View metadata, citation and similar papers at core.ac.uk

brought to you by CORE

provided by Bilkent University Institutional Repository

APPLICATION OF DEADBEAT CONTROLLERS AND POLE PLACEMENT METHODOLOGIES FOR FRICTION COMPENSATION IN MECHANICAL SYSTEMS

A THESIS SUBMITTED TO

THE GRADUATE SCHOOL OF ENGINEERING AND SCIENCE

OF BILKENT UNIVERSITY

IN PARTIAL FULFILLMENT OF THE REQUIREMENTS FOR

THE DEGREE OF

MASTER OF SCIENCE

IN

ELECTRICAL AND ELECTRONICS ENGINEERING

By

Çınar Yeşil Karahasanoğlu

September, 2015

Application of Deadbeat Controllers and Pole Placement Methodologies
for Friction Compensation in Mechanical Systems
By Çınar Yeşil Karahasanoğlu
September, 2015

We certify that we have read this thesis and that in our opinion it is fully adequate, in scope and in quality, as a thesis for the degree of Master of Science.

Prof. Dr. Ömer Morgül(Advisor)

Prof. Dr. Hitay Özbay

Prof. Dr. Mehmet Önder Efe

Approved for the Graduate School of Engineering and Science:

Prof. Dr. Levent Onural
Director of the Graduate School

ABSTRACT

APPLICATION OF DEADBEAT CONTROLLERS AND POLE PLACEMENT METHODOLOGIES FOR FRICTION COMPENSATION IN MECHANICAL SYSTEMS

Çınar Yeşil Karahasanoğlu
M.S. in Electrical and Electronics Engineering
Advisor: Prof. Dr. Ömer Morgül
September, 2015

Friction is an almost unavoidable component of many mechanical systems. When not taken into account in designing control systems, the effect of friction may result in the degradation of controlled system performance. This thesis deals with the problem of designing a control system, for friction compensation in mechanical systems, via pole placement and deadbeat methodologies. Pole placement design is based on different performance measures and indices such as settling time, overshoot and ITAE. Deadbeat controller design is based on parameterization of Diophantine equations which depend on the reference signal to be tracked. System performance is analyzed on simulation level by the application of the two methodologies in a hierarchical feedback system structure, which provides both position and velocity control separately. Simulation results show that both methodologies provide acceptable performance as compared to the existing compensation schemes in literature and control performances are improved with respect to their accuracy of tracking. In addition, deadbeat controller is observed to be more promising in terms of minimum settling time.

Keywords: Friction, Coulomb Friction, Friction Compensation, Pole Placement, Deadbeat Controller, Diophantine Equations.

ÖZET

MEKANİK SİSTEMLERDE SÜRTÜNME GİDERİMİ İÇİN DEADBEAT DENETLEYİCİ VE KUTUP YERLEŞTİRME DENETİMİ UYGULAMASI

Çınar Yeşil Karahasanoğlu
Elektrik ve Elektronik Mühendisliği Bölümü , Yüksek Lisans
Tez Danışmanı: Prof. Dr. Ömer Morgül
Eylül, 2015

Sürtünme, mekanik sistemlerde kaçınılmaz bir şekilde oluşur. Kontrol sistemleri tasarlanırken sürtünmenin gözardı edilmesi, kontrol sisteminin performansını düşürmektedir. Bu tezde, tasarlanan kontrol sistemlerinde kutup yerleştirme ve deadbeat metodolojilerini kullanarak, mekanik sistemler için sürtünme giderme yöntemleri sunulmaktadır. Kutup yerleştirme temelli tasarım ITAE, oturma zamanı ve maksimum aşma gibi değişik performans kriterlerine göre yapılmıştır. Deadbeat denetleyici temelli tasarım ise referans sinyaline bağlı olarak parametrize edilen Diophantine denklemlerine göre yapılmıştır. Ayrı ayrı hem hız hem pozisyon kontrolü sağlayan hiyerarşik kontrol yapısı kullanılarak, sistem performansı simülasyonlarla analiz edilmiştir. Simülasyon sonuçları, iki yöntemin de, mevcut sürtünme giderme yöntemlerine kıyasla, uygulandığı sistemin performansını kabul edilebilir ölçüde geliştirdiğini ortaya koymuştur. Ayrıca, simülasyonlar, takip hassasiyeti baz alındığında da kontrol performansının arttığını göstermiştir. Deadbeat denetleyicinin ise minimum oturma zamanı baz alındığında daha umut vaat eden bir kontrol yöntemi olduğu gözlenmiştir.

Anahtar sözcükler: Sürtünme, Coulomb Sürtünme, Sürtünme Giderimi, Kutup Yerleştirme, Deadbeat Denetleyici, Diophantine Denklemleri.

Acknowledgement

I would like to express my sincere gratitude to Prof. Dr. Ömer Morgül, for his supervision and support throughout my graduate study and endless guidance throughout my thesis. He has been a constant source of help, ideas and inspiration. It is a great honor to be one of his students and a rare privilege to be able to work with him.

I would also like to thank Prof. Dr. Hitay Özbay and Prof. Dr. Mehmet Önder Efe for being members of my thesis committee.

I would like to express my special gratitude to Dr. Ömür Yüksel Baş. I appreciate her taking the time to talk to me about my thesis and providing many useful suggestions.

I am thankful to my dear friends Mert, Orçun, Elif, Esra and Ezgi for their support and encouragement. I feel fortunate having them in my life and they are the sources of my motivation and strength till the end.

Most importantly, I would like to deeply thank my father Mahir, my mother Zeliha and my sister Zeynep Aslı for all their love, inspiration and support in my whole life. I humbly extend my thanks to my second family Orhan, Hülya and Özlem, for their love and passionate encouragement throughout my graduate study.

Last but not least, I am indebted to my dearest Cicoş and Daco. I greatly value their lifelong love, care and belief in me...

Words will not be enough to thank my husband Onur, for his patience, infinite support and encouragement during my thesis. He was always there, stood by me through good times and bad and helped me stay sane through these difficult years. His endless love and interest made it possible for me to complete this thesis.

Contents

List of Figures

List of Tables

To Onur...

Chapter 1

Introduction

Friction plays an important role in the performance of high precision mechanical systems as it is a highly nonlinear component that may give rise to poor performance and cause undesirable effects such as steady state errors, tracking errors, time delays, oscillations and limit cycling [1]. It is one of the main limiting factors for the precision of positioning and pointing in the motion system, if it is not compensated. Therefore, it is desirable to minimize the frictional effects by friction compensation, for the design of motion control approach, as classical feedback laws may be insufficient for the compensation of frictional effects [2].

An effective control strategy would achieve a good transient response and tracking of any reference input with zero steady-state error. Tracking error should diminish as fast as possible because the systems lose the most time at zero or near-zero velocities, trying to overcome the dominant and discontinuous disturbance factor, which is the friction.

1.1 Motivation

The goal of this study is to develop a control strategy that both compensates for the frictional effects and achieves certain performance criteria, such as overshoot and settling time optimization, etc. This goal is important especially for position and speed control in critically-timed firing, shooting and weapon systems or mechanical motion platforms with which these systems are integrated. These systems need to satisfy high tracking accuracy demands in a short amount of time. To this end, a deadbeat controller, employing the parameterization of Diophantine equations, is utilized to a plant of motion system with nonlinear friction.

The study primarily focuses on position tracking of a plant that experiences high number of velocity reversals or low magnitude demand, in which Viscous friction, combined with Coulomb friction, is the most dominant disturbance factor. In these systems, typical procedures for orienting the system to the given input as in linear systems, are no longer valid because of the nonlinearity region and robustness issues. Furthermore, suitable friction compensation methods may have additional performance based drawbacks such as time delays, overshoots, bad disturbance rejection and higher control effort. By the utilization of the deadbeat controller, output of the system tracks the reference input from any initial state, with zero steady state error and minimum settling time [3].

The design process of the deadbeat controller consists of 2 main steps. The first step is feedback linearization, in which, the nonlinear system is linearized and stabilized by using state and output feedbacks with integral and gain controller. Feedback linearization is also related to the pole placement in the case of linear systems [4]. The second step includes polynomial approach, in which, the controller's parameters are obtained by solutions of the two independent Diophantine equations, constructed

for the transfer function of the linearized and stabilized nonlinear plant [5]. The general structure of the controlled mechanical system studied in this thesis is shown in Figure 1.1:

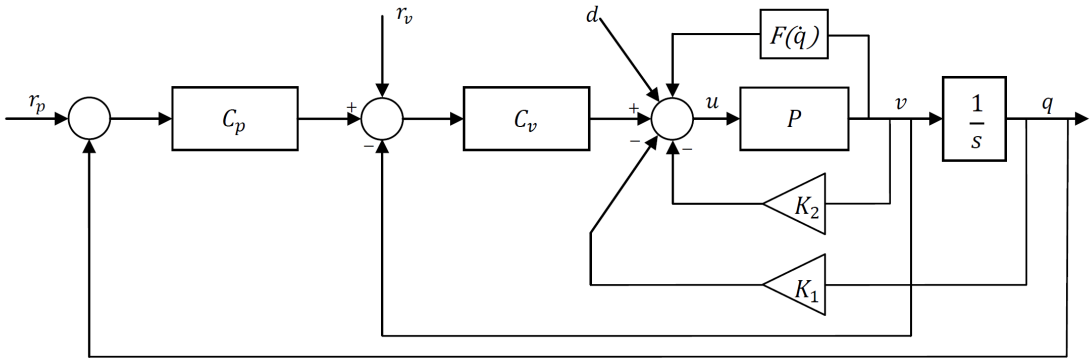

Figure 1.1: Block diagram of overall feedback system

In Figure 1.1, P represents the plant, $F(\dot{q})$ represents the friction force. The gains K_1 and K_2 are are utilized for pole placement after linearization of the plant. C_p and C_v blocks represent the controllers, one for stabilization of the position loop and one for the stabilization of the velocity loop respectively. Moreover, the signals r_p and r_v represent the command inputs for position and velocity respectively. Position output is represented by q, whereas $v = \dot{q}$ is the velocity output. Finally, d stands for the disturbance acting on the plant and u is the control input applied to the plant.

Such structures have been investigated in various systems, see [6], [7] and [8]. The proposed deadbeat controller will be added to the structure given in Figure 1.1 in subsequent sections, see e.g. section 3.2.

For position control, velocity command input r_v must be equal to zero ($r_v = 0$). For velocity control, position command input r_p must be equal to zero ($r_p = 0$) and the position loop must be switched off by making $C_p = 0$.

1.2 Background

Various control strategies have been developed, in order to eliminate frictional effects and to deal with problems such as instabilities, steady state and tracking errors, oscillations, time delays and limit cycles caused by friction. These strategies can be categorized as model-based and non-model based friction compensation, according to their control approach towards friction phenomena [9].

1.2.1 Non-model-based Friction Compensation

If the friction cannot be accurately modeled or it depends on varying and uncontrollable conditions in the system, non-model based friction compensation schemes are suitable for overcoming problems caused by friction. These schemes compensate not only for friction, but also other nonlinearities. The survey paper [10] overviewed the important contributions on non-model based friction compensation and classified available methods having different accuracy levels.

Most known compensation schemes are introducing Dither signal into the system [11], [12], [13], [14], [15] and [16], Linear Feedback Controllers [17], [18], [19], [20], [21], [22], [23], [24] and [25], Joint Torque Control [26], [27], [28], [29], [30], [31], [32], [33], [34] and [35], Impulsive Control [36], [37] and [38], Dual Mode Controllers [39], [40] and [41] and Disturbance Observers [42], [43], [44], [45], [46], [47] and [48].

Dither is a smoothing technique for the discontinuities, in which a high frequency signal is introduced to the control signal such that the total applied force overcomes the static friction force at velocity reversals [13]. Figure 1.2 shows addition of Dither with unit feedback:

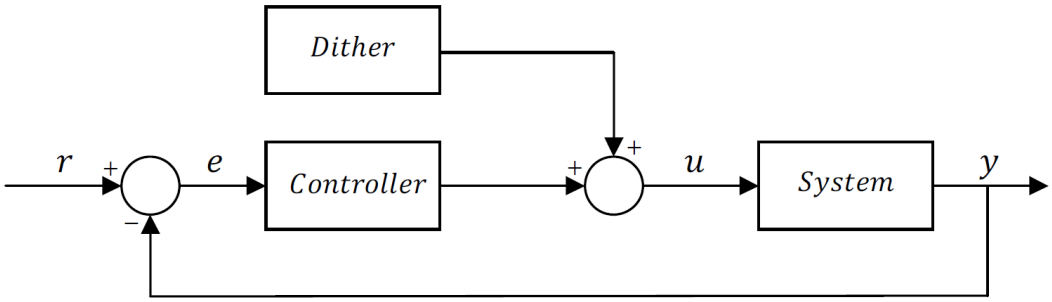

Figure 1.2: Representation of dither method

Despite its simplicity and effectiveness, Dither is not suggested especially for direct drive mechanical systems as more noise is introduced into the control process. Controller output might no longer be the same as the plant input as one of the natural frequencies of the plant might be excited with the addition of Dither [14]. Furthermore, hysteresis may appear due to wear problems caused by the vibrations [16].

Linear Feedback Controllers include all types and combinations of Proportional (P), Integral (I) and Derivative (D) controllers, which are widely used in control applications. The PID algorithm is described by:

$$u(t) = K_p \mathrm{e}(t) + K_i \int_0^t \mathrm{e}(\tau), \mathrm{d}\tau + K_d \frac{\mathrm{d}e(t)}{\mathrm{d}t}$$

where K_p , K_i and K_d are controller parameters, u(t) and e(t) are control signal and error, respectively [21]. P-term is proportional to the error, I-term is proportional to the integral of the error and D-term is proportional to the derivative of the error.

The study in [24] shows the design and implementation of a nonlinear PID controller including the application of time-varying and switching state feedback gains as a function of system state and errors. Yet, this study focuses only on the stability of the system under frictional disturbances and does not offer any methodology for performance goals. The study in [22] exposes the fact that the stick-slip limit cycle is inevitable in systems with Coulomb friction combined with static friction even if another first-order linear compensator in the feedback loop is added for reduction of the amplitude of the limit cycle. The work in [20] clarifies that no combinations of P, I and D parameters can eliminate the stick-slip friction unless nonlinear modifications, such as tuning of PID parameters, are made.

Rate varying and Reset-off integral controllers are studied in [19], especially for reduction of steady-state errors. Although rate varying integrator eliminated the steady state errors originating from stick friction, it couldn't handle the tracking errors originating from slip friction. The Reset-off integrator reduced the start-up errors and oscillations, but couldn't compensate for slip friction. Therefore; the integral controllers were not successful and effective enough for compensation of friction at low velocities and velocity reversals.

Position tracking with a PD controller in a steady, low velocity motion is explored in [18]. The study indicates that velocity feedback, combined with position feedback gains above a critical value, is crucial for friction compensation. Nevertheless, maximum gains of velocity and position feedback are limited by possible loop instabilities and steady-state tracking errors.

Joint torque control includes the design of a joint torque sensor which is introduced to the commanded torque, with a feedback loop between the actuator and the plant so that applied torque follows the commanded torque [26]. Figure 1.3 shows addition of torque controller with unit feedback. In the inner torque loop, friction compensation and torque maintenance is made whereas in the outer loop, execution of the overall

system is carried out.

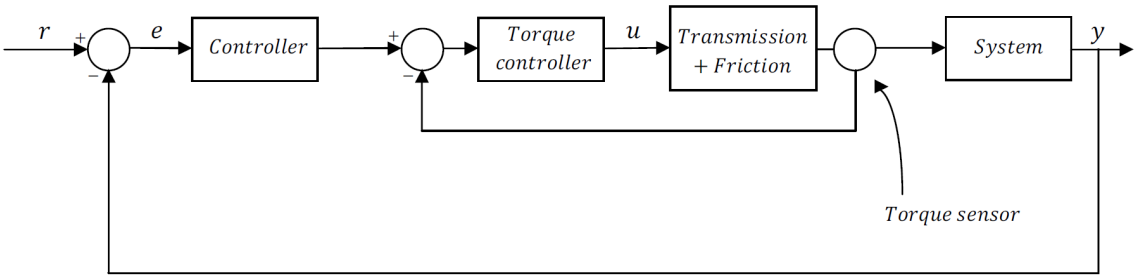

Figure 1.3: Representation of the joint torque control

The studies in [27] and [31] focus on sensing and compensating for nonlinear dynamics in robotics by the design of joint torque control. The studies in [28] and [29] implement the control for compensation of actuator disturbances and transmission flexibilities. The study in [30] uses a joint torque sensing technique that complying harmonic-drive elasticity in a single joint arm. All of these studies address single axis sensing for each joint whereas the study in [33] proposes using six axes of force/torque sensing per joint. Despite the results showing that performance of the system is increased with almost indistinguishable steady state tracking errors, the main challenge of this method is non-collocated sensing, caused by the separation of actuator and sensor by the compliance of the transducer.

Impulsive control proposes generation of the control signal as a sequence of pulses to perform the desired motion [38]. The study in [37] proposes a state-dependent impulsive feedback control scheme, for set-point stabilization in motion systems with uncertain friction. The study in [16] extends the study in [37], by the addition of a pulse sequence to the control signal. However, control is limited to the dynamics of the system and limitations of the controller, as the system is at rest between the impulsive actions [36]. Furthermore, pulses should be of great magnitude to overcome

the friction at low velocities and the control method is challenged by estimating velocity accurately.

Usage of different controllers due to different frictional disturbances in the same system is known as variable structural control strategy [39]. A special case of this strategy is Dual Mode Control [40], in which two different controllers are used depending on the active stage of friction. Figure 1.4 depicts the control strategy:

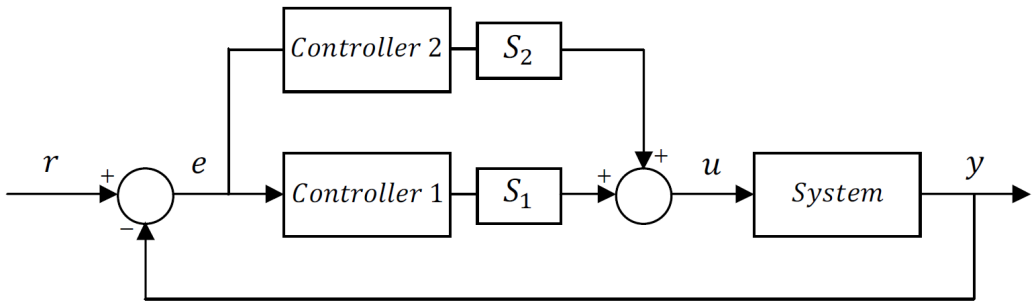

Figure 1.4: Representation of dual mode control

If the friction dynamics are drastically different, i.e. dual dynamic modes, this control strategy could be adapted by switching so that each controller is used for each frictional behavior. However, this strategy requires repetitive initialization of the state of each controller right after switching, which may be a challenging task. In addition to this, switching decision could be a difficult task due to the problems caused by identification of the friction [41].

Disturbance observers' ability is to realize the unidentified disturbances such as parameter variations and parametric uncertainties without use of any additional sensor [43]. For friction compensation schemes, disturbance observers are used in the control strategy widely in order to estimate friction. These schemes are observed

to provide improved tracking and robustness [42]. As seen in Figure 1.5, if the system dynamics are known, the disturbance observer estimates the disturbance with the measurement of system output and applied torque [47]. Indeed, output of the disturbance observer minimizes the frictional effects.

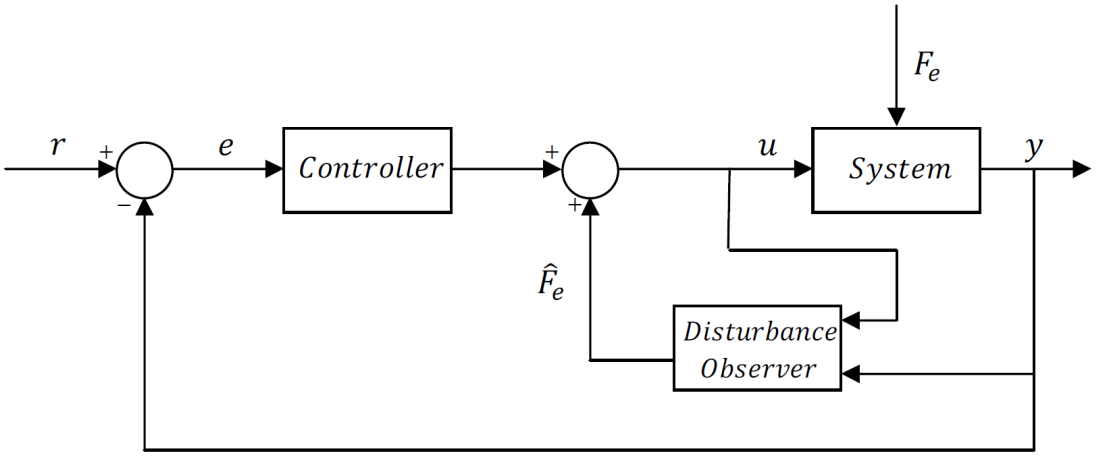

Figure 1.5: Representation of the disturbance observer structure

The study in [44] proposes an extended Kalman-Bucy filter relying on an accurate system model to estimate friction. This approach treats friction as an unknown state element whereas in [48], friction is treated as a load disturbance torque in a tracking servo system. In addition to Kalman filter based approach, stability and performance analysis of predictive filter based approach and local function estimation approach are studied in [45]. Although the results show increased tracking performance, decreased frictional uncertainties and stability for a wide range of frictional behavior, disturbance observers have limited disturbance rejection bandwidths and limited capability of friction compensation at velocity reversals [46].

1.2.2 Model-based Friction Compensation

If friction can be modeled mathematically or the information of friction is available, model-based friction compensation schemes are used to compensate for friction just by applying an equivalent and opposite control force to the instantaneous friction in the system [49]. Figure 1.6 illustrates the basic idea behind model-based friction compensation:

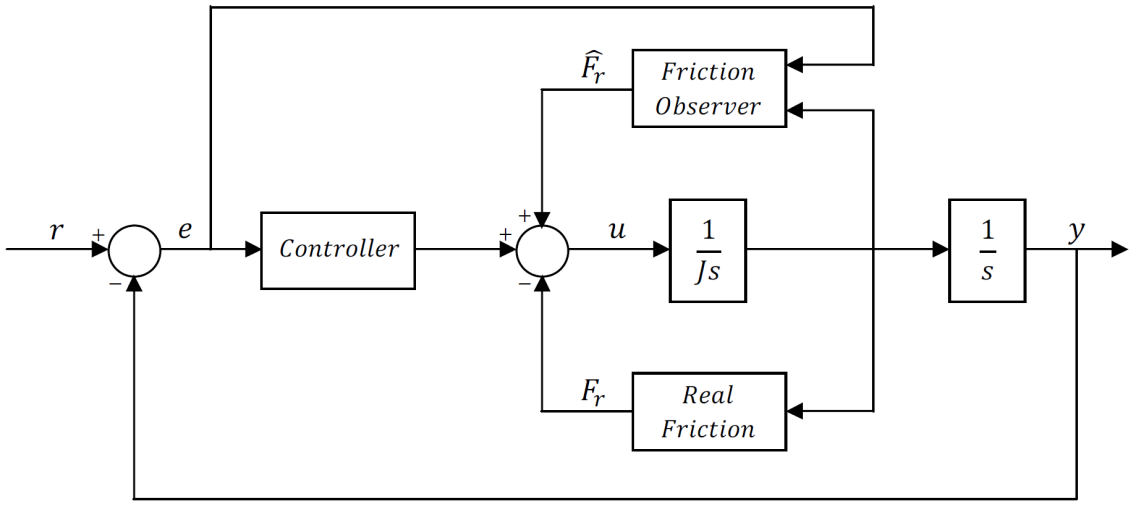

Figure 1.6: Representation of model-based friction compensation

As knowledge and accuracy of the model increases, these schemes are more promising [9]. The papers [10] and [1] overviewed the important contributions on model-based friction compensation and classified available methods having different accuracy levels.

Most known compensation schemes are Adding Fixed Friction Compensation Term as in [50], [51], [52], [53], [54], [55] and [56], Compensation in Feedforward [57], [58], [59], [60], [6] and [7], Compensation in Feedback [61], [62], [63], [64] and

[65], Adaptive and Learning Controllers combined with Friction Estimators and Observers [6], [66], [67], [68], [69], [70], [71], [72], [73], [74] and [75].

Fixed Friction Compensation introduces a fixed compensation term to the real friction in the system, with an equal and opposite control force composed of an accurate off-line estimate of the friction force [76].

The study in [54] explores friction compensation by the use of kinematics and dynamics of a three revolute joints robot. The friction parameters are estimated on the basis of the assigned three-sigmoid function model. The study in [55] verifies the performance of the proposed methodology in [54] by kinetic friction parameter estimation experimentally in a servomechanism. For dynamic friction models in systems, observers are inserted in the velocity loops of systems and the fixed compensation term is introduced on the basis of the estimated dynamic friction as studied in [52] and [53].

Feedforward and feedback schemes are the most widely used forms of model based friction compensation. Feedforward is used for improvement of the tracking performance, whereas feedback deals mostly with stability and disturbance rejection issues [1]. A detailed comparison study, with the application of feedforward and feedback approaches to a robotic gripper, is presented in [77]. This study makes a distinction between two approaches: feedback tries to reject frictional disturbances whereas feedforward tries to provide accurate tracking. The block diagram of a feedforward controller combined with a unit feedback is illustrated in Figure 1.7. The major difference between feedforward and feedback approaches is the use of information for compensation. Feedforward approach uses a precalculated friction depending on the reference, whereas feedback approach makes use of the actual friction for the calculation of compensation [1].

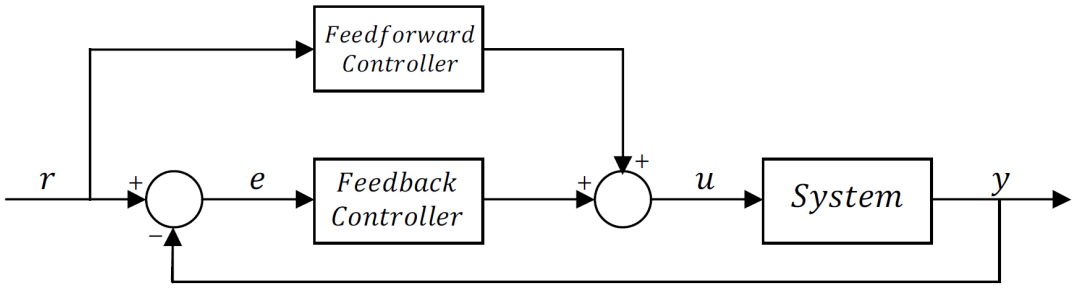

Figure 1.7: Representation of unit feedback and feedforward

The study in [46] offers design of feedforward compensation for various friction models such as Dahl, LuGre, Leuven and Generalized Maxwell-slip (GMS) [49]. The approach in [46] is also used in [58] with Karnopp friction model and it's been observed that potential limit cycles are eliminated. In [57], Viscous damping added Coulomb friction is compensated by an adaptive feedforward controller. A feedforward compensation is designed in [59], for a static model combined with GMS friction model especially for compensating the tracking errors caused by the complex nonlinear behavior of friction at velocity reversals. The study in [60] is an enhanced version of the study in [59] in which the feedforward controller is combined with a repetitive controller and a disturbance observer, thus resulting in an almost complete elimination of the remaining frictional disturbances and effects of cutting forces.

Feedback compensation of friction usually uses velocity information as a feedback variable and uses actual values of the velocity state in the friction model [64]. However, in [62], an estimation algorithm for velocity is proposed and feedback is

introduced with the estimated velocity instead of measured velocity. In [65], a feedback compensation structure is developed in order to overcome friction of a printer system, in which feedback controller is combined with an Iterative Learning Controller used for learning the repetitive error and identifying friction parameters in the system up to a higher frequency.

Both feedforward and feedback compensation schemes depend on desired reference friction model, accurate identification of friction parameters or measurement of actual friction. Therefore; feedforward compensation is limited by the used reference friction model especially at very low velocities whereas feedback compensation is limited by the measurability of the internal friction state, especially for the dynamic friction models.

Modeling and parameter identification, required for model-based compensation, is challenging because friction varies with temperature, wear, contact material properties, velocity and position etc [72]. Adaptive and learning controllers try to lead the system to adapt such changes by employing friction parameters and forward corrections - obtained by online identification - to the system [69].

The studies in [66] and [67] propose a control scheme in which frictional effects are compensated adaptively with the use of an observer to estimate static friction models and parameters in servo systems. The performance benefited from the control strategy since the system spends a little amount of time around zero velocity. Nonetheless, the approach is not suggested for systems with dynamic friction models. This problem is overcome in [68], in which an adaptive nonlinear model provides a reconstruction method for the velocity reversals by the help of a linear observer and in [51] in which a neural-network based online learning feedforward controller for repetitive low-velocity motions. Furthermore, the study in [73] demonstrates an adaptive sliding control scheme for the estimation of friction and force ripple dynamics around zero velocity and velocity reversals and the study in [71] features a dual

observer for the estimation of friction parameters. The studies in [74] and [75] deal with dynamic friction models and propose stable adaptive compensators with low tracking errors. However, the study in [70] proves that if the friction state is unmeasureable, it is difficult to adapt the friction dynamics and compensate for uncertain friction throughout the mechanical system as adaptive compensators work only if the plant and disturbance dynamics are available. Another drawback is the restrictive assumptions made through the design process such as constant plant parameters which may not work in practical case.

1.2.3 Deadbeat Control

Deadbeat Control strategy offers a solution to the steady-state optimal control problem with its fastest settling time feature. Although this feature is one of the principal concepts in system control theory as it is crucial to reach the desired reference from any initial condition in minimum time, it is not explored much and the strategy was not studied frequently in literature [78].

The theory of Deadbeat Control problem was apparently first addressed in [3], in which four different types of controller, using different columns of the controllability matrix of a system for state space construction and state transfer in minimum time, are proposed. The designs lack robustness with respect to possible system parameter variations.

The study in [79] approaches the deadbeat control problem by the formulation of an optimal control problem which is established to solve the associated eigenvalue problem. Generalized eigenvalue technique is used to place the poles at the origin by the obtained feedback gain. The resulting controller, which is constructed with the internal model of the reference input, provides robust tracking. The study in [80] extends the results of [79] and [78] to linear multivariable generalized state-space

systems, by the use of properties of linear quadratic regulator theory to obtain the deadbeat controller classes.

Solution of a singular Riccati equation associated with the optimization problem for a linear time-invariant system, leads to the design of a time variable deadbeat controller by the minimization of a quadratic cost function, in [81]. The study is extended in [82], which proves that a time varying Kalman gain sequence, computed by the solution of a singular Riccati equation, always leads to the design of a deadbeat controller.

These studies do not deal with the intersample ripples that may appear in the continuous-time output. Ripple is an undesirable feature of deadbeat controllers, which appear between sampling instants after settling time as an error between the reference and actual output. The study in [83] proposes a ripple-free deadbeat controller, which also minimizes a quadratic cost function with the aid of H_2 norm, for minimization of tracking error and control signal.

Very large values of control signals are one of the main drawbacks of deadbeat controllers in most of the studies that offer minimum settling time. This is because of the fact that the main objective is to beat all of the states of the system to the origin in minimum time. The study in [84] offers a solution to this problem by the use of transfer function factorization approach, which presents characterization of all stabilizing deadbeat controls in terms of control input. The approach is illustrated in a system with two-degree-of-freedom controllers: a feedforward block minimizing the control input and a feedback block guaranteeing robustness. A trade-off is clearly observed between settling time and magnitude of the control signal.

Performance based design quantities such as settling time, overshoot, undershoot, slew rate and l_1, l_2 , l_∞ norms are used for obtaining a matrix parameterization of the deadbeat controller in [85]. This controller is used as an optimal ripple-free

control problem with time delayed systems. The study is further extended by the study in [86], in which the matrix parameterization is made for all causal output periodic feedback controllers using polynomial methods. The controllers provide ripple-free behavior of the output of a linear time-invariant plant with a general multirate control scheme.

The study in [5] proposes a hybrid, two-degree-of-freedom and ripple-free deadbeat controller, which is designed according to performance and robustness specifications. The design is based on the internal model principle and the solution of two Diophantine equations: one equation for determining the performance property, another equation for determining the robustness property. This design process is treated as a solution for the fixed-order constrained optimization problem. Approaching this problem with a given performance and robustness program, one has to minimize performance and robustness cost functions subject to controller constraints. Figure 1.8 illustrates the configuration for the realization of the proposed deadbeat controller, [5]:

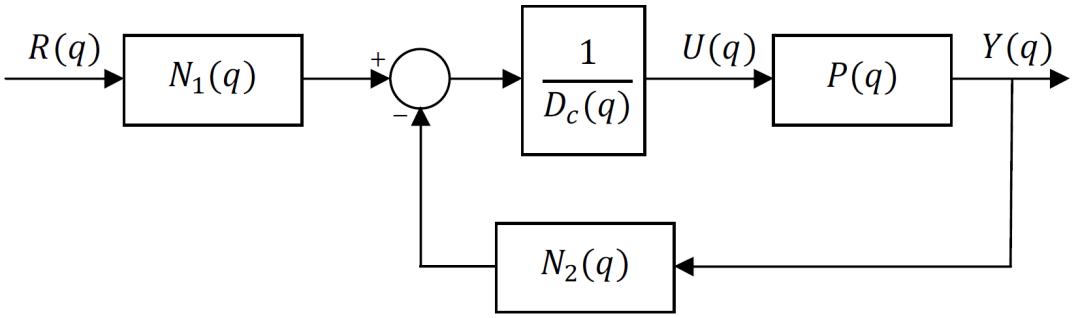

Figure 1.8: Implementation of the deadbeat controller

The controller polynomials N_1 , N_2 and D_c are obtained by the solution of two Diophantine equations:

$$N_p(q)N_1(q) + D_r(q)Q_1(q) = 1 \tag{1.1}$$

$$N_p(q)N_2(q) + D_p(q)D_c(q) = 1 \tag{1.2}$$

where Q_1 is also a polynomial like N_1, N_2 and D_c, N_p is the numerator of the plant, D_p is the denominator of the plant and D_r is the denominator of the reference input $R(q) = \frac{N_r(q)}{D_r(q)}$, $P(q) = \frac{N_p(q)}{D_p(q)}$. The plant and reference inputs are polynomials in Q-domain, which corresponds to rational functions in Z-domain. The results of this study, validated with examples throughout the paper, show a good performance with small settling times but high control signals.

The studies listed above, which gives a much better understanding of the capabilities and limitations of minimum-time and deadbeat controllability, treats linear systems only [87]. The insight of this control strategy for linear systems raises a big question in mind: whether a deadbeat controller can be designed also for nonlinear systems or not. This problem is apparently worth investigating.

The first attempt for deadbeat control of nonlinear systems is made in the study [87], in which a system with one zero at infinity is one step output deadbeat controlled. This study shows that, if the system's zero dynamics are stable, the deadbeat controller beats all states of the system to the origin. The study in [88] proposes a contribution to the investigation, with an input-output approach given for stability of one dimensional explicit zero dynamics. The study in [89] offers the best generalized solutions especially for minimum phase nonlinear polynomial systems.

As observed from literature, there has been no work on design and application of a deadbeat controller to the nonlinear friction compensation in mechanical motion systems.

1.2.4 Contributions of the Thesis

This thesis presents a pole placement methodology and design of a deadbeat controller to solve the tracking, disturbance rejection and friction compensation problems in a mechanical system with nonlinear friction. Presented scheme is based on a hierarchical closed loop feedback structure proposed in [6] and [7] whereas the deadbeat controller formulation is based on [5]. Thus, the presented controller combines two different types of controllers: one for internally stabilizing the system and one for providing fast settling time and robustness.

1.2.5 Organization of the Thesis

The thesis is organized as follows. In Chapter 2, structure of the plant and the controller are defined, the design of the controller is presented. In Chapter 3, analysis of the proposed control scheme is given. Performance of the designed controller is investigated under different scenarios and compared with the performance of a high gain feedback controller in terms of friction compensation. Concluding remarks are made in Chapter 4.

Chapter 2

Control Design of Mechanical Systems with Friction

2.1 Plant Structure

A typical motion system is characterized by the following general equation:

$$J\ddot{q} + F(\dot{q}) = u \tag{2.1}$$

where J is the moment of inertia, q is the position, u is the applied force and $F(\dot{q})$ is the friction force. Equation 2.1 will be used in the next part to derive state space of linearized model of the plant.

In this system, output is position or velocity whereas input is the force applied. The acceleration of the system as produced by the acceleration force is directly proportional to the magnitude of the net force, in the same direction as the net

force and inversely proportional to the moment of inertia of the system according to Newton's second law of motion [90]. When there is no friction force, acceleration is proportional to the applied force.

The following block diagram depicts the motion dynamics of a typical motion system, with the representation of nonlinear friction force.

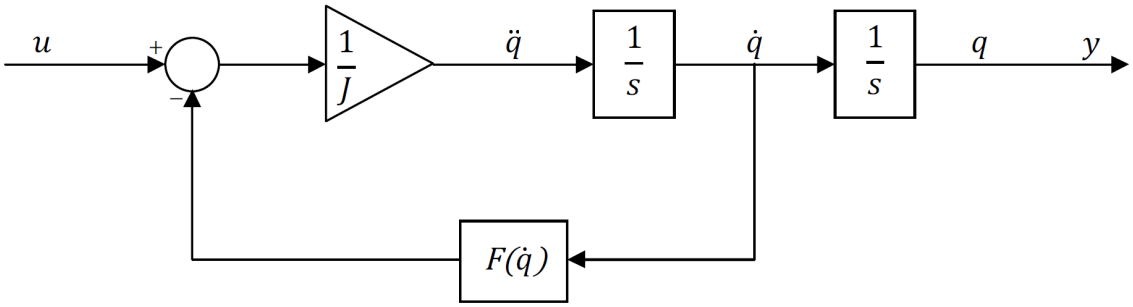

Figure 2.1: Block diagram of the mechanical system

Forward path includes an integrator from applied force to velocity as it is obvious from Newton's Law. Velocity is integrated into position. In addition to the integrator, there is a gain inversely proportional to the moment of inertia.

Friction is introduced to the system in the velocity loop. It acts against the applied force as characterized by the subtraction in the block diagram. The difference between the applied force and the friction force is applied to the plant dynamics. This difference is used for acceleration. Therefore; performance of the system degrades.

In order to overcome the friction force, a proper model of friction is essential. A useful and simple model capturing the essential properties of friction is Coulomb friction, where the friction force depends on the sign of the velocity, and a linear viscous friction [49].

Let us assume that the plant contains Coulomb friction and linear viscous damping, which describe a static relationship between the friction force and velocity as given below:

$$F(\dot{q}) = F_c \text{sgn}(\dot{q}) + F_v \dot{q} \tag{2.2}$$

Here, F_c is the magnitude of Coulomb friction which is proportional to the normal force, i.e. $F_c = \mu F$, and $\mu < 1$ is the coefficient of friction. F_v is the magnitude of Viscous friction. The friction force contains a discontinuity at zero relative velocity as observed from the presence of signum function in the equation [91]. This discontinuity may possibly be alleviated by replacing the model by a smoothing function such as $\tanh(\lambda\dot{q})$. Hyperbolic tangent is an approximation of signum function without being discontinuous. As λ approaches infinity, it reduces to signum function [92]. Thus, the friction model will be approximated as:

$$F(\dot{q}) = F_c \tanh(\lambda\dot{q}) + F_v \dot{q} \tag{2.3}$$

The motion of equation depends on the type of friction model. Throughout the thesis, simulations will be carried out with the original Coulomb friction model, which includes signum function, whereas the design of the controller will be based on three different friction models. Table 2.1 shows the friction models and the resultant equations of motion:

Table 2.1: Equation of Motions for Friction Models

Friction Model	Friction Force	Equation of Motion
Viscous	$F(\dot{q}) = F_v\dot{q}$	$\ddot{q} = \frac{1}{J}(u - (F_v\dot{q}))$
Viscous+Coulomb (based on sgn(x))	$F(\dot{q}) = F_c\text{sgn}(\dot{q}) + F_v\dot{q}$	$\ddot{q} = \frac{1}{J}(u - (F_c\text{sgn}(\dot{q}) + F_v\dot{q}))$
Viscous+Coulomb (based on $\tanh(x)$)	$F(\dot{q}) = F_c\tanh(\lambda\dot{q}) + F_v\dot{q}$	$\ddot{q} = \frac{1}{J}(u - (F_c\tanh(\lambda\dot{q}) + F_v\dot{q}))$

2.2 Deadbeat Controller Structure

In this section, design methodology for deadbeat controller is given. The theory is illustrated for position control of a motion system as an example.

2.2.1 Feedback Linearization

The goal of feedback linearization approach is to produce a linear model of the dynamics by canceling the nonlinearities in the system, with the use of nonlinear state feedback design. State feedback design relies on pole placement such that the closed loop nonlinear system dynamics is algebraically transformed into a linear form [4].

For the first step of state feedback design, full-state feedback control law is utilized for the state space representation of the system - the mathematical model of the system including the set of input, output and state variables - which is derived after linearization around operating point [93]. Figure 2.2 illustrates the block diagram of full-state feedback:

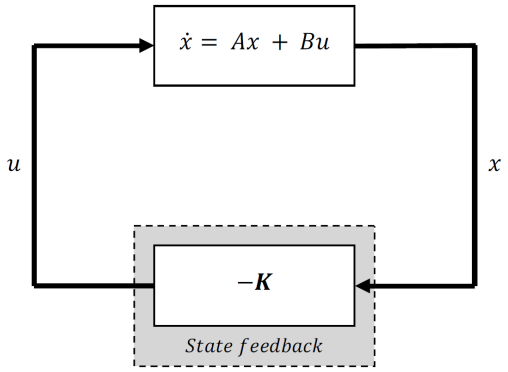

Figure 2.2: Block diagram of full-state feedback

In order to obtain state space representation of the system, let us define variable transformation:

$$x_1 = q \tag{2.4}$$

$$x_2 = \dot{q} \tag{2.5}$$

Substituting (2.4) and (2.5) into equation 2.1, we obtain:

$$\dot{x_1} = x_2 \tag{2.6}$$

$$\dot{x_2} = -\frac{1}{J}F(x_2) + \frac{1}{J}u \tag{2.7}$$

Equations (2.6) and (2.7) are first order state equations in the form:

$$\begin{aligned} \dot{x_1} &= \quad f_1(x_1, x_2) \\ \dot{x_2} &= f_2(x_1, x_2) + \frac{1}{J}u \end{aligned} \tag{2.8}$$

Here, $f_1(x_1, x_2) = x_2$ and $f_2(x_1, x_2) = -\frac{1}{J}F(x_2)$

Using the state variable expression in (2.8), linearization around equilibrium point is given by [4]:

$$\dot{x_1} = \left.\frac{\partial f_1}{\partial x_1}\right|_{\substack{x_1=x_{10}\\x_2=x_{20}}} x_1 + \left.\frac{\partial f_1}{\partial x_2}\right|_{\substack{x_1=x_{10}\\x_2=x_{20}}} x_2 \tag{2.9}$$

$$\dot{x_2} = \left.\frac{\partial f_2}{\partial x_1}\right|_{\substack{x_1=x_{10}\\x_2=x_{20}}} x_1 + \left.\frac{\partial f_2}{\partial x_2}\right|_{\substack{x_1=x_{10}\\x_2=x_{20}}} x_2 + \frac{1}{J}u \tag{2.10}$$

Here (x_{10}, x_{20}) is the equilibrium point of the system. At equilibrium, the system is fixed at position x_1, then velocity is equal to zero; i.e. we have:

$$\begin{aligned} x_1 &= x_{10} \\ x_2 &= \ 0 \end{aligned}$$

Equations (2.9) and (2.10) could be put into the following matrix form:

$$\begin{bmatrix} \dot{x_1} \\ \dot{x_2} \end{bmatrix} = A \begin{bmatrix} x_1 \\ x_2 \end{bmatrix} + Bu$$

$$y = C \begin{bmatrix} x_1 \\ x_2 \end{bmatrix} + Du$$

Where $A = \left.\begin{bmatrix} \frac{\partial f_1}{\partial x_1} & \frac{\partial f_1}{\partial x_2} \\ \frac{\partial f_2}{\partial x_1} & \frac{\partial f_2}{\partial x_2} \end{bmatrix}\right|_{\substack{x_1=x_{10}\\x_2=0}}$, $B = \begin{bmatrix} 0 \\ \frac{1}{j} \end{bmatrix}$, $C = \begin{bmatrix} 1 & 0 \end{bmatrix}$ and $D = 0$

By using the friction model in (2.3) and related equation of motion in Table 2.1, state space representation of the linearized system can be derived as:

$$\dot{x_1} = x_2$$

$$\dot{x_2} = \frac{1}{J}u - \frac{1}{J}(F_c\lambda + F_v)x_2$$

Where we use the fact that $\frac{d}{dx_2}(\tanh(\lambda x_2))\big|_{x_2=0} = \lambda$

Each friction model yields a different linear approximation. Table 2.2 shows the friction models and the resultant state space representation of linearized system:

Table 2.2: State Space Matrices for Friction Models

Friction Force	State Space Representation	State Space Matrix
$F(\dot{q}) = F_v\dot{q}$	$\dot{x_1} = x_2$ $\dot{x_2} = \frac{1}{J}u - \frac{1}{J}(F_v)x_2$	$A = \begin{bmatrix} 0 & 1 \\ 0 & -\frac{1}{J}F_v \end{bmatrix}$ $\mathrm{B} = \begin{bmatrix} 0 \\ \frac{1}{J} \end{bmatrix}$ $C = \begin{bmatrix} 1 & 0 \end{bmatrix}$ $D = 0$
$F(\dot{q}) = F_c\mathrm{sgn}(\dot{q}) + F_v\dot{q}$	$\dot{x_1} = x_2$ $\dot{x_2} = \frac{1}{J}u - \frac{1}{J}F_vx_2$	$A = \begin{bmatrix} 0 & 1 \\ 0 & -\frac{1}{J}F_v \end{bmatrix}$ $\mathrm{B} = \begin{bmatrix} 0 \\ \frac{1}{J} \end{bmatrix}$ $C = \begin{bmatrix} 1 & 0 \end{bmatrix}$ $D = 0$
$F(\dot{q}) = F_c\tanh(\lambda\dot{q}) + F_v\dot{q}$	$\dot{x_1} = x_2$ $\dot{x_2} = \frac{1}{J}u - \frac{1}{J}(F_c\lambda + F_v)x_2$	$A = \begin{bmatrix} 0 & 1 \\ 0 & -\frac{1}{J}F_c\lambda - \frac{1}{J}F_v \end{bmatrix}$ $\mathrm{B} = \begin{bmatrix} 0 \\ \frac{1}{J} \end{bmatrix}$ $C = \begin{bmatrix} 1 & 0 \end{bmatrix}$ $D = 0$

REMARK 2.1

We note that the second row in Table 2.2 does not correspond to an exact linearization since the signum function $\mathrm{sgn}(\dot{q})$ is not differentiable at $\dot{q} = 0$. Here we basically omit the effect of Coulomb friction hence, in essence, we consider the system given by (2.1) without a Coulomb friction term in controller design. As a result, the linear models in the first 2 rows of Table 2.2 are exactly the same. For this reason,

we will consider only the linear systems given in last 2 rows in our controller designs. However, note that Coulomb friction is always used in our simulations.

The block diagram of state space representation of the linearized system is shown in figure 2.3:

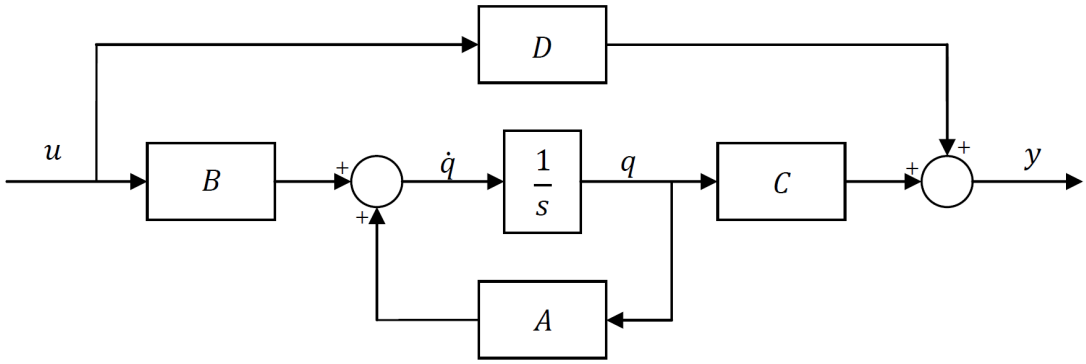

Figure 2.3: Block diagram representation of state space

The transfer function associated with the block diagram in Figure 2.3 is given as:

$$T(s) = C(sI - A)^{-1}B + D \tag{2.11}$$

Here, $T(s)$ is the transfer function of the linearized system. By using the friction model in (2.3) and related state space matrices A, B and C from Table 2.2, we obtain:

$$T(s) = \frac{\frac{I}{J}}{s^2 + \left(\frac{1}{J}F_c\lambda + \frac{1}{J}F_v\right)s}$$

2.2.2 Controllability and Observability

In state variable format, poles of the closed-loop system are the eigenvalues of the system. The ability to place the poles precisely at the desired locations, in order to meet the performance specifications, depends only on the controllability and observability of the system.

Before the design of feedback linearization controller, Controllability and Observability tests must be carried out to figure out if it is possible to construct a state vector, get a feedback from states and drive the state vector to its final state by assigning the system eigenvalues [5].

Controllability concerns with whether the system could be forced into a particular state by the design of an appropriate control input. The controllability of a system can be determined by the algebraic condition:

$$rank\begin{bmatrix} B & AB & A^2B & \dots & A^{n-1}B \end{bmatrix} = n \tag{2.12}$$

Here, A is a $n \times n$ matrix, B is a $n \times 1$ matrix, $P_C = \begin{bmatrix} B & AB & A^2B & \dots & A^{n-1} \end{bmatrix}$ is the $n \times n$ controllability matrix and n is the number of states.

Controllability Theorem states that if the determinant of P_C is nonzero; i.e P_C has full rank, the system is controllable [93].

Observability concerns with whether the state variables of a system could be determineqd in order to apply feedback linearization. The observability of a system can be determined by the algebraic condition:

$$rank \begin{bmatrix} C \\ CA \\ \vdots \\ CA^{n-1} \end{bmatrix} = n \tag{2.13}$$

Here, C is a $1 \times n$ row vector,$P_O = \begin{bmatrix} C \\ CA \\ \vdots \\ CA^{n-1} \end{bmatrix} = n$ is the $n \times n$ observability matrix and n is the number of states.

Observability Theorem states that if the determinant of P_O is nonzero; i.e P_O has full rank, the system is observable [93].

Substituting state space matrices found in Table 2.2 into (2.12) and (2.13), controllability and observability tests are carried out. By using the friction model in (2.3) and related state space matrices in Table 2.2, controllability and observability matrices of the linearized system can be calculated as:

$$P_C = \begin{bmatrix} B & AB \end{bmatrix} = \begin{bmatrix} 0 & \frac{1}{J} \\ \frac{1}{J} & -\frac{1}{J^2}F_v \end{bmatrix}$$

$$P_O = \begin{bmatrix} C \\ CA \end{bmatrix} = \begin{bmatrix} 1 & 0 \\ 0 & 1 \end{bmatrix}$$

Since P_C and P_O have full rank, system is controllable and observable. Therefore; state feedback and pole placement are possible.

2.2.3 Pole Placement

Eigenvalues of a system, which control the characteristics of the system response, correspond to location of the system poles. Pole placement provides a control, in which state variables are fed back to the system through a state-feedback gain matrix K, for placing the system poles to a desired location [94], Block diagram representation is seen in Figure 2.4 with the calculated state space after linearization:

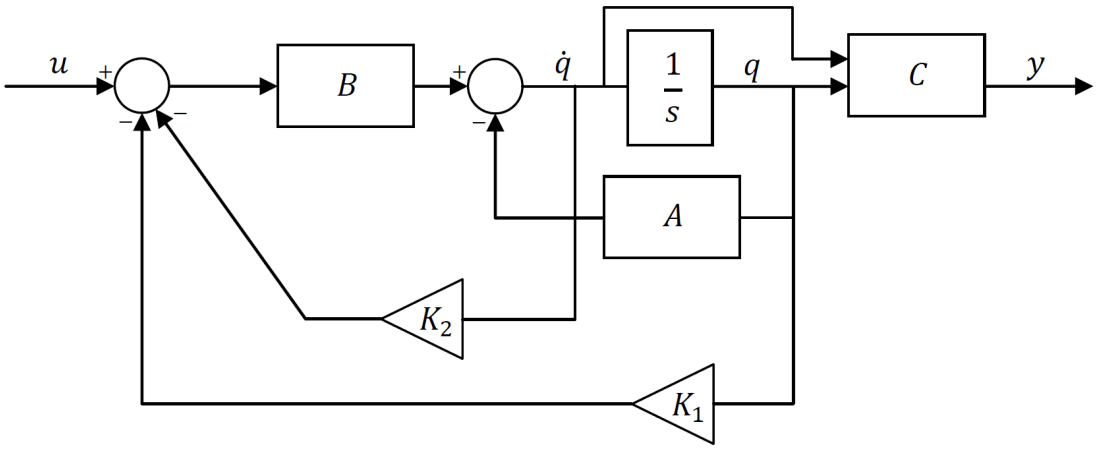

Figure 2.4: Block diagram representation of pole placement

The state space representation of the system after pole placement is:

$$\begin{bmatrix} \dot{x_1} \\ \dot{x_2} \end{bmatrix} = (A - BK) \begin{bmatrix} x_1 \\ x_2 \end{bmatrix} + Bu \tag{2.14}$$

$$y = C \begin{bmatrix} x_1 \\ x_2 \end{bmatrix}$$

Transfer function after pole placement, $T_{new(s)}$, is found by the use of equations

(2.11) and (2.14):

$$T_{new}(s) = C(sI - (A - BK))^{-1}B \tag{2.15}$$

By using the friction model in (2.3) and substituting related state space matrices A, B and C from Table 2.2 into (2.15), we obtain:

$$T_{new}(s) = \frac{\frac{1}{J}}{s^2 + s(\frac{1}{J}F_c\lambda + \frac{1}{J}F_v + \frac{1}{J}K_1) + \frac{1}{J}K_2} \tag{2.16}$$

Here, K is a 2×1 matrix, i.e. $K = \begin{bmatrix} K_1 \\ K_2 \end{bmatrix}$.

The state-feedback gain matrix is computed according to a specified transfer function, which is obtained by performance measures that are defined in terms of the step response such as settling time and overshoot or performance indices such as ITAE (Integral of the Time Multiplied by Absolute Error) [95]. The comparison between the actual output and reference step input is usually measured by the percent overshoot $P.O.$ and settling time T_s.

Throughout this thesis, we will treat settling time as the time required for the system to settle within a 2% of the unit step input. Therefore;

$$T_s = \frac{4}{\zeta\omega_n} \tag{2.17}$$

Here, ζ is the damping ratio and ω_n is the normalized frequency.

Maximum Overshoot for a step input is defined as the maximum amount of the output response, proceeding above the reference input. It is expressed by a percentage, called Percent Overshoot, as:

$$P.O. = 100e^{-\zeta\pi/\sqrt{1-\zeta^2}} \tag{2.18}$$

In addition to the step response properties, performance indices such as ITAE are used to reduce the tracking error by measuring and trying to minimize it over time range [96]. ITAE index is used to reduce the effect of initial error to the value of the performance integral and to stress errors occurring later in the response [97].

$$ITAE = \int_0^T t|e(t)|dt \tag{2.19}$$

As seen from equation (2.19), ITAE integrates an additional time multiplier and the absolute error over time. This results in heavy weighted errors existing after a long time, whereas light weighted errors at the start of the response. It provides the best selectivity than the other performance indices as it provides much more quick settled systems, but with lazy initial response [98].

The transfer function of a closed-loop second order system is:

$$\frac{Y(s)}{U(s)} = \frac{\omega_n^2}{s^2 + \zeta\omega_n s + \omega_n^2} \tag{2.20}$$

In order to obtain a specified function, percent overshoot and settling time is used to find the damping ratio and natural frequency as:

$$\zeta = \sqrt{\frac{ln(P.O.)^2}{ln(P.O.)^2 + \pi^2}} \tag{2.21}$$

$$\omega_n = -\frac{ln(P.O.\sqrt{1-\zeta^2})}{\zeta T_s} \tag{2.22}$$

Throughout the thesis, we choose $T_s = 0.01$ seconds and $P.O. = 5\%$, unless stated otherwise. Integrating these values in equations (2.21) and (2.22), damping ratio is calculated as $\zeta = 0.6901$ and natural frequency is calculated as $\omega_n = 480.95$. Substituting these values into equation (2.20), the specified transfer function is found as:

$$\frac{Y(s)}{U(s)} = \frac{2.313 \times 10^5}{s^2 + 663.8s + 2.313 \times 10^5} \tag{2.23}$$

Roots of characteristic equation give desired pole locations: $-331.91 \pm 348.07j$. In order to place the poles to the desired pole locations and obtain state-feedback gain matrix K, characteristic equation found in (2.16) must be equal to the characteristic equation found in (2.23). By equating the characteristic equations, we can solve for K:

$$\begin{aligned} \frac{1}{J}F_c\lambda + \frac{1}{J}F_v + \frac{1}{J}K_1 &= 663.8 \\ \frac{1}{J}K_2 &= 2.313 \times 10^5 \end{aligned}$$

State-feedback gain matrix K changes with the friction model. Table 2.3 shows the friction models and the equations used to solve for K:

Table 2.3: Pole placement design for friction models based on settling time and overshoot

Friction Force	State Space Matrix	Pole Placement Design
$F(\dot{q}) = F_v\dot{q}$	$A = \begin{bmatrix} 0 & 1 \\ 0 & -\frac{1}{J}F_v \end{bmatrix}$ $\mathrm{B} = \begin{bmatrix} 0 \\ \frac{1}{J} \end{bmatrix}$ $C = \begin{bmatrix} 1 & 0 \end{bmatrix}$	$\frac{1}{J}F_v + \frac{1}{J}K_1 = 663.8$ $\frac{1}{J}K_2 = 2.313 \times 10^5$
$F(\dot{q}) = F_c\mathrm{sgn}(\dot{q}) + F_v\dot{q}$	$A = \begin{bmatrix} 0 & 1 \\ 0 & -\frac{1}{J}F_v \end{bmatrix}$ $\mathrm{B} = \begin{bmatrix} 0 \\ \frac{1}{J} \end{bmatrix}$ $C = \begin{bmatrix} 1 & 0 \end{bmatrix}$	$\frac{1}{J}F_v + \frac{1}{J}K_1 = 663.8$ $\frac{1}{J}K_2 = 2.313 \times 10^5$
$F(\dot{q}) = F_c\tanh(\lambda\dot{q}) + F_v\dot{q}$	$A = \begin{bmatrix} 0 & 1 \\ 0 & -\frac{1}{J}F_c\lambda - \frac{1}{J}F_v \end{bmatrix}$ $\mathrm{B} = \begin{bmatrix} 0 \\ \frac{1}{J} \end{bmatrix}$ $C = \begin{bmatrix} 1 & 0 \end{bmatrix}$	$\frac{1}{J}F_c\lambda + \frac{1}{J}F_v + \frac{1}{J}K_1 = 663.8$ $\frac{1}{J}K_2 = 2.313 \times 10^5$

REMARK 2.2

Note that as stated in Remark 2.1, the calculations given in first two rows of Table 2.3 are exactly the same. Hence as a result, we will consider only the calculations given in the last two rows of Table 2.3.

Pole placement design based on ITAE criterion for a Step Input uses a table of optimum coefficients of a transfer function that minimizes the ITAE performance and the step response of a normalized transfer function using these optimum coefficients [93]. According to the table in [93], the characteristic equation for a second order

system is:

$$\Delta(s) = s^2 + 1.4w_n s + w_n^2 \tag{2.24}$$

In addition to this, examining the step response of a normalized transfer function for $n = 2$, the settling time is estimated to be approximately 8 seconds in normalized time:

$$w_n T_s = 8$$

As $T_s = 0.01$, w_n is found to be 800 rad/s. From equation (2.17), $\zeta = 0.5$. Substituting w_n into (2.24), the characteristic equation is obtained. The same process is carried out by equating the characteristic equations in (2.16) and (2.24), to solve for K.

The transfer function of the closed loop system after pole placement is obtained as:

$$\frac{Y(s)}{U(s)} = \frac{\frac{1}{J}}{s^2 + 2\zeta\omega_n s + \omega_n^2} \tag{2.25}$$

2.2.4 Integral Controller and Root Locus Control Design

An integral controller, combined with a unit feedback from the output, is added as a feedforward controller in the velocity loop to the system after pole placement. The aim of the feedback path is to form the error whereas integrator is added in order to reduce the error and increase system type [94]. Figure 2.5 depicts the block diagram of the closed loop system, from velocity command input to output.

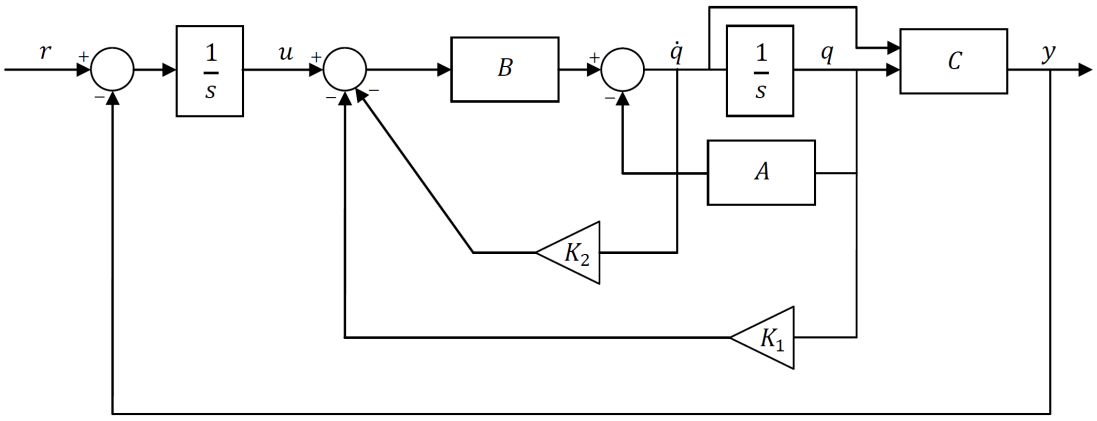

Figure 2.5: Block diagram of added integral controller and feedback path

In order to examine how the roots of the system change with the variation of a gain, P, root locus analysis is carried out. The value of P is determined so that step response should not have any overshoot, by observing how the poles of the closed loop transfer function of the overall system are located as a function of P. The block diagram of root locus method is given in Figure 2.6:

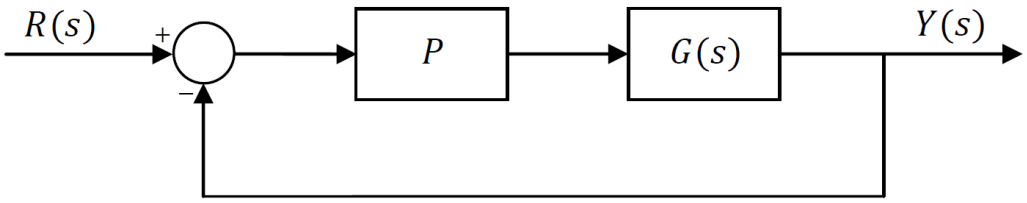

Figure 2.6: Block diagram of the closed loop system with P controller

In Figure 2.6, $G(s)$ represents the plant from velocity command input to output depicted in Figure 2.5. The block diagram of the overall control design discussed so

far is given in Figure 2.7:

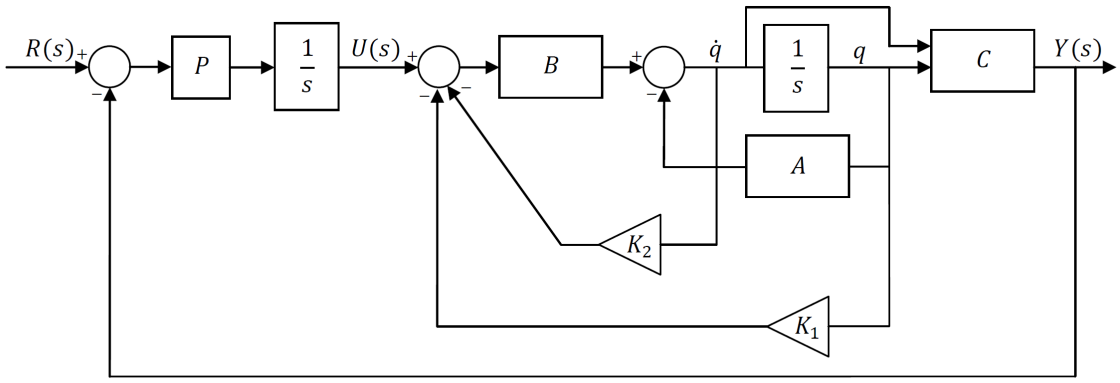

Figure 2.7: Block diagram of the overall closed loop system

The transfer function of the overall closed loop system is obtained as:

$$T_f(s)\frac{P\frac{1}{J}}{s^2 + 2\zeta\omega_n s^2 + \omega_n^2 s + P\frac{1}{J}} \tag{2.26}$$

2.2.5 Application of Diophantine Equations

The Diophantine Control methodology is a transfer function based control scheme, providing a simple parameterization of all controllers that stabilize a given plant in terms of a factorized transfer function [99].

The transfer function of the linearized and stabilized nonlinear plant structure, given in Figure 2.1, is obtained in (2.26). The design procedure of the deadbeat controller operates on this transfer function as depicted in figure 2.8:

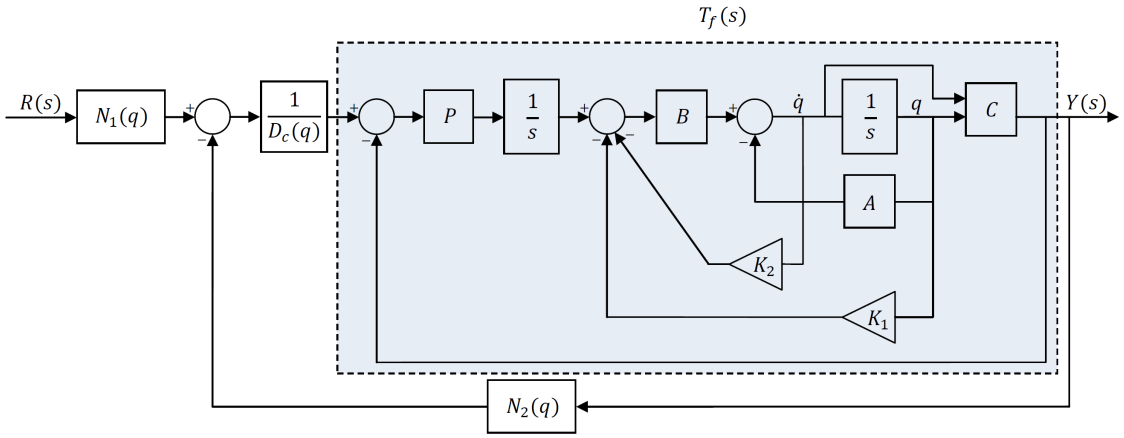

Figure 2.8: Block diagram of the deadbeat controller

Discrete time model of (2.26) is obtained with a sampling period of T:

$$P(q) = \left\{ \frac{1 - e^{-sT}}{s} T_f(s) \right\} \Bigg|_{q=z^{-1}} \tag{2.27}$$

The discretized transfer function can be factorized as:

$$P(q) = \frac{N_p(q)}{D_p(q)} \tag{2.28}$$

Here, N_p is the numerator and D_p is the denominator of the plant in Q-domain.

The reference input $R(s)$ is also discretized and factorized as:

$$R(q) = \left\{ \frac{1 - e^{-sT}}{s} \right\} \Bigg|_{q=z^{-1}} = \frac{N_r(q)}{D_r(q)} \tag{2.29}$$

The design is based on finding the controller polynomials N_1, N_2 and D_c by the solution of two independent Diophantine equations constructed for the transfer function in (2.28) and the given arbitrary reference input in (2.29) [5]:

$$N_p(q)N_1(q) + D_r(q)Q_1(q) = 1 \tag{2.30}$$

$$N_p(q)N_2(q) + D_p(q)D_c(q) = 1 \tag{2.31}$$

Note that, $N_p(q)$ and $D_r(q)$ must be co-prime in discrete-time to ensure that there is no pole zero cancellation [5].

Let us define:

$$N_p(q) = N_p(4)q^3 + N_p(3)q^2 + N_p(2)q + N_p(1) \tag{2.32}$$

$$D_p(q) = D_p(4)q^3 + D_p(3)q^2 + D_p(2)q + D_p(1)$$

$$N_r(q) = N_r(3)q^2 + N_r(2)q + N_r(1)$$

$$D_r(q) = D_r(3)q^2 + D_r(2)q + D_r(1)$$

Minimum order of N_1 and Q_1 is one less than the maximum of orders of $N_p(q)$ and $D_r(q)$: $\max(\text{order}(N_p(q))|\text{order}(D_r(q))) - 1 = 2$.

Minimum order of N_2 and D_c is one less than the maximum of orders of $N_p(q)$ and $D_p(q)$: $\max(\text{order}(N_p(q))|\text{order}(D_p(q))) - 1 = 2$.

Let:

$$N_1(q) = aq^2 + bq + c \tag{2.33}$$

$$Q_1(q) = dq^2 + eq + f$$

$$N_2(q) = gq^2 + hq + i$$

$$D_c(q) = jq^2 + kq + l$$

where $a, b, c, d, e, f, g, h, i, j, k$ and l are unknowns.

Substituting (2.32) and (2.33) into (2.30) and (2.31), we can solve for the unknowns:

$$\begin{bmatrix} a \\ b \\ c \\ d \\ e \\ f \\ g \\ h \\ i \\ j \\ k \\ l \end{bmatrix} = \begin{bmatrix} N_p(4) & 0 & 0 & 0 & 0 & 0 & 0 & 0 & 0 & 0 & 0 & 0 \\ N_p(3) & N_p(4) & 0 & D_r(3) & 0 & 0 & 0 & 0 & 0 & 0 & 0 & 0 \\ N_p(2) & N_p(3) & N_p(4) & D_r(2) & D_r(3) & 0 & 0 & 0 & 0 & 0 & 0 & 0 \\ N_p(1) & N_p(2) & N_p(3) & D_r(1) & D_r(2) & D_r(3) & 0 & 0 & 0 & 0 & 0 & 0 \\ 0 & N_p(1) & N_p(2) & 0 & D_r(1) & D_r(2) & 0 & 0 & 0 & 0 & 0 & 0 \\ 0 & 0 & N_p(1) & 0 & 0 & D_r(1) & 0 & 0 & 0 & 0 & 0 & 0 \\ 0 & 0 & 0 & 0 & 0 & 0 & N_p(4) & 0 & 0 & D_p(4) & 0 & 0 \\ 0 & 0 & 0 & 0 & 0 & 0 & N_p(3) & N_p(4) & 0 & D_p(3) & D_p(4) & 0 \\ 0 & 0 & 0 & 0 & 0 & 0 & N_p(2) & N_p(3) & N_p(4) & D_p(2) & D_p(3) & D_p(4) \\ 0 & 0 & 0 & 0 & 0 & 0 & N_p(1) & N_p(2) & N_p(3) & D_p(1) & D_p(2) & D_p(3) \\ 0 & 0 & 0 & 0 & 0 & 0 & 0 & N_p(1) & N_p(2) & 0 & D_p(1) & D_p(2) \\ 0 & 0 & 0 & 0 & 0 & 0 & 0 & 0 & N_p(1) & 0 & 0 & D_p(1) \end{bmatrix}^{-1} \begin{bmatrix} 0 \\ 0 \\ 0 \\ 0 \\ 0 \\ 1 \\ 0 \\ 0 \\ 0 \\ 0 \\ 0 \\ 1 \end{bmatrix} \tag{2.34}$$

Thus, controller polynomials N_1, N_2 and D_c are obtained by the solution of (2.34).

2.3 Deadbeat Controller Based Velocity Control

In this section, the design methodology given in section 2.2 is applied for velocity control.

In order to obtain state space representation of the system, let us define variable

transformation:

$$x_1 = \dot{q} \tag{2.35}$$

Substituting (2.35) into equation 2.1, we obtain:

$$\dot{x_1} = -\frac{1}{J}F(x_1) + \frac{1}{J}u \tag{2.36}$$

Equation (2.36) is a first order state equation in the form:

$$\dot{x_1} = f_1(x_1) + \frac{1}{J}u \tag{2.37}$$

Here, $f_1(x_1) = -\frac{1}{J}F(x_1)$.

Using the state variable expression in (2.37), linearization around equilibrium point is given by [4]:

$$\dot{x_1} = \left.\frac{\partial f_1}{\partial x_1}\right|_{x_1=x_{10}} x_1 \tag{2.38}$$

Equations (2.9) and (2.10) could be put into the following matrix form:

$$\dot{x_1} = Ax_1 + Bu$$
$$y = Cx_1 + Du$$

Where $A = \left.\frac{\partial f_1}{\partial x_1}\right|_{x_1=0}$, $B = \frac{1}{J}$, $C = 1$, $D = 0$.

By using the friction model in (2.3) and related equation of motion in Table 1.1, state space representation of the linearized system can be derived as:

$$\dot{x}_1 = \frac{1}{J}u - \frac{1}{J}(F_v)x_1$$

Where we use the fact that $\frac{d}{dx_1}(\tanh(\lambda x_1))\big| = \lambda$.

Each friction model yields a different linear approximation. Table 2.4 shows the friction models and the resultant state space representation of linearized system:

Table 2.4: State Space Matrices for Friction Models

Friction Force	State Space Representation	State Space Matrix
$F(\dot{q}) = F_v\dot{q}$	$\dot{x}_1 = \frac{1}{J}u - \frac{1}{J}(F_v)x_1$	$A = -\frac{1}{J}F_v$ $B = \frac{1}{J}$ $C = 1$ $D = 0$
$F(\dot{q}) = F_c\text{sgn}(\dot{q}) + F_v\dot{q}$	$\dot{x}_1 = \frac{1}{J}u - \frac{1}{J}(F_v)x_1$	$A = -\frac{1}{J}F_v$ $B = \frac{1}{J}$ $C = 1$ $D = 0$
$F(\dot{q}) = F_c\tanh(\lambda\dot{q}) + F_v\dot{q}$	$\dot{x}_1 = \frac{1}{J}u - \frac{1}{J}(F_v\lambda + F_v)x_1$	$A = -\frac{1}{J}F_c\lambda - \frac{1}{J}F_v$ $B = \frac{1}{J}$ $C = 1$ $D = 0$

See Remark 2.1

By using the friction model in (2.3) and related state space matrices A, B and C from Table 2.4, we obtain:

$$T(s) = \frac{\frac{1}{J}}{s + (\frac{1}{J}F_c\lambda) + \frac{1}{J}F_v}$$

Substituting state space matrices found in Table 2.4 into (2.12) and (2.13), controllability and observability tests are carried out. By using the friction model in (2.3) and related state space matrices in Table 2.4, controllability and observability matrices of the linearized system can be calculated as:

$$P_C = \Big[B\Big] = \Big[\tfrac{1}{J}\Big]$$
$$P_O = \Big[C\Big] = \Big[1\Big]$$

Since P_C and P_O have full rank, system is controllable and observable. Therefore; state feedback and pole placement are possible.

By using the friction model in (2.3) and substituting related state space matrices A, B and C from Table 2.4 into (2.15), we obtain:

$$T_{new}(s) = \frac{\frac{1}{J}}{s + (\frac{1}{J}F_c\lambda + \frac{1}{J}F_v + \frac{1}{J}K)} \tag{2.39}$$

Here, K is a 1×1 matrix.

The transfer function of the closed loop system after pole placement is obtained as:

$$\frac{Y(s)}{U(s)} = \frac{\frac{1}{J}}{s + \omega_n} \tag{2.40}$$

The transfer function of the overall closed loop system after addition of the integral controller and root locus design is obtained as:

$$T_f(s) = \frac{P\frac{1}{J}}{s^2 + \omega_n s + P\frac{1}{J}} \tag{2.41}$$

By substituting (2.41) into equation (2.27), the transfer function is discretized and factorized as in (2.28). The reference input $R(s)$ is also discretized and factorized as in (2.29):

Let us define:

$$N_p(q) = N_p(3)q^2 + N_p(2)q + N_p(1) \tag{2.42}$$

$$D_p(q) = D_p(3)q^2 + D_p(2)q + D_p(1)$$

$$N_r(q) = N_r(3)q^2 + N_r(2)q + N_r(1)$$

$$D_r(q) = D_r(3)q^2 + D_r(2)q + D_r(1)$$

Minimum order of N_1 and Q_1 is one less than the maximum of orders of $N_p(q)$ and $D_r(q)$: $\max(\text{order}(N_p(q))|\text{order}(D_r(q))) - 1 = 1$.

Minimum order of N_2 and D_c is one less than the maximum of orders of $N_p(q)$ and $D_p(q)$: $\max(\text{order}(N_p(q))|\text{order}(D_p(q))) - 1 = 1$.

Let:

$$N_1(q) = aq + b \tag{2.43}$$

$$Q_1(q) = cq + d$$

$$N_2(q) = eq + f$$

$$D_c(q) = gq + h$$

Where a, b, c, d, e, f, g and h are unknowns.

Substituting (2.42) and (2.43) into (2.30) and (2.31), we can solve for the unknowns:

$$\begin{bmatrix} a \\ b \\ c \\ d \\ e \\ f \\ g \\ h \end{bmatrix} = \begin{bmatrix} N_p(3) & 0 & D_r(3) & 0 & 0 & 0 & 0 & 0 \\ N_p(2) & N_p(3) & D_r(2) & D_r(3) & 0 & 0 & 0 & 0 \\ N_p(1) & N_p(2) & D_r(1) & D_r(2) & 0 & 0 & 0 & 0 \\ 0 & N_p(1) & 0 & D_p(1) & 0 & 0 & 0 & 0 \\ 0 & 0 & 0 & 0 & N_p(3) & 0 & D_p(3) & 0 \\ 0 & 0 & 0 & 0 & N_p(2) & N_p(3) & D_p(2) & D_p(3) \\ 0 & 0 & 0 & 0 & N_p(1) & N_p(2) & D_p(1) & D_p(2) \\ 0 & 0 & 0 & 0 & 0 & N_p(1) & 0 & D_p(1) \end{bmatrix}^{-1} \begin{bmatrix} 0 \\ 0 \\ 0 \\ 1 \\ 0 \\ 0 \\ 0 \\ 1 \end{bmatrix} \tag{2.44}$$

Thus, controller polynomials N_1, N_2 and D_c are obtained by the solution of (2.44).

Chapter 3

Simulations and Results

In this section, system performance of the hierarchical feedback system structure, by the applications of pole placement and deadbeat methodologies is analyzed. Simulations are made using simple plant model in Equation (2.1), with the friction models in Table 2.1. For our simulations, let us choose the values given below:

$$\begin{aligned} J &= \quad 0.0023 Nm^2 \\ F_c &= \quad 0.28 Nm \\ F_v &= 0.0176 Nms/rad \end{aligned} \tag{3.1}$$

The performance is criticized in terms of reference input tracking and disturbance rejection. For both velocity and position control, step and sinusoidal input tracking with and without disturbance cases are analyzed.

We note that during the design process, Coulomb friction is either omitted or approximated by $\tanh(\lambda\dot{q})$ function, whereas in all our simulations, we

use Coulomb+Viscous friction model based on $sgn(\dot{q})$ function. Since we apply pole placement and deadbeat controller design methodologies, for each reference/disturbance input, we consider the following cases:

- **Case 1** - Coulomb friction is omitted and the design is based on pole placement
- **Case 2** - Coulomb friction is approximated by $tanh(\lambda\dot{q})$ function and the design is based on pole placement
- **Case 3** - Coulomb friction is omitted and the design is based on pole placement + deadbeat Controller
- **Case 4** - Coulomb friction is approximated by $tanh(\lambda\dot{q})$ function and the design is based on pole placement + deadbeat Controller

As for the reference input to be tracked, we choose a step input $r(t) = u(t)$ and a sinusoidal signal $r(t) = Asin(wt)$, where we choose $A = 3$ and $w = 2$ rad/sec for simplicity. The reference input is discretized and factorized as in (2.29). Throughout the thesis, sampling time is taken as 0.01 seconds. Table 3.1 shows the reference inputs and related transforms in s-domain and q-domain:

Table 3.1: Laplace and Q Transforms for Reference Inputs

Reference Input	Laplace Transform	Q Transform
$r(t) = u(t)$	$R(s) = \frac{1}{s}$	$R(q) = \frac{1}{1-q}$
$r(t) = 3\sin(2t)$	$R(s) = \frac{6}{s^2+4}$	$R(q) = \frac{0.0003q^2+0.0003q}{q^2-2q+1}$

3.1 Pole Placement Based Velocity Control: Step Input without disturbance

After linearization around operating point, pole of the first order system is placed based on settling time and ITAE index. The characteristic equation of a first order system with optimum coefficients based on ITAE index is $\Delta(s) = s+w_n$. As $T_s = 0.01$ seconds, w_n is chosen to be 400 rad/s. The transfer function of the closed loop system using (2.40) is obtained as:

$$T(s) = \frac{434.8}{s + 400} \tag{3.2}$$

With the addition of an integral controller, root locus analysis is carried out. By using SISO Design Tool in MATLAB, the value of P is determined from the Root Locus Diagram. Note that by the addition of the integral controller, poles of the closed loop system are moved towards right in the complex plane. Therefore; settling time criterion might no longer be satisfied with the addition of a new pole at $s = 0$.

Figure 3.1 depicts the root locus diagram of the system. The design requirements are indicated in terms of percent overshoot and settling time, i.e $P.O. = 5\%$ and minimum settling time that could be achieved after design is 0.03 seconds. In addition, the locations of the new poles are also shown in the diagram. The value of P, satisfying the percent overshoot and minimum settling time criteria, is found to be 50.975.

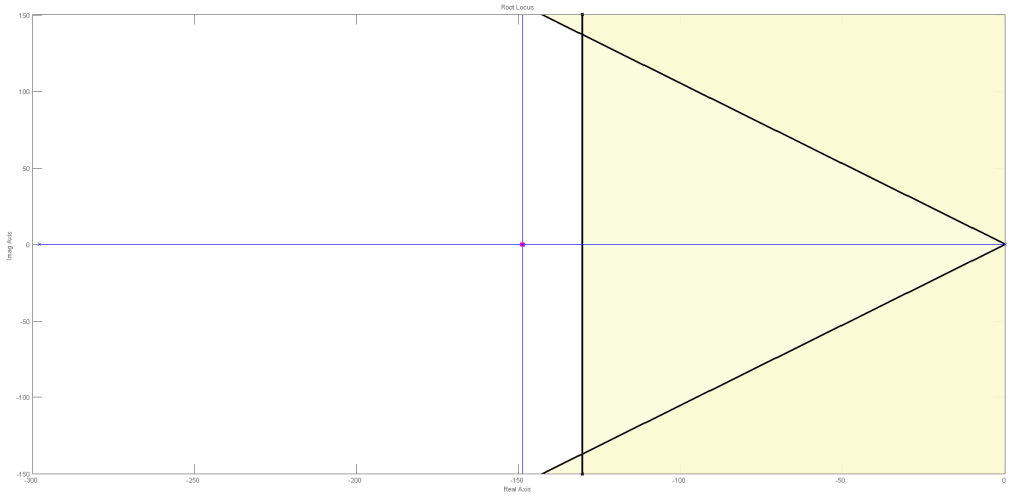

Figure 3.1: Root Locus Diagram for Pole Placement Based Velocity Control

The transfer function of the overall system, after Root Locus Design, is obtained by the equation (2.45). This transfer function changes according to the friction models used. It should be noted that, when designing a controller based on the friction model in (2.3), the value of λ has also an effect on the transfer function.

We note that for higher λ values, $\tanh(\lambda\dot{q})$ function approximates $sgn(\dot{q})$ with better accuracy [92]. However, as can be seen from Figure 3.2, for some smaller λ values we obtain better tracking performance for unit step input. Same behavior is also observed for the tracking of other inputs as well. For this reason, we choose $\lambda = 2$ throughout our simulations.

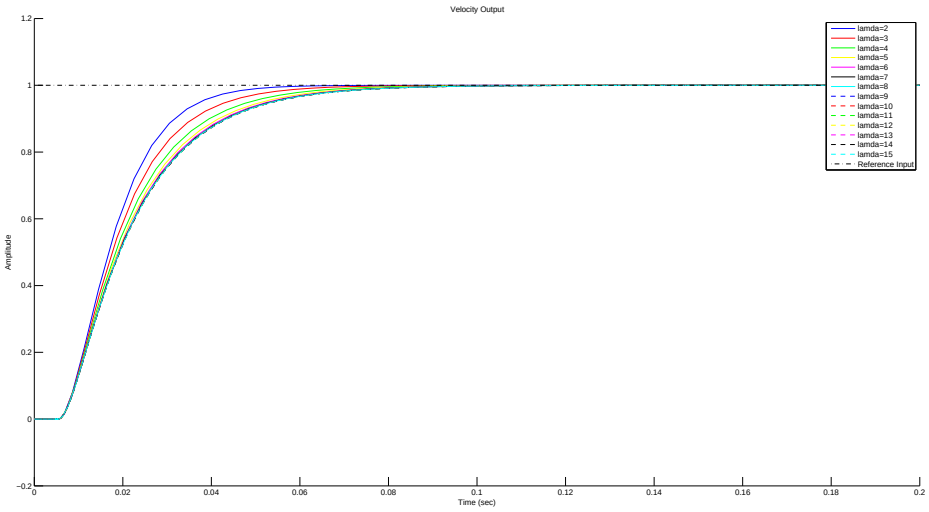

Figure 3.2: Unit Step Response of the closed loop system for different λ values

Unit Step Responses and corresponding errors for pole placement based control designs are shown in Figure 3.3 and Figure 3.4 respectively. Settling time is slightly decreased when Coulomb friction is approximated by $tanh(\lambda\dot{q})$ (Case 2). The reason for this situation is that the friction model in which Coulomb friction is approximated by $\tanh(\lambda\dot{q})$, captures the Coulomb force component and properties of friction at low velocities better.

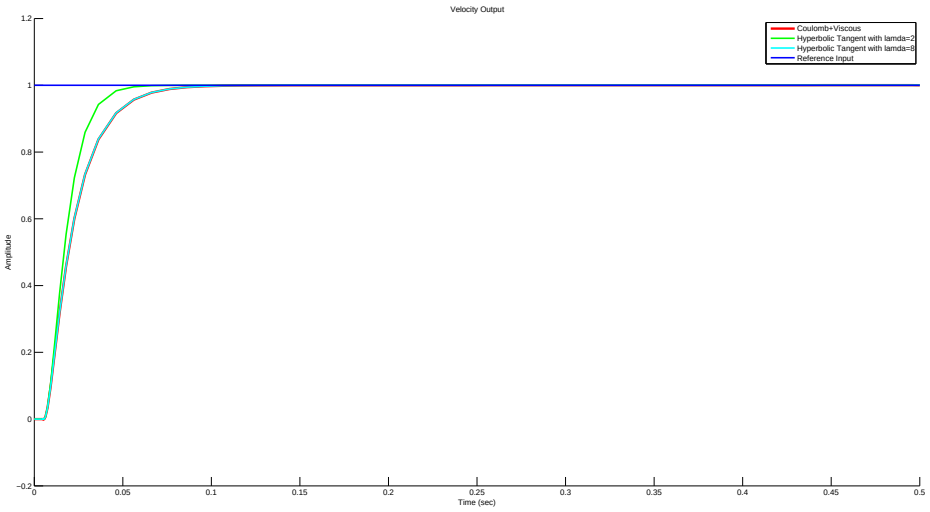

Figure 3.3: Unit Step Response of Velocity Control without disturbance based on Pole Placement Methodology

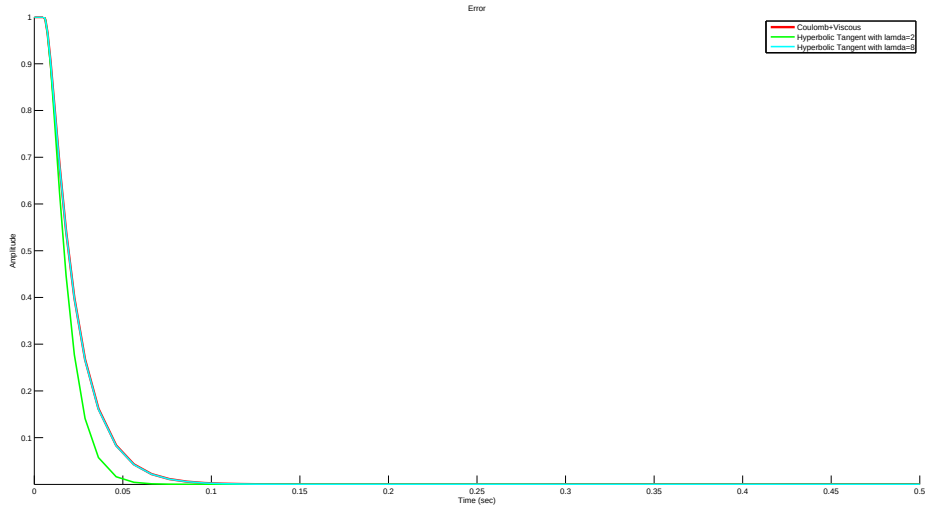

Figure 3.4: Error Signal of Velocity Control for a unit step without disturbance based on Pole Placement Methodology

3.2 Deadbeat Controller Based Velocity Control: Step input without disturbance

The deadbeat controller is added to the overall system designed in Section 3.1 as shown in Figure 2.8. The transfer function of the closed loop system, before applying the deadbeat controller is obtained using (2.41):

$$T_f(s) = \frac{221.6 \times 10^2}{s^2 + 400s + 221.6 \times 10^2}$$

By choosing the related reference input from Table 3.1 and the discretized transfer function $P(q)$ obtained using (2.27), Diophantine Equations are constructed:

$$\begin{aligned} (0.1019q^2 + 0.3663q)(aq + b) + (1 - q)(cq + d) &= 1 \\ (0.1019q^2 + 0.3663q)(eq + f) + (0.01832q^2 - 0.5502q)(gq + h) &= 1 \end{aligned} \tag{3.3}$$

Thus, controller polynomials N_1, N_2 and D_c are obtained by the solution of (2.44). These controllers are utilized to the overall system as seen in Figure 2.8.

Figure 3.5 and Figure 3.6 show Unit Step Responses and corresponding errors for deadbeat controller based designs, respectively. It might seem that deadbeat controller does not have an acceptable superiority compared to pole placement Methodology. However, as it can be observed from Figure 3.6, steady-state error is zero without any distortion and smoother compared to Figure 3.4.

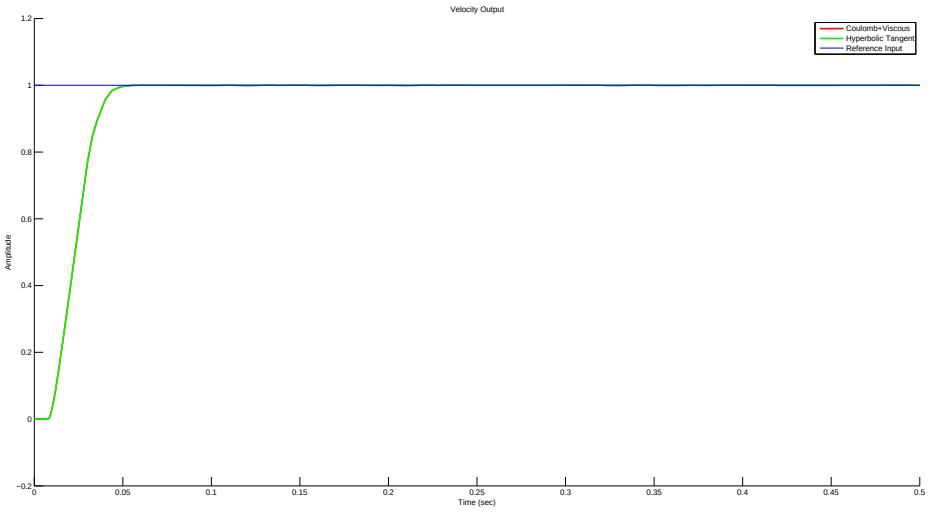

Figure 3.5: Unit Step Response of Velocity Control without disturbance based on Deadbeat Controller

With the design based on pole placement, in which Coulomb friction is approximated by $\tanh(\lambda\dot{q})$ function (Case 1), settling time is found to be approximately 0.060 seconds, whereas with the design based on Pole Placement + deadbeat controller (Case 3), it is reduced to approximately 0.035 seconds. We conclude that, deadbeat controller provides shorter settling time.

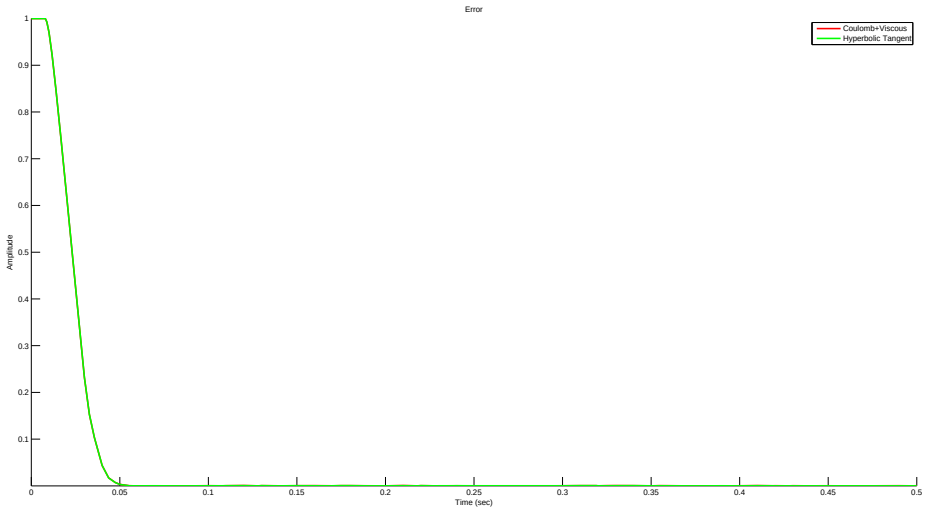

Figure 3.6: Error Signal of Velocity Control for a unit step without disturbance based on Deadbeat Controller

3.3 Pole Placement Based Velocity Control: Sinusoidal input without disturbance

The overall control system designed in Section 3.1 is also used for the tracking of the sinusoidal input, as pole placement method does not require any additional design step for hierarchical closed loop feedback structure and does not depend on the reference input to be tracked. Sinusoidal Responses and corresponding errors for pole placement based control designs are shown in Figure 3.7 and Figure 3.8 respectively.

In Figure 3.7, velocity output is observed to be tracking the reference input, with a delay of approximately 0.02 seconds, which results in an apparent steady-state error in Figure 3.8, similar for both friction models (Case 1 and Case 2). Furthermore,

there occurs a large tracking error especially around low velocities and when the direction of velocity changes. Therefore, the system needs extra time to track the reference input in a new direction. This might be caused by the integrator, which becomes insufficient when needed the most at velocity reversals to overcome stiction [10].

Integral control is almost always introduced to a mechanical system in forward path in order to minimize the steady-state errors [19], as in Section 3.1 for a unit step input. However, it is observed to be less effective for the sinusoidal input, in which repetitive velocity reversals occur in the reference input, compared to the unit step input. This situation is called "integral windup" and can be prevented by either resetting the integrator when the direction of velocity changes or limiting the accumulation of the integrator by setting upper and lower bounds [100]. In addition to this, a different control strategy based on sinusoidal reference tracking could have been adapted instead of an integral control.

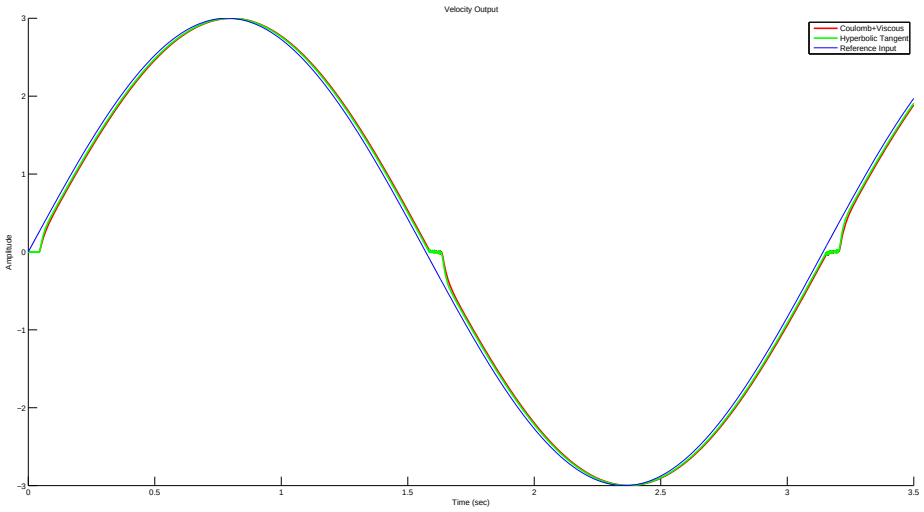

Figure 3.7: Sinusoidal Response of Velocity Control without disturbance based on Pole Placement Methodology

As it is clearly observed from Figure 3.8, the case of approximation of Coulomb friction by $tanh(\lambda\dot{q})$ (Case 2) yields a better response to sinusoidal input, compared to the case in which Coulomb friction is omitted (Case 1). Moreover, the system needs less time to track the reference input in a new direction after direction reversals, in Case 2. This situation may be caused by modeling errors of the Coulomb+Viscous friction at low velocities in MATLAB. Therefore; approximation of Coulomb friction by $\tanh(\lambda\dot{q})$ represents the original friction model much more realistically. This is because this model takes Coulomb force into account for control design.

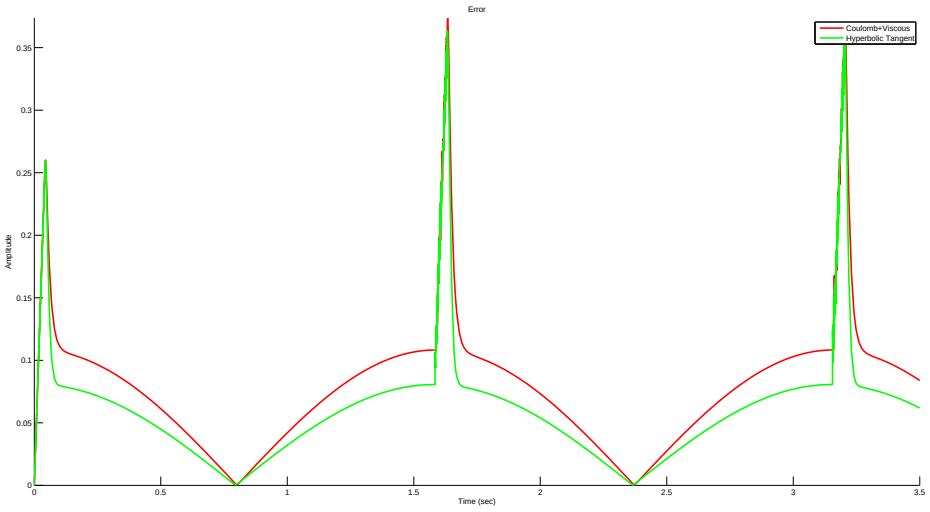

Figure 3.8: Error Signal of Velocity Control for a sinusoid without disturbance based on Pole Placement Methodology

3.4 Deadbeat Controller Based Velocity Control: Sinusoidal input without disturbance

The deadbeat controller is added to the overall system designed in Section 3.3 as shown in Figure 2.8. The transfer function of the closed loop system, before applying the deadbeat controller is obtained using (2.41). By choosing the related reference input from Table 3.1 and the discretized transfer function $P(q)$ obtained using (2.27), Diophantine Equations are constructed:

$$\begin{aligned}(0.1019q^2 + 0.3663q)(aq + b) + (0.0003q^2 + 0.0003q)(cq + d) = 1\\ (0.1019q^2 + 0.3663q)(eq + f) + (0.01832q^2 - 0.5502q)(gq + h) = 1\end{aligned} \tag{3.4}$$

Thus, controller polynomials N_1, N_2 and D_c are obtained by the solution of (2.44). These controllers are utilized to the overall system as seen in Figure 2.8.

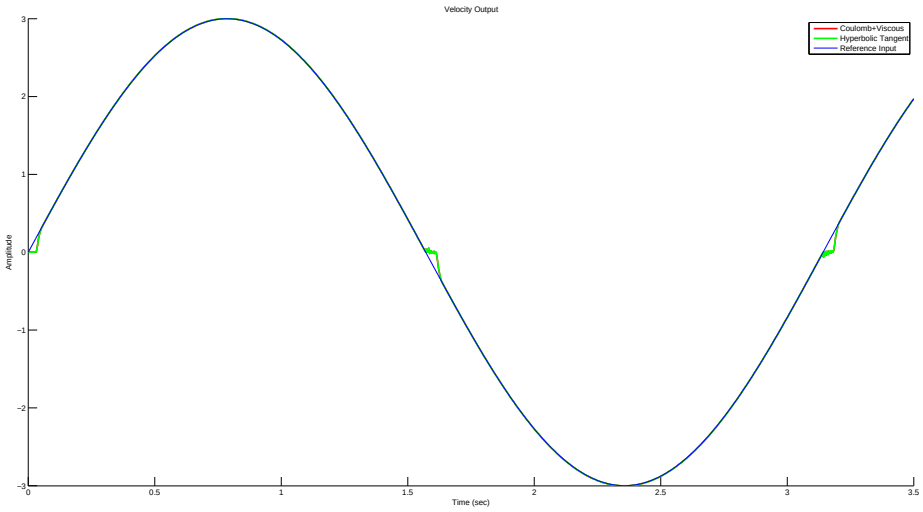

Figure 3.9: Sinusoidal Response of Velocity Control without disturbance based on Deadbeat Controller

In Figure 3.9, velocity output is observed to be following the reference input, without any delay and with zero steady-state error, except near-zero velocities and velocity reversals, similar for both friction models (Case 1 and Case 2).

In Figure 3.10, peaks are observed similar to the ones in Figure 3.8. However, deadbeat controller is apparently more successful in compensating for friction throughout the overall design, as errors occur only when the direction of velocity changes. This might also be caused by the integrator, which becomes insufficient to compensate for Coulomb friction.

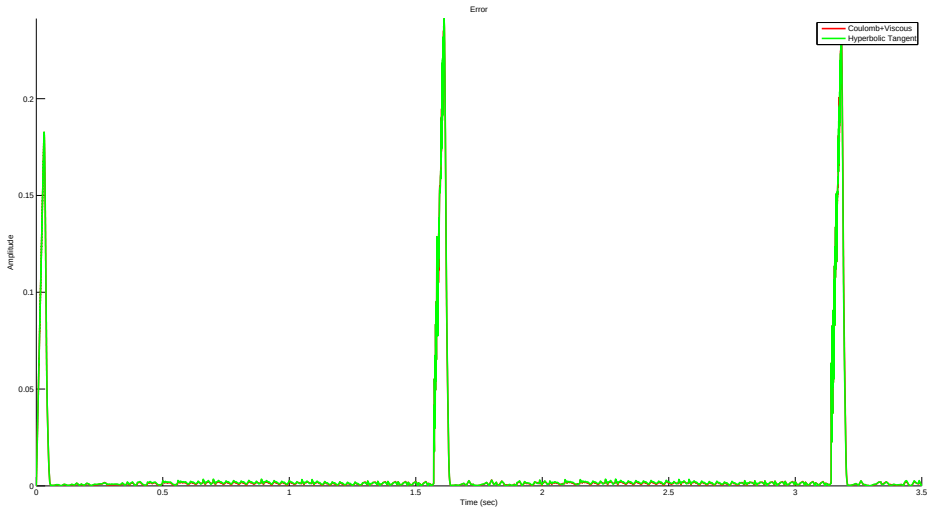

Figure 3.10: Error Signal of Velocity Control for a sinusoid without disturbance based on Deadbeat Controller

3.5 Pole Placement Based Velocity Control: Step input with disturbance

The overall control system designed in Section 3.1 is also used for disturbance rejection. The disturbance input is added to the overall system designed in Section 3.1, as shown in Figure 1.1. For the disturbance input, we apply a step input $d(t) = u(t)$ and a sinusoidal signal $d(t) = Asin(2\pi ft)$, where we choose $A = 0.5$ and $f = 0.5$ rad/sec for simplicity.

3.5.1 Step Disturbance

Unit Step Responses and corresponding errors for pole placement based control designs, for a Unit Step Disturbance, are shown in Figure 3.11 and Figure 3.12 respectively.

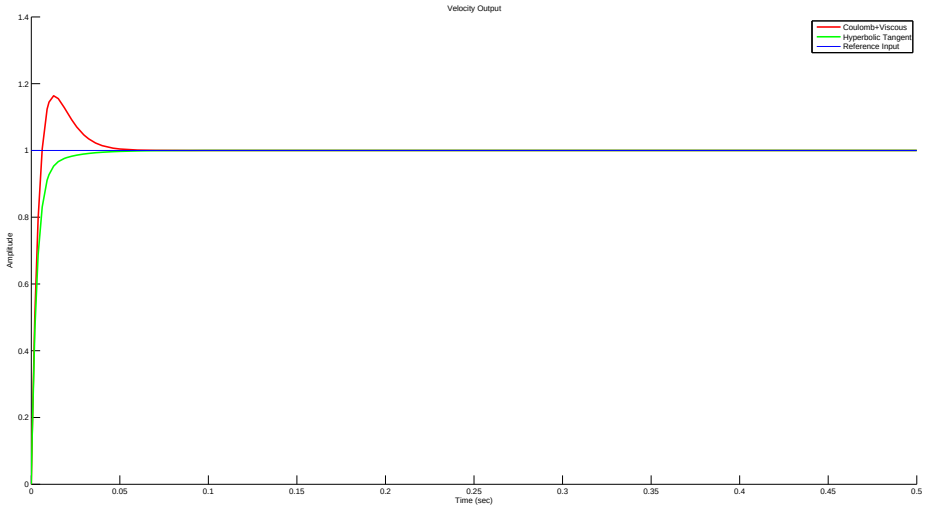

Figure 3.11: Unit Step Response of Velocity Control with unit step disturbance based on Pole Placement Methodology

From Figure 3.11, velocity output is observed to be tracking the reference input, both for Case 1 and 2. However, disturbance leads to an increase of approximately 0.02 seconds in terms of settling time also for both cases. In addition, as it is previously observed in Section 3.1, settling time is also slightly decreased when Coulomb friction is approximated by $\tanh(\lambda\dot{q})$ (Case 2).

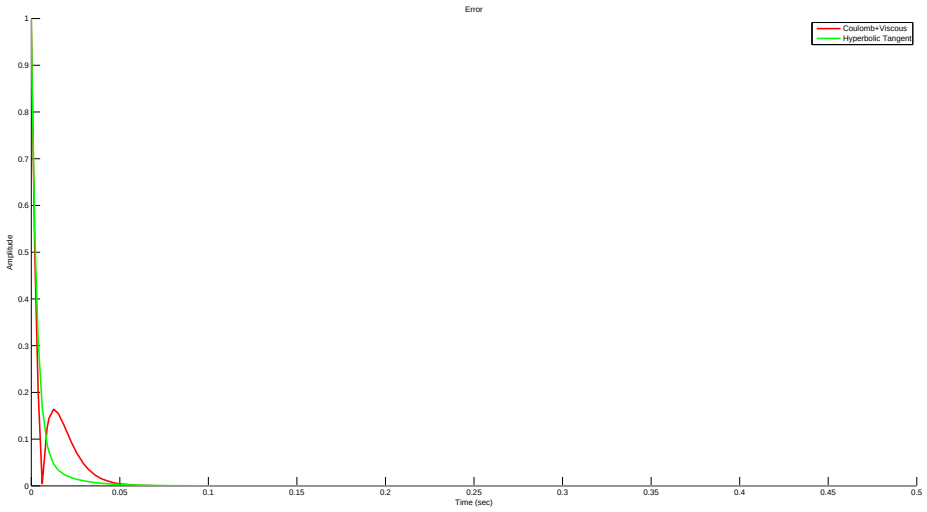

Figure 3.12: Error Signal of Velocity Control for a unit step with unit step disturbance based on Pole Placement Methodology

3.5.2 Sinusoidal Disturbance

Unit Step Responses and corresponding errors for pole placement based control designs, for a Sinusoidal Disturbance, are shown in Figure 3.13 and Figure 3.14 respectively.

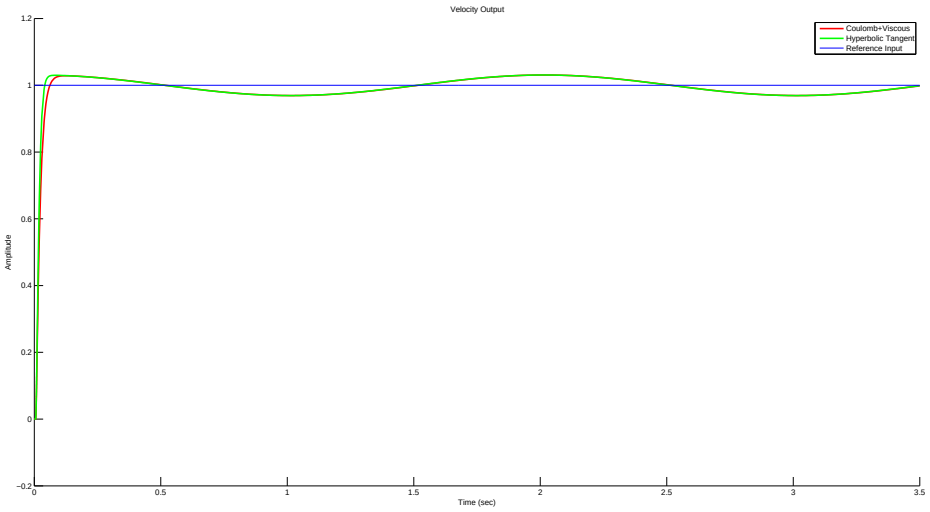

Figure 3.13: Unit Step Response of Velocity Control with Sinusoidal disturbance based on Pole Placement Methodology

From Figure 3.13, velocity output is not accepted to be settled and tracking the reference input, as the response does not remain within the 2% of the unit step input, both for Case 1 and 2. This is because the disturbance leads to a distinct oscillation and the proposed controller cannot reject the disturbance and there occurs a large tracking error as observed in Figure 3.14. This might also be caused by the integrator, which becomes insufficient to reject the sinusoidal disturbance.

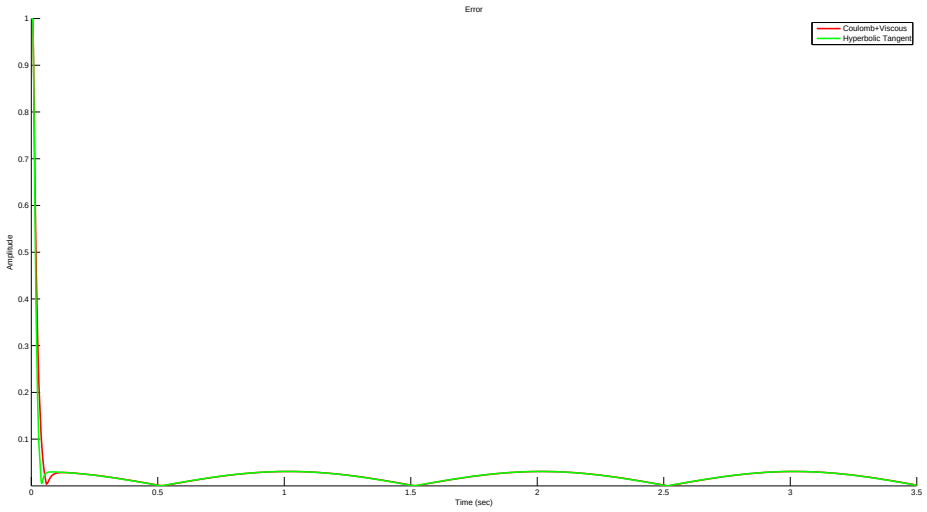

Figure 3.14: Error Signal of Velocity Control for a unit step with Sinusoidal disturbance based on Pole Placement Methodology

3.6 Deadbeat Controller Based Velocity Control: Step input with disturbance

The overall control system designed in Section 3.2, is also used for disturbance rejection. The disturbance input is added to the overall system designed in Section 3.2, as shown in Figure 1.1. For the disturbance input, we apply a step input d(t)=u(t) and a sinusoidal signal $d(t) = Asin(2\pi ft)$, where we choose $A = 0.5$ and $f = 0.5$ rad/sec for simplicity.

3.6.1 Step Disturbance

Unit Step Responses and corresponding errors for pole placement + Deadbeat controller based control designs, for a Unit Step Disturbance, are shown in Figure 3.15 and Figure 3.16 respectively.

It is clearly observed in Figure 3.15 that deadbeat controller has a better disturbance rejection performance, compared to Figure 3.11. Settling time is apparently shorter compared to Section 3.5.1.

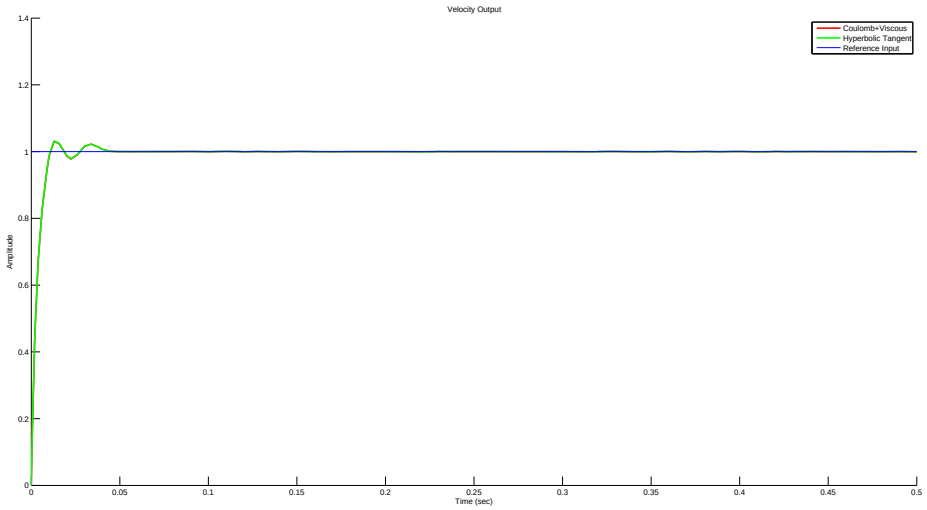

Figure 3.15: Unit Step Response of Velocity Control with unit step disturbance based on Deadbeat Controller

Comparing Figure 3.12 and Figure 3.16, a similar conclusion can be drawn as in Section 3.2 concerning steady-state errors. Especially for the case where Coulomb friction is omitted, steady-state error is less for pole placement + deadbeat controller based control design.

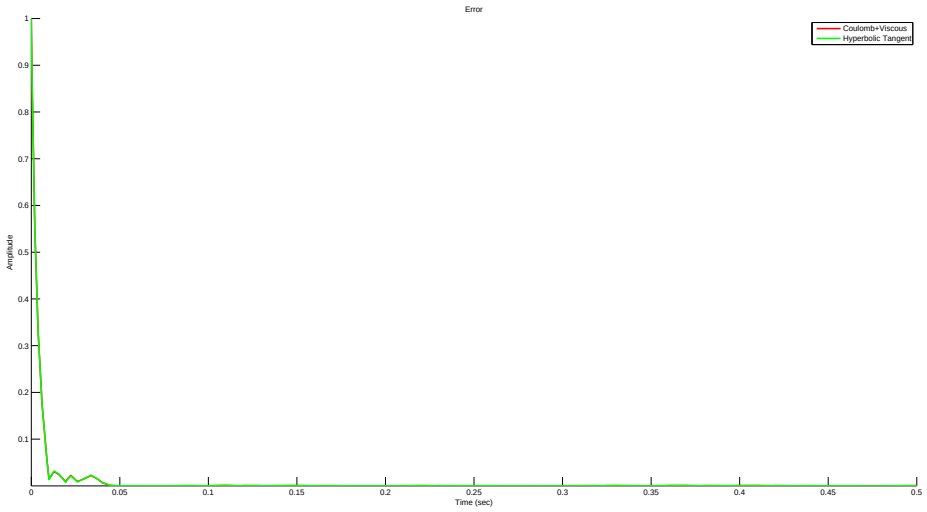

Figure 3.16: Error Signal of Velocity Control for a unit step with unit step disturbance based on Deadbeat Controller

3.6.2 Sinusoidal Disturbance

Unit Step Responses and corresponding errors for pole placement + Deadbeat controller based control designs, for a Sinusoidal Disturbance, are shown in Figure 3.17 and Figure 3.18 respectively.

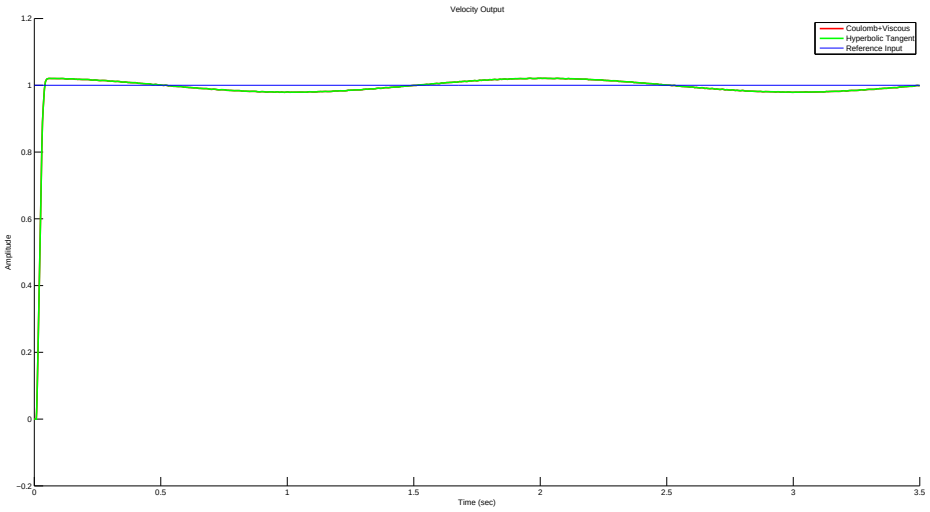

Figure 3.17: Unit Step Response of Velocity Control with Sinusoidal disturbance based on Deadbeat Controller

From Figure 3.17, velocity output is accepted to be settled and tracking the reference input, as the response remains within the 2% of the unit step input, both for Case 1 and 2. Therefore; we can conclude that deadbeat controller based design is more effective in terms of sinusoidal disturbance rejection. Yet, the disturbance leads to a distinct oscillation with a large tracking error, similar to the result in Figure 3.13.

Comparing Figure 3.14 and Figure 3.18, we can conclude that for the sinusoidal disturbances, the design based on pole placement + deadbeat controller has a better disturbance rejection property for both cases, i.e. when Coulomb friction is approximated by $\tanh(\lambda\dot{q})$ function and when it is omitted.

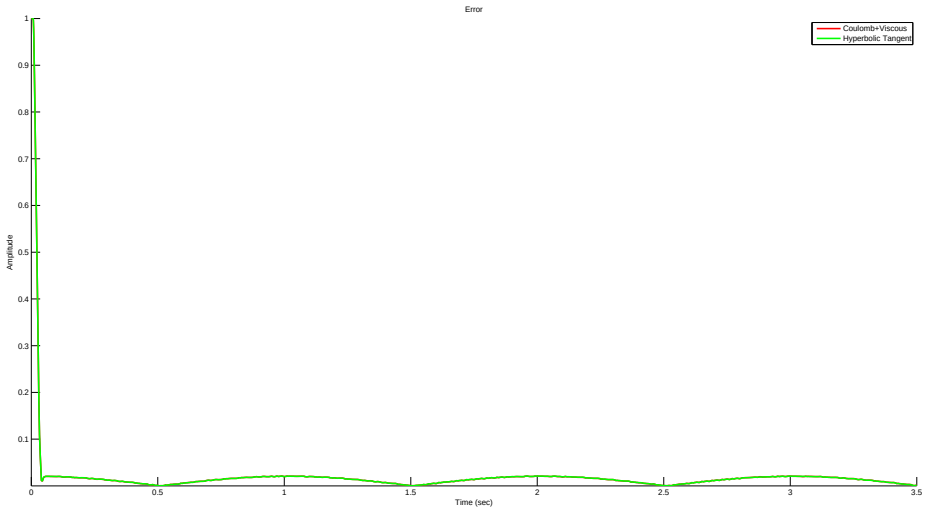

Figure 3.18: Error Signal of Velocity Control for a unit step with Sinusoidal disturbance based on Deadbeat Controller

3.7 Pole Placement Based Velocity Control: Sinusoidal input with disturbance

The overall control system designed in Section 3.3 is also used for disturbance rejection. The disturbance input is added to the overall system designed in Section 3.3, as shown in Figure 1.1. For the disturbance input, we choose a step input $d(t) = u(t)$ and a sinusoidal signal $d(t) = Asin(2\pi ft)$, where we choose $A = 0.5$ and $f = 0.5$ rad/sec for simplicity.

3.7.1 Step Disturbance

Sinusoidal Responses and corresponding errors for pole placement based control designs, for a Unit Step Disturbance, are shown in Figure 3.19 and Figure 3.20 respectively.

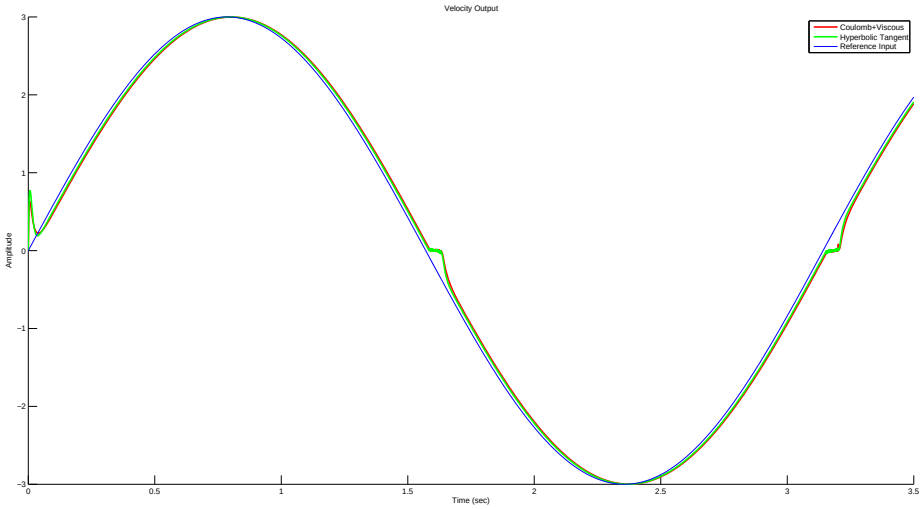

Figure 3.19: Sinusoidal Response of Velocity Control with unit step disturbance based on Pole Placement Methodology

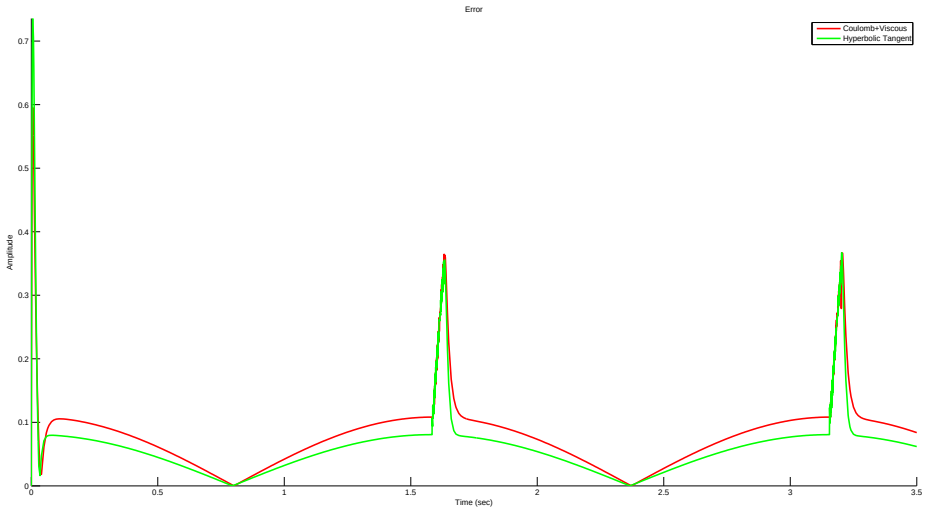

Figure 3.20: Error Signal of Velocity Control for a Sinusoid with unit step disturbance based on Pole Placement Methodology

When the amplitude of the error signals in Figure 3.20 and Figure 3.8 are compared, disturbance rejection performance of the control design based on Pole Placement, for a step input seems successful. However, the unit step disturbance is observed to introduce a delay of approximately 0.01 seconds to the settling time when compared to Section 3.3.

3.7.2 Sinusoidal Disturbance

Sinusoidal Responses and corresponding errors for pole placement based control designs, for a Sinusoidal Disturbance, are shown in Figure 3.21 and Figure 3.22 respectively.

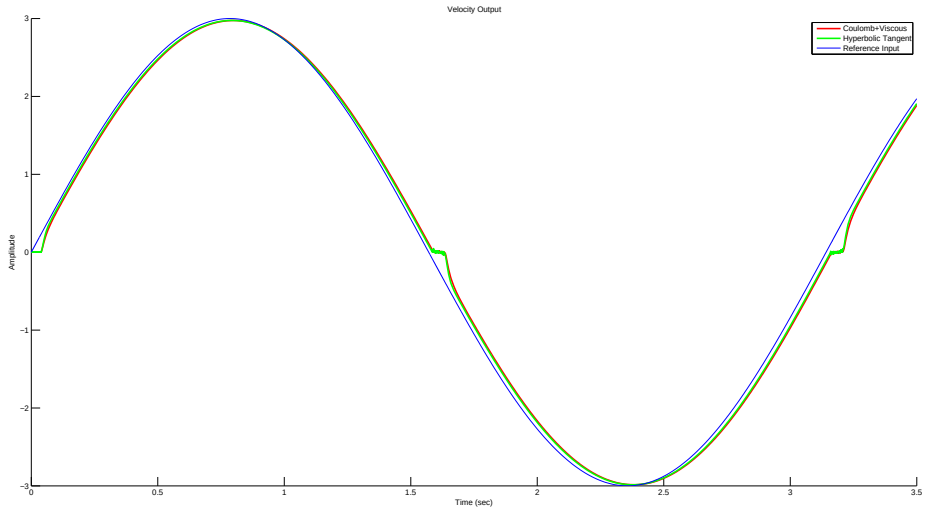

Figure 3.21: Sinusoidal Response of Velocity Control with Sinusoidal disturbance based on Pole Placement Methodology

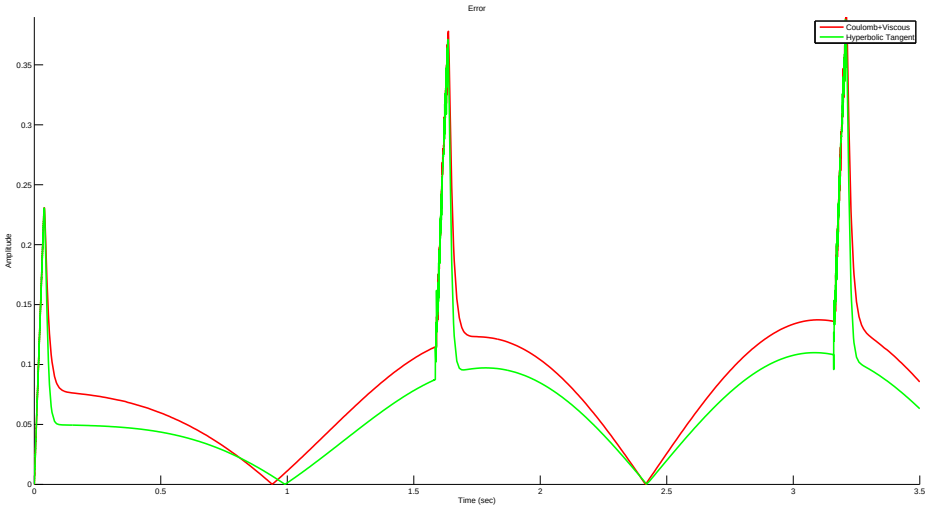

Figure 3.22: Error Signal of Velocity Control for a Sinusoid with Sinusoidal disturbance based on Pole Placement Methodology

When the amplitude of the error signals in Figure 3.22 and Figure 3.8 are compared, adding a sinusoidal disturbance does not change the performance of the control design based on pole placement. Yet, the problem of compensating the Coulomb friction at velocity reversals remains the same.

3.8 Deadbeat Controller Based Velocity Control: Sinusoidal input with disturbance

The overall control system designed in Section 3.4, is also used for disturbance rejection. The disturbance input is added to the overall system designed in Section 3.4, as shown in Figure 1.1. For the disturbance input, we choose a step input $d(t) = u(t)$ and a sinusoidal signal $d(t) = Asin(2\pi ft)$, where we choose $A = 0.5$ and $f = 0.5$ rad/sec for simplicity.

3.8.1 Step Disturbance

Sinusoidal Responses and corresponding errors for pole placement + Deadbeat Controller based control designs, for a Unit Step Disturbance, are shown in Figure 3.23 and Figure 3.24 respectively.

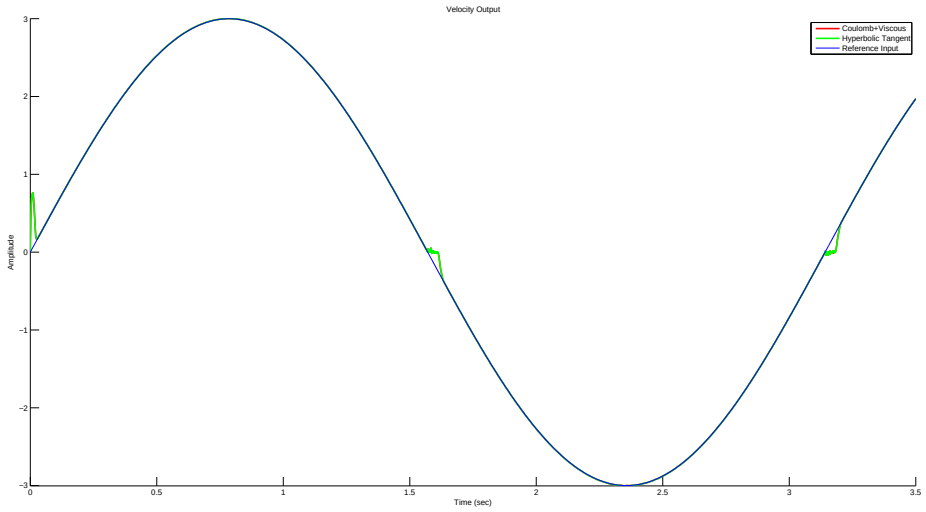

Figure 3.23: Sinusoidal Response of Velocity Control with unit step disturbance based on Deadbeat Controller

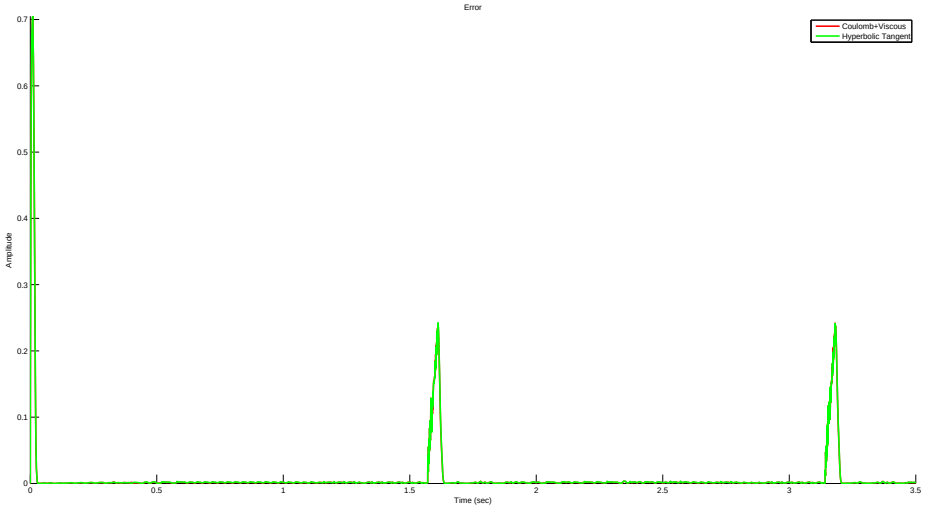

Figure 3.24: Error Signal of Velocity Control for a Sinusoid with unit step disturbance based on Deadbeat Controller

When the amplitude of the error signals in Figure 3.24 and Figure 3.10 are compared, disturbance rejection performance of the control design based on deadbeat controller, for a step input, is observed to be successful.

3.8.2 Sinusoidal Disturbance

Sinusoidal Responses and corresponding errors for pole placement + Deadbeat Controller based control designs, for a Sinusoidal Disturbance, are shown in Figure 3.25 and Figure 3.26 respectively.

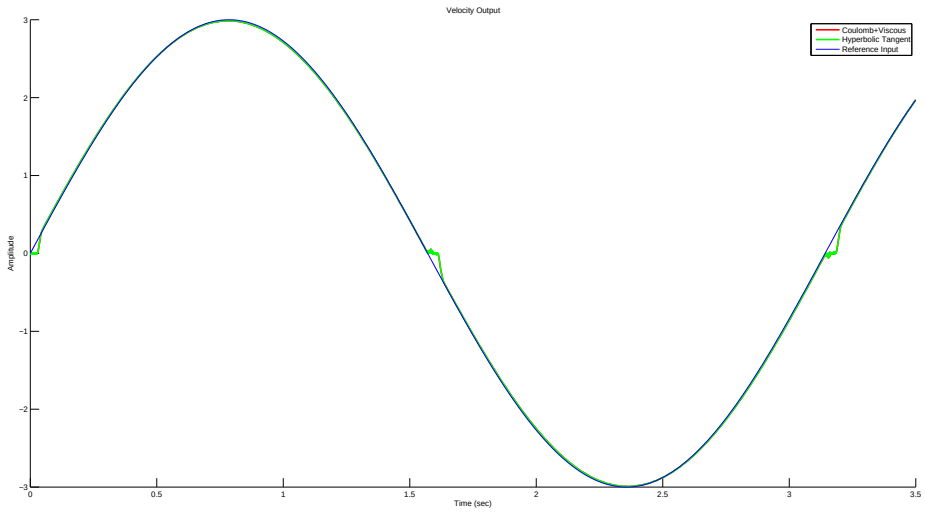

Figure 3.25: Sinusoidal Response of Velocity Control with Sinusoidal disturbance based on Deadbeat Controller

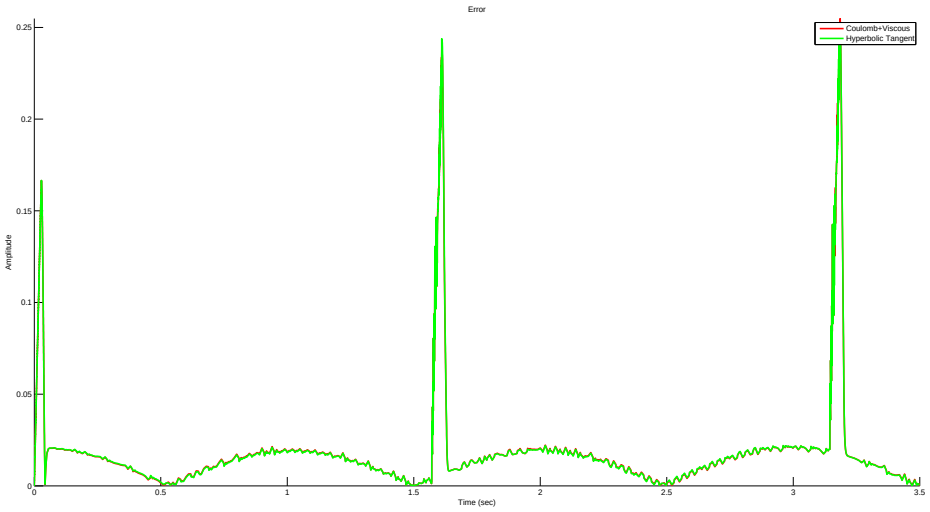

Figure 3.26: Error Signal of Velocity Control for a Sinusoid with Sinusoidal disturbance based on Deadbeat Controller

When the amplitude of the error signals in Figure 3.26 and Figure 3.10 are compared, deadbeat controller is observed to be insufficient for sinusoidal disturbance rejection. In addition, the problem of compensating the Coulomb friction at velocity reversals remains the same, similar to the result in Section 3.7.2. Yet, when the errors in Figure 3.26 and Figure 3.22 are compared, it is clearly observed that Deadbeat methodology gives a better disturbance rejection performance.

3.9 Pole Placement Based Position Control: Step input without disturbance

3.9.1 Pole Placement based on settling time and overshoot

After linearization around operating point, poles of the second order system are placed based on settling time and overshoot. The transfer function of the closed loop system using (2.26) is obtained as:

$$T(s) = \frac{434.8}{s^2 + 663.8s + 231.3 \times 10^5}$$

As integral controller is added in the velocity loop, we do not introduce an additional integrator for the position loop. Root locus analysis is carried out. By using SISO Design Tool in MATLAB, the value of P is determined from the Root Locus Diagram.

Figure 3.27 depicts the root locus diagram of the system. The design requirements are indicated in terms of percent overshoot and settling time, i.e $P.O. = 5\%$ and minimum settling time that could be achieved after design is 0.03 seconds. In addition, the locations of the new poles are also shown in the diagram. The value of P, satisfying the percent overshoot and minimum settling time criteria, is found to be 1500.

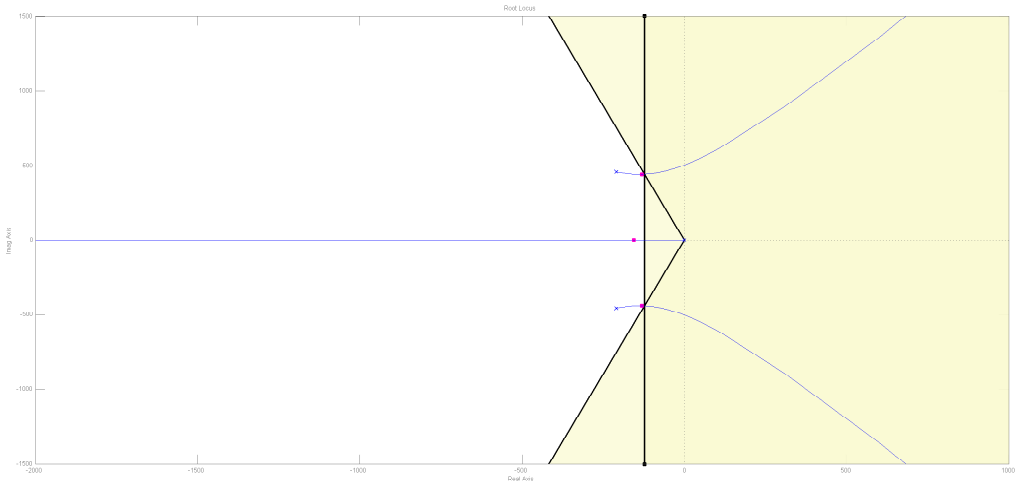

Figure 3.27: Root Locus Diagram for Pole Placement Based Position Control in terms of settling time and overshoot

Unit Step Responses and corresponding errors for pole placement based control designs are shown in Figure 3.28 and Figure 3.29 respectively.

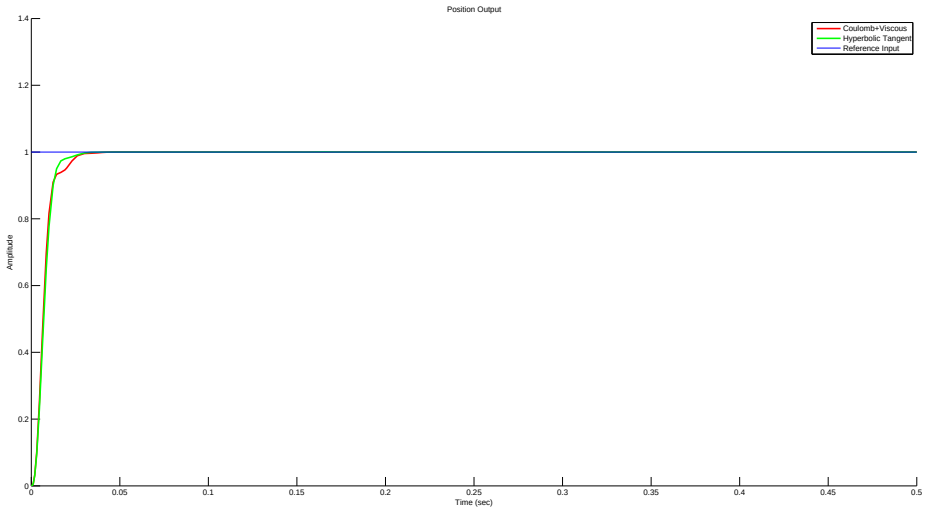

Figure 3.28: Unit Step Response of Position Control without disturbance based on Pole Placement Methodology in terms of settling time and overshoot

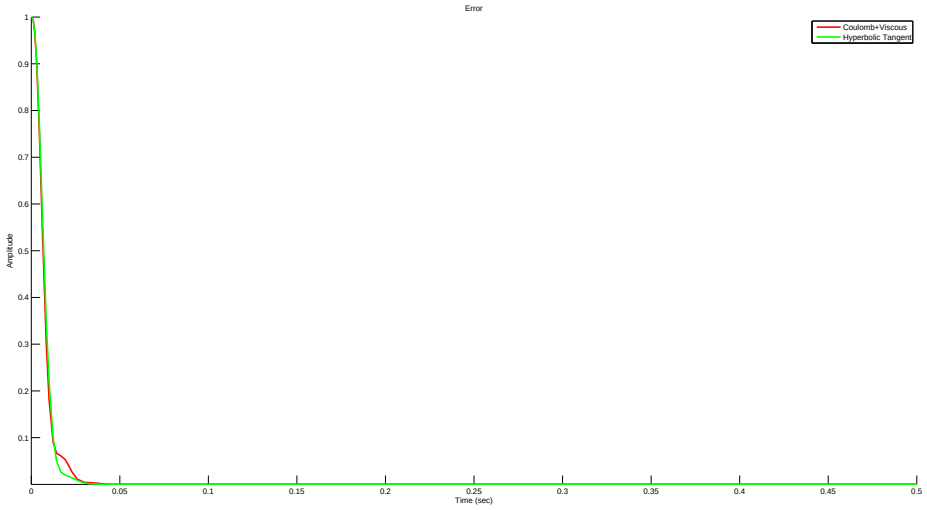

Figure 3.29: Error Signal of Position Control for a unit step without disturbance based on Pole Placement Methodology in terms of settling time and overshoot

3.9.2 Pole Placement based on ITAE

After linearization around operating point, poles of the second order system are placed based on settling time and ITAE index. The transfer function of the closed loop system using (2.26) is obtained as:

$$T(s) = \frac{434.8}{s^2 + 1120s + 231.3 \times 10^5}$$

As integral controller is added in the velocity loop, we do not introduce an additional integrator for the position loop. Root locus analysis is carried out. By using SISO Design Tool in MATLAB, the value of P is determined from the Root Locus Diagram.

Figure 3.30 depicts the root locus diagram of the system. The design requirements are indicated in terms of percent overshoot and settling time, i.e $P.O. = 5\%$ and minimum settling time that could be achieved after design is 0.01 seconds. In addition, the locations of the new poles are also shown in the diagram. The value of P, satisfying the percent overshoot and minimum settling time criteria, is found to be 5000.

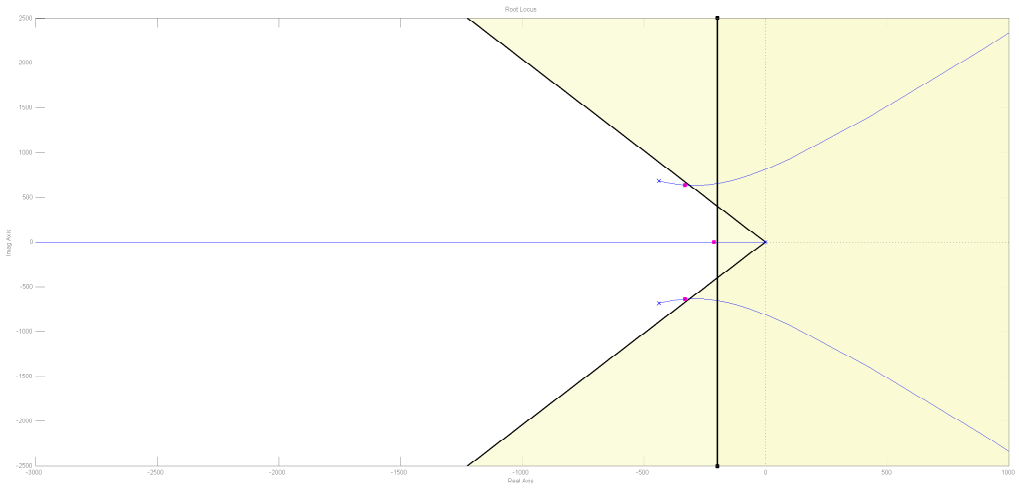

Figure 3.30: Root Locus Diagram for Pole Placement Based Position Control in terms of ITAE index

Unit Step Responses and corresponding errors for pole placement based control designs are shown in Figure 3.31 and Figure 3.32 respectively.

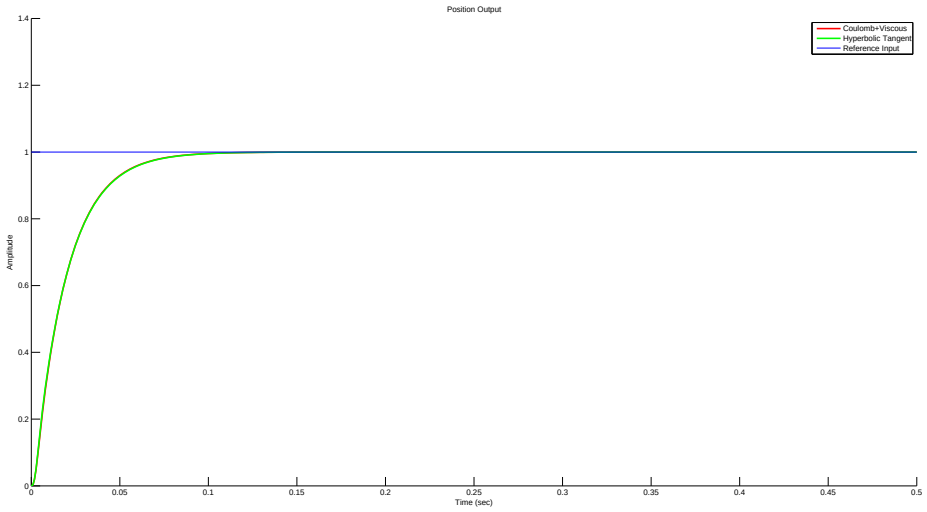

Figure 3.31: Unit Step Response of Position Control without disturbance based on Pole Placement Methodology in terms of ITAE index

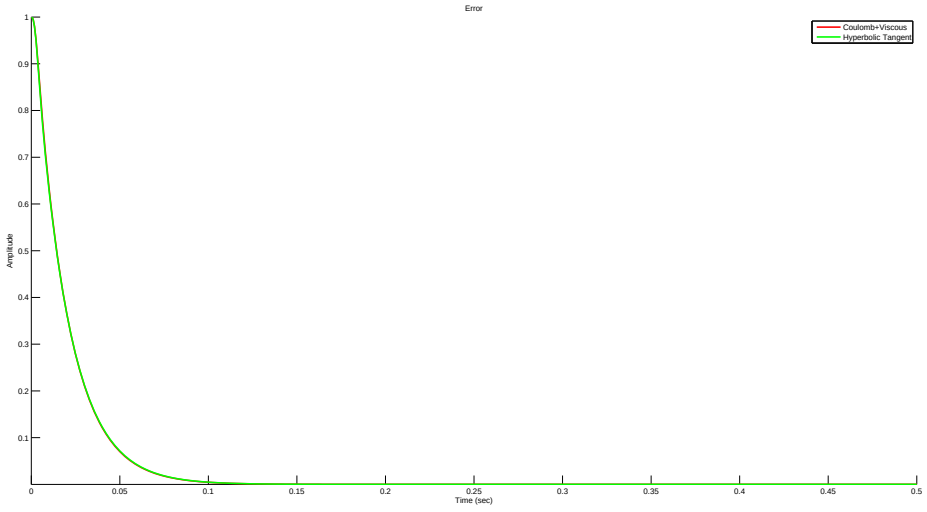

Figure 3.32: Error Signal of Position Control for a unit step without disturbance based on Pole Placement Methodology in terms of ITAE index

3.10 Deadbeat Controller Based Position Control: Step input without disturbance

The deadbeat controller is added to the overall system designed in Section 3.9.1 as shown in Figure 2.8. The transfer function of the closed loop system, before applying the deadbeat controller is obtained using (2.26):

$$T_f(s) = \frac{332.4 \times 10^5}{s^3 + 420.3s^2 + 253.5 \times 10^3 s + 332.4 \times 10^5}$$

By choosing the related reference input from Table 3.1 and the discretized transfer function $P(q)$ obtained using (2.27), Diophantine Equations are constructed:

$$\begin{aligned}(0.08342q^3 + 0.03057q^2 + 0.8587q)(aq + b)\\ +(1 - q)(cq + d) = 1\\ (0.08342q^3 + 0.03057q^2 + 0.8587q)(eq + f)+\\ (-0.01494q^3 + 0.03872q^2 - 0.0511q + 1)(gq + h) = 1\end{aligned}$$

Thus, controller polynomials N_1, N_2 and D_c are obtained by the solution of (2.34). These controllers are utilized to the overall system as seen in Figure 2.8.

Figure 3.33 and Figure 3.34 show Unit Step Responses and corresponding errors for deadbeat controller based designs, respectively.

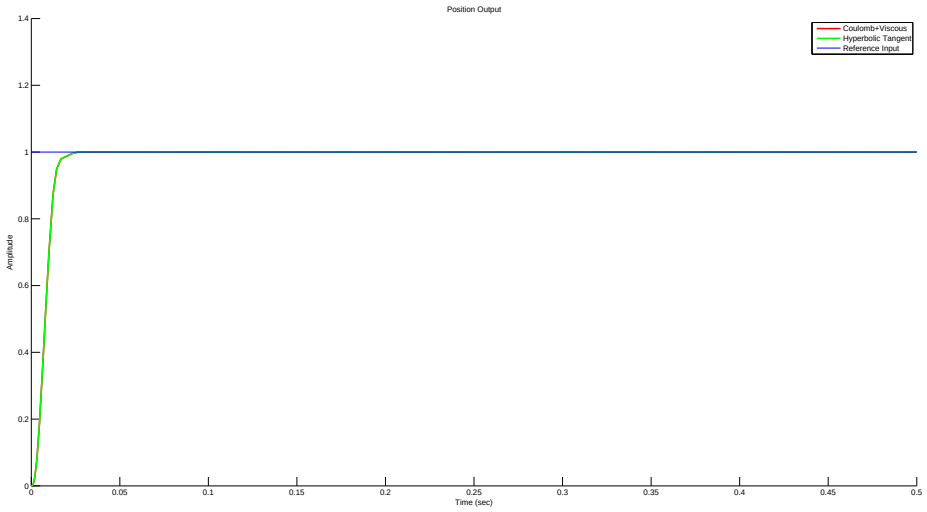

Figure 3.33: Unit Step Response of Position Control without disturbance based on Deadbeat Controller

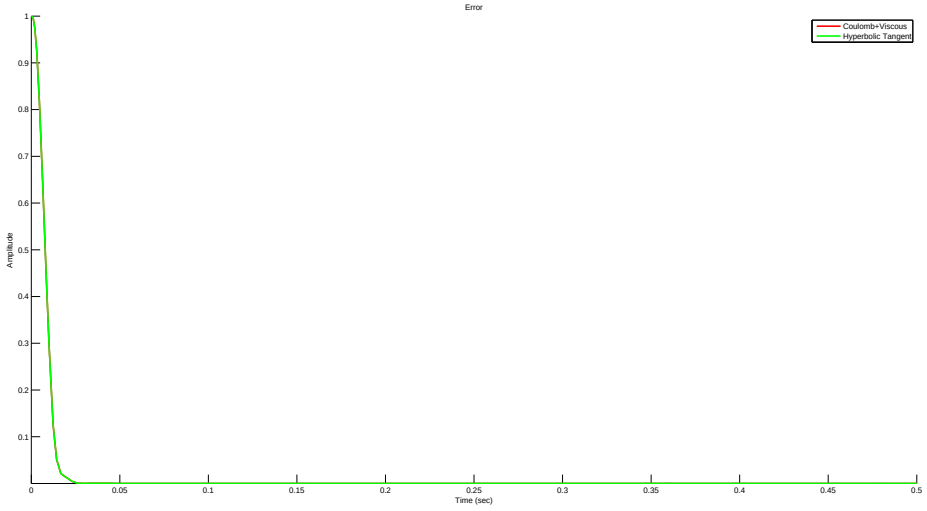

Figure 3.34: Error Signal of Position Control for a unit step without disturbance based on Deadbeat Controller

3.11 Pole Placement Based Position Control: Sinusoidal input without disturbance

The overall control system designed in Section 3.9 is also used for the tracking of the sinusoidal input, as pole placement method does not require any additional design step for hierarchical closed loop feedback structure and does not depend on the reference input to be tracked.

3.11.1 Pole Placement based on settling time and overshoot

Sinusoidal Responses and corresponding errors for pole placement based control designs are shown in Figure 3.35 and Figure 3.36 respectively.

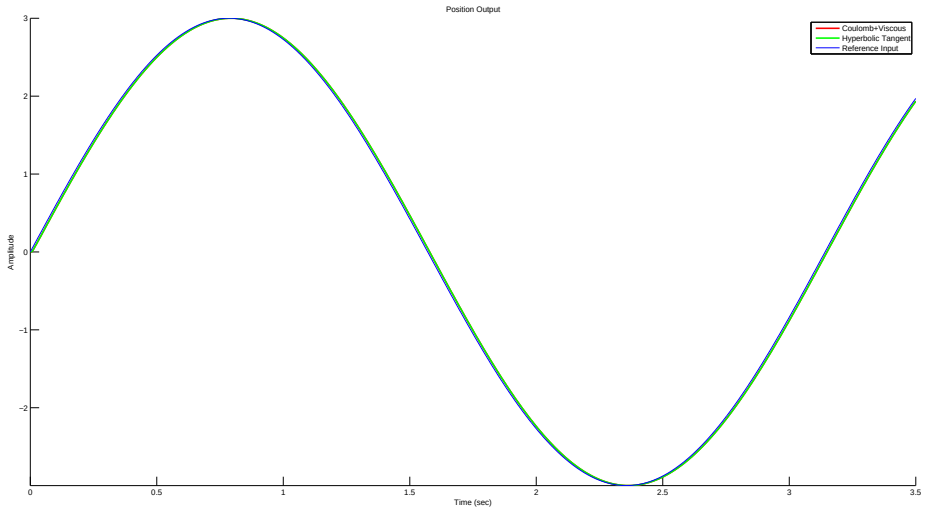

Figure 3.35: Sinusoidal Response of Position Control without disturbance based on Pole Placement Methodology in terms of settling time and overshoot

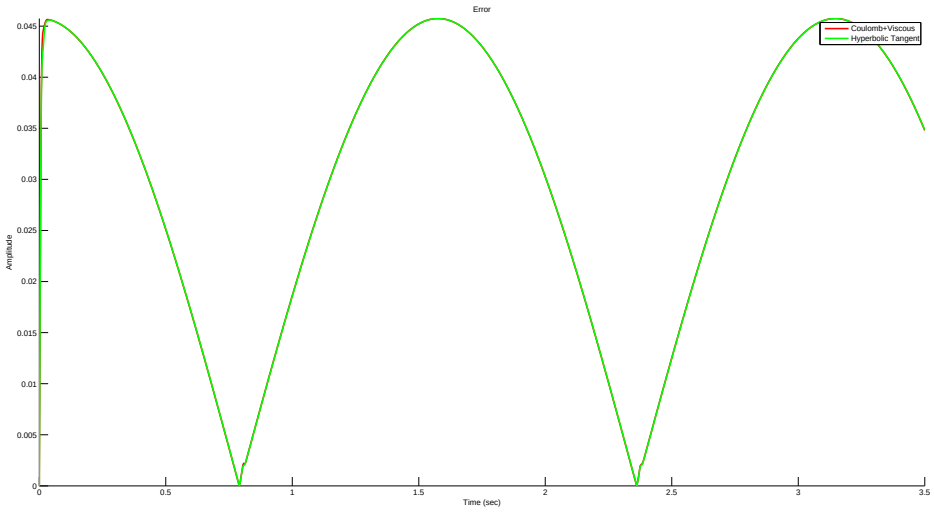

Figure 3.36: Error Signal of Position Control for a sinusoid without disturbance based on Pole Placement Methodology in terms of settling time and overshoot

3.11.2 Pole Placement based on ITAE

Sinusoidal Responses and corresponding errors for pole placement based control designs are shown in Figure 3.37 and Figure 3.38 respectively.

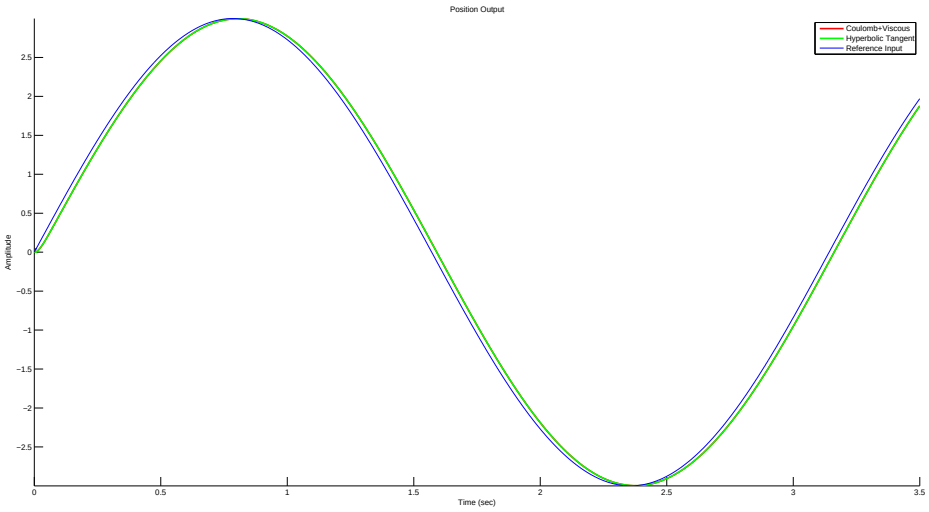

Figure 3.37: Sinusoidal Response of Position Control without disturbance based on Pole Placement Methodology in terms of ITAE index

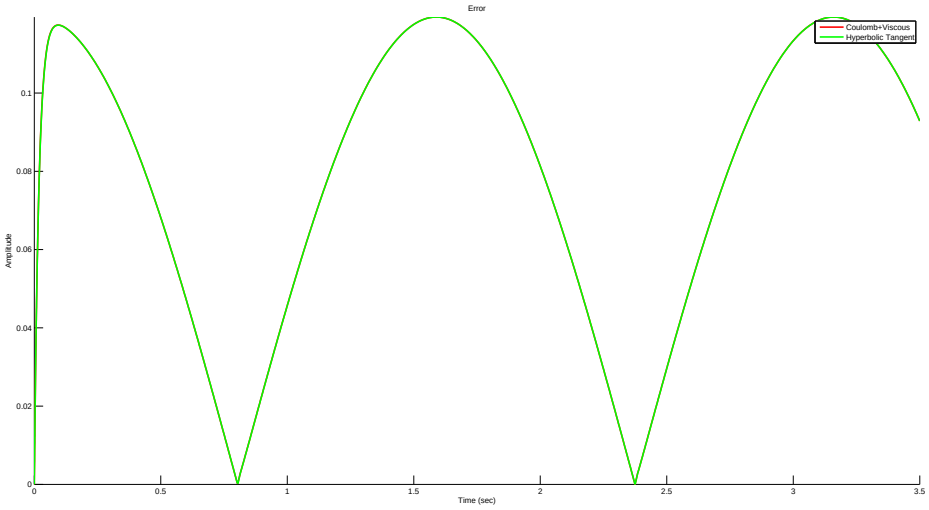

Figure 3.38: Error Signal of Position Control for a sinusoid without disturbance based on Pole Placement Methodology in terms of ITAE index

3.12 Deadbeat Controller Based Position Control: Sinusoidal input without disturbance

The deadbeat controller is added to the overall system designed in Section 3.11.1 as shown in Figure 2.8. The transfer function of the closed loop system, before applying the deadbeat controller is obtained using (2.41). By choosing the related reference input from Table 3.1 and the discretized transfer function $P(q)$ obtained using (2.27), Diophantine Equations are constructed:

$$\begin{aligned}(0.08342q^3 + 0.03057q^2 + 0.8587q)(aq + b) + \\ (0.0003q^2 + 0.0003q)(cq + d) = 1 \\ (0.08342q^3 + 0.03057q^2 + 0.8587q)(eq + f) + \\ (-0.01494q^3 + 0.03872q^2 - 0.0511q + 1)(gq + h) = 1\end{aligned}$$

Thus, controller polynomials N_1, N_2 and D_c are obtained by the solution of (2.34). These controllers are utilized to the overall system as seen in Figure 2.8.

Sinusoidal Responses and corresponding errors for pole placement + Deadbeat Controller based control designs are shown in Figure 3.39 and Figure 3.40 respectively.

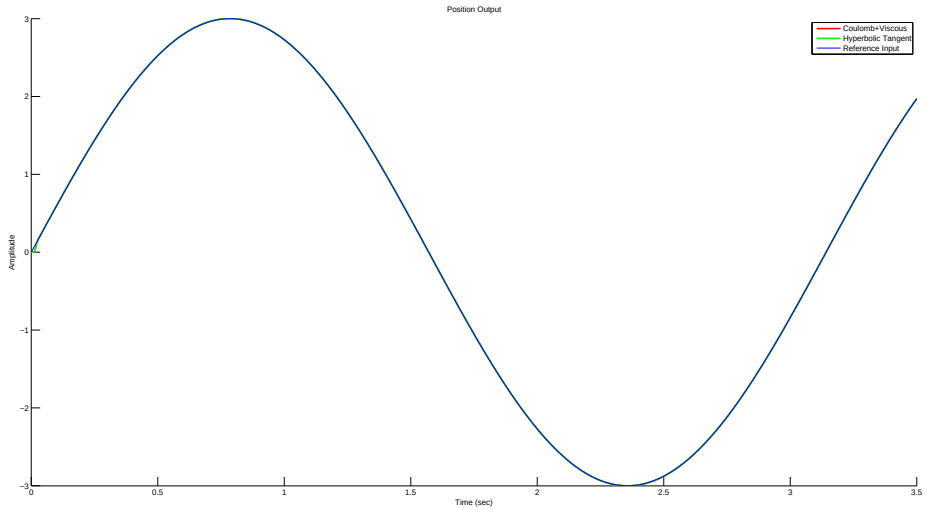

Figure 3.39: Sinusoidal Response of Position Control without disturbance based on Deadbeat Controller

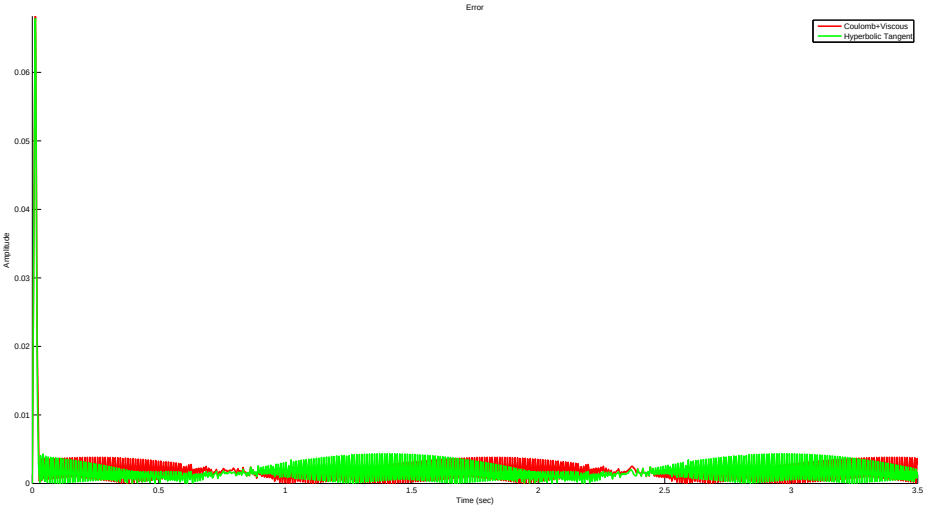

Figure 3.40: Error Signal of Position Control for a sinusoid without disturbance based on Deadbeat Controller

3.13 Pole Placement Based Position Control: Step input with disturbance

The overall control system designed in Section 3.9 is also used for disturbance rejection. The disturbance input is added to the overall system designed in Section 3.9, as shown in Figure 1.1. For the disturbance input, we choose a step input $d(t) = u(t)$ and a sinusoidal signal $d(t) = Asin(2\pi ft)$, where we choose $A = 0.5$ and $f = 0.5$ rad/sec for simplicity.

3.13.1 Pole Placement based on settling time and overshoot

3.13.1.1 Step Disturbance

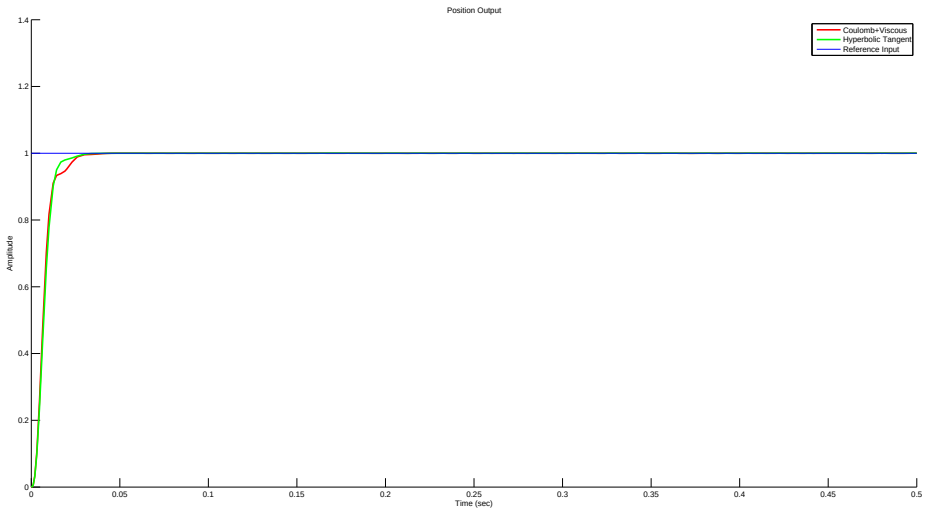

Figure 3.41: Unit Step Response of Position Control with Unit Step disturbance based on Pole Placement Methodology in terms of settling time and overshoot

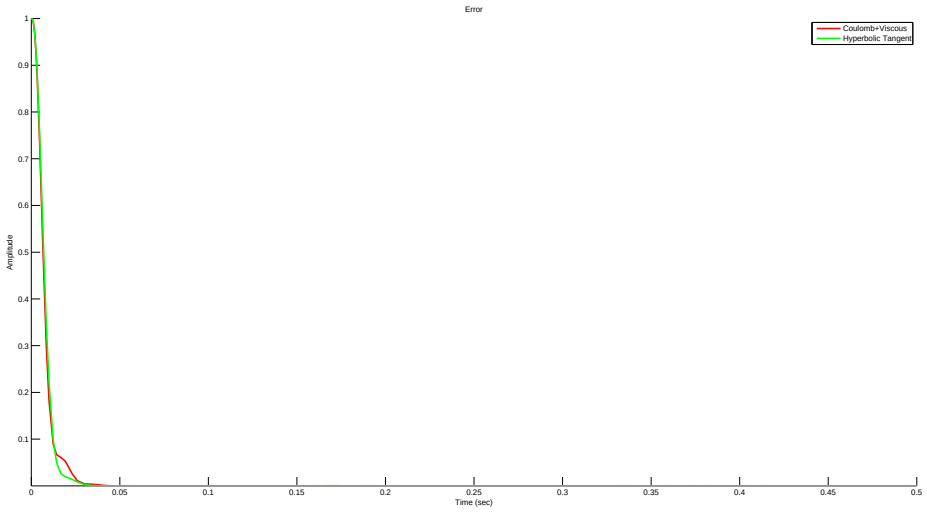

Figure 3.42: Error Signal of Position Control for a Unit Step with Unit Step disturbance based on Pole Placement Methodology in terms of settling time and overshoot

3.13.1.2 Sinusoidal Disturbance

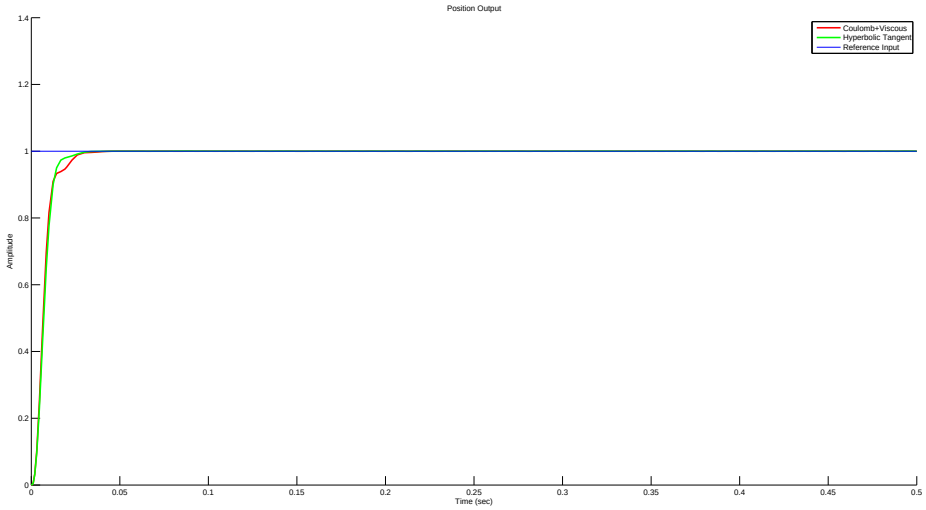

Figure 3.43: Unit Step Response of Position Control with Sinusoidal disturbance based on Pole Placement Methodology in terms of settling time and overshoot

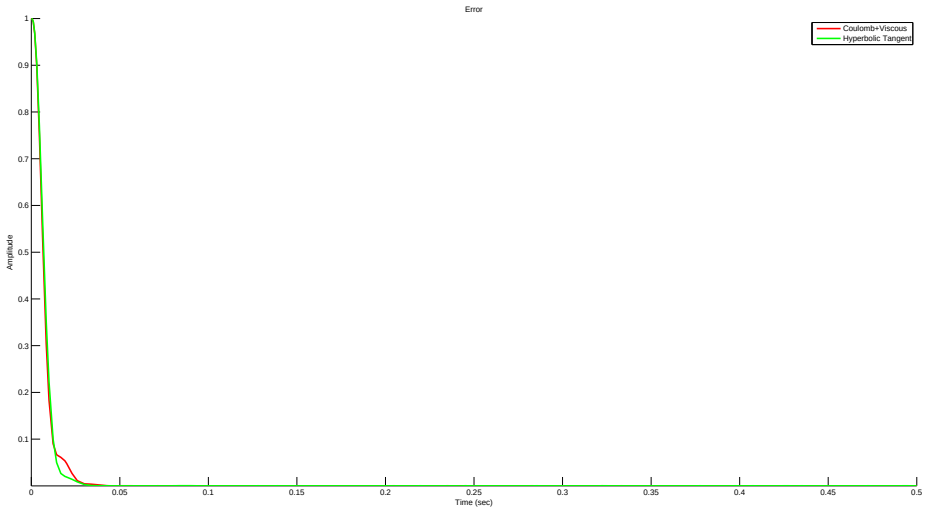

Figure 3.44: Error Signal of Position Control for a Unit Step with Sinusoidal disturbance based on Pole Placement Methodology in terms of settling time and overshoot

3.13.2 Pole Placement based on ITAE

3.13.2.1 Step Disturbance

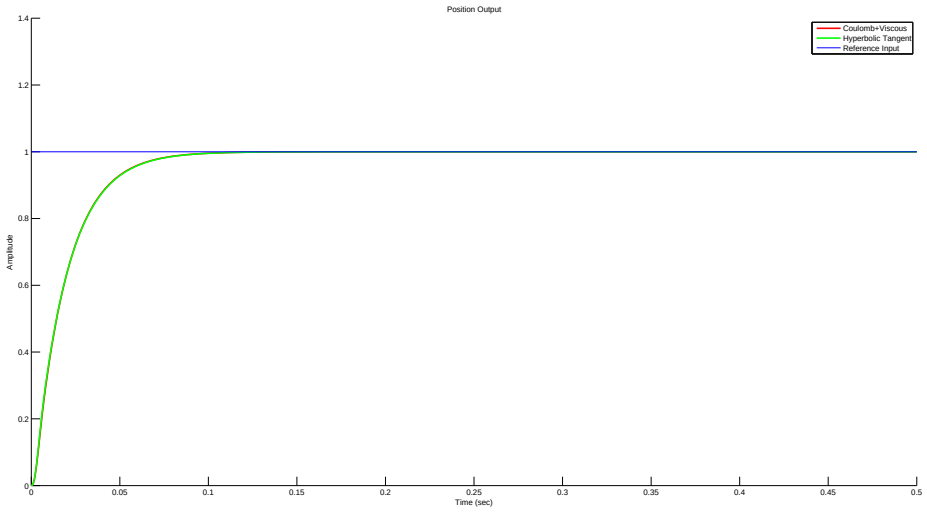

Figure 3.45: Unit Step Response of Position Control with Unit Step disturbance based on Pole Placement Methodology in terms of ITAE index

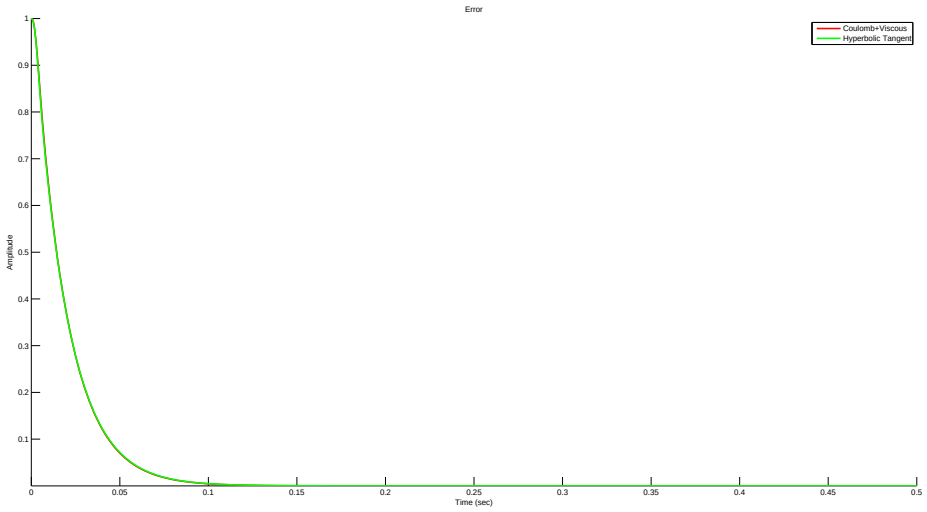

Figure 3.46: Error Signal of Position Control for a Unit Step with Unit Step disturbance based on Pole Placement Methodology in terms of ITAE index

3.13.2.2 Sinusoidal Disturbance

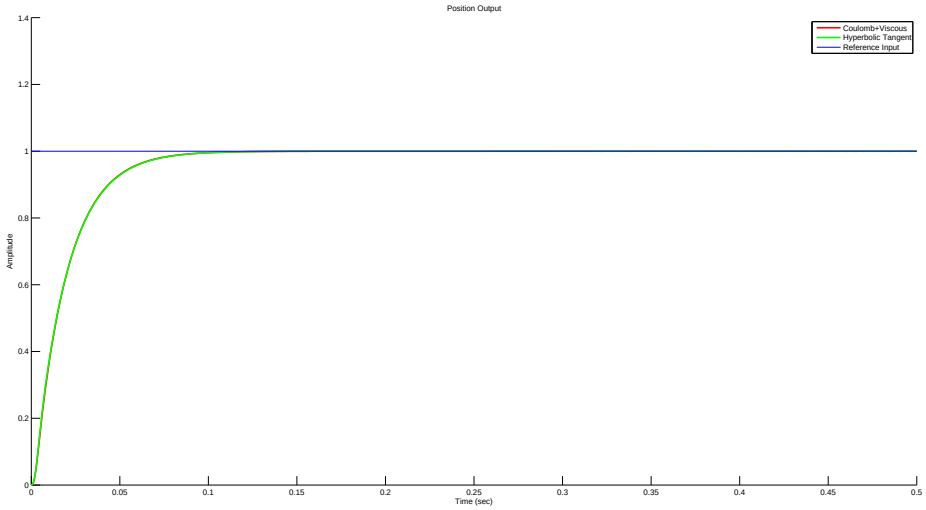

Figure 3.47: Unit Step Response of Position Control with Sinusoidal disturbance based on Pole Placement Methodology in terms of ITAE index

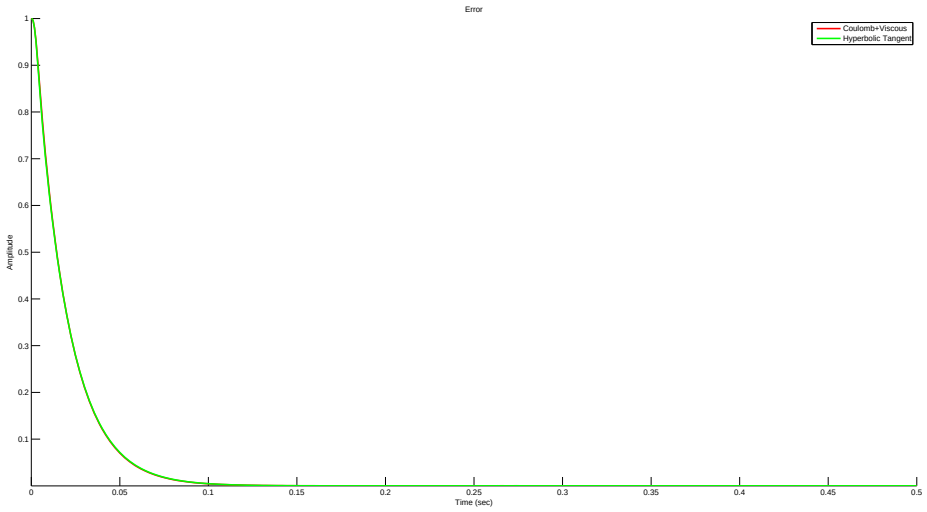

Figure 3.48: Error Signal of Position Control for a Unit Step with Sinusoidal disturbance based on Pole Placement Methodology in terms of ITAE index

3.14 Deadbeat Controller Based Position Control: Step input with disturbance

The overall control system designed in Section 3.10, is also used for disturbance rejection. The disturbance input is added to the overall system designed in Section 3.10, as shown in Figure 1.1. For the disturbance input, we choose a step input $d(t) = u(t)$ and a sinusoidal signal $d(t) = Asin(2\pi ft)$, where we choose $A = 0.5$ and $f = 0.5$ rad/sec for simplicity.

3.14.1 Step Disturbance

Unit Step Responses and corresponding errors for pole placement + Deadbeat controller based control designs, for a Unit Step Disturbance, are shown in Figure 3.49 and Figure 3.50 respectively.

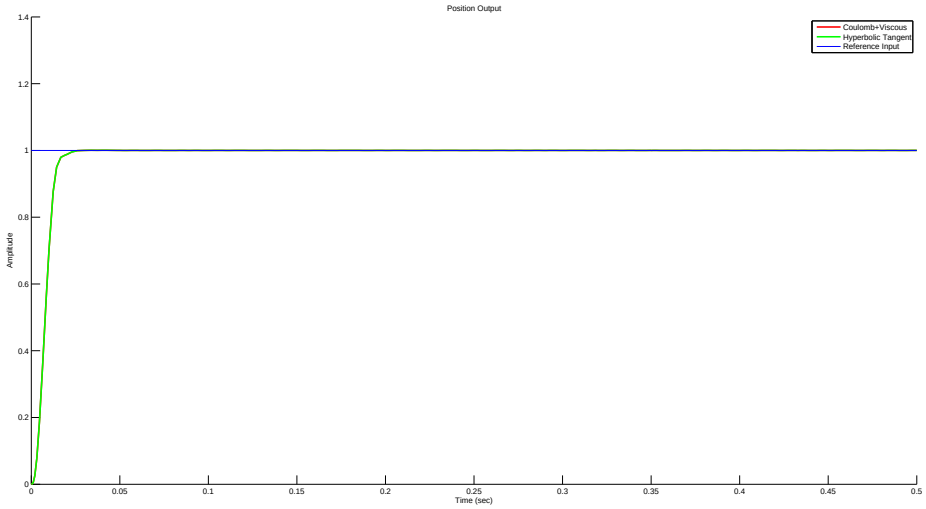

Figure 3.49: Unit Step Response of Position Control with Unit Step disturbance based on Deadbeat Controller in terms of settling time and overshoot

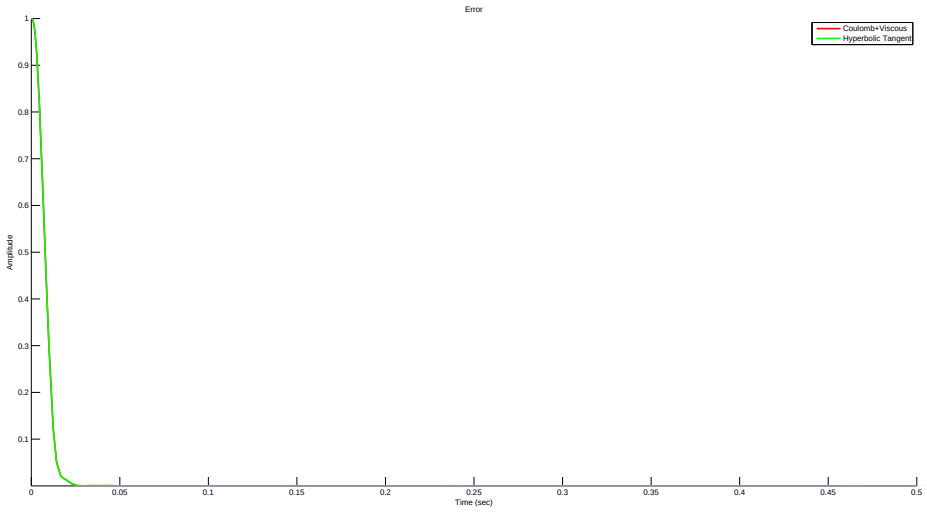

Figure 3.50: Error Signal of Position Control for a Unit Step with Unit Step disturbance based on Deadbeat Controller in terms of settling time and overshoot

3.14.2 Sinusoidal Disturbance

Unit Step Responses and corresponding errors for pole placement + Deadbeat controller based control designs, for a Sinusoidal Disturbance, are shown in Figure 3.51 and Figure 3.52 respectively.

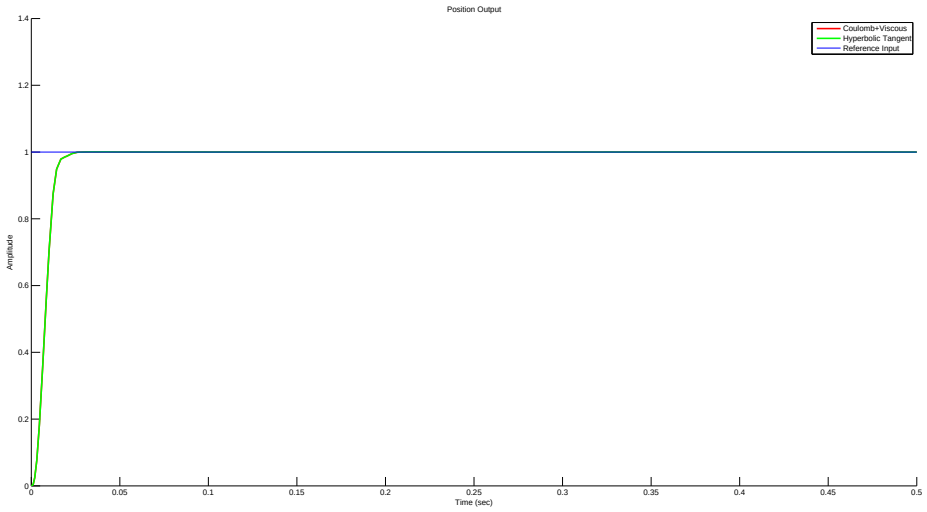

Figure 3.51: Unit Step Response of Position Control with Sinusoidal disturbance based on Deadbeat Controller in terms of settling time and overshoot

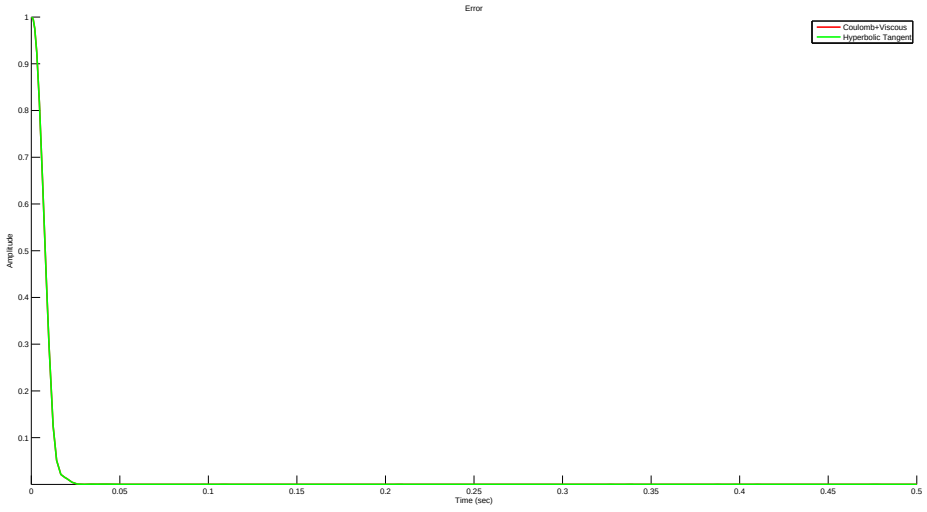

Figure 3.52: Error Signal of Position Control for a Unit Step with Sinusoidal disturbance based on Deadbeat Controller in terms of settling time and overshoot

3.15 Pole Placement Based Position Control: Sinusoidal input with disturbance

3.15.1 Pole Placement based on settling time and overshoot

3.15.1.1 Step Disturbance

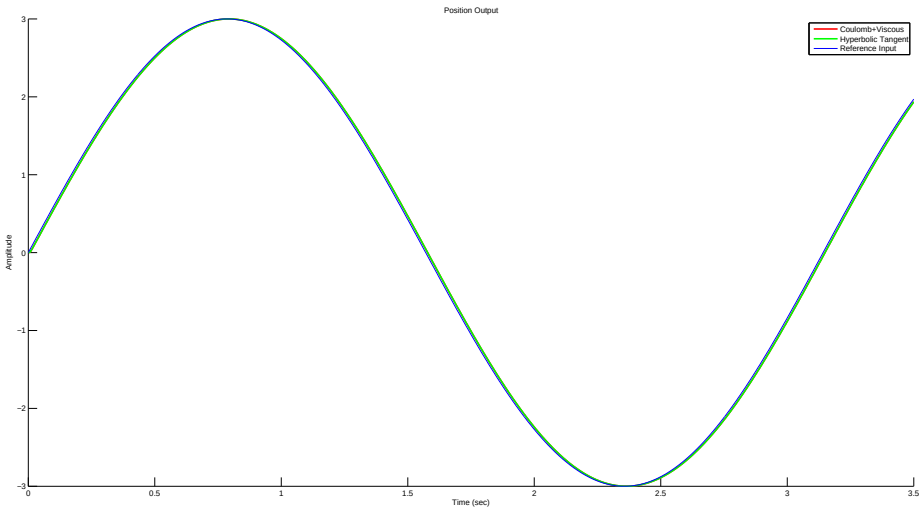

Figure 3.53: Sinusoidal Response of Position Control with Unit Step disturbance based on Pole Placement Methodology in terms of settling time and overshoot

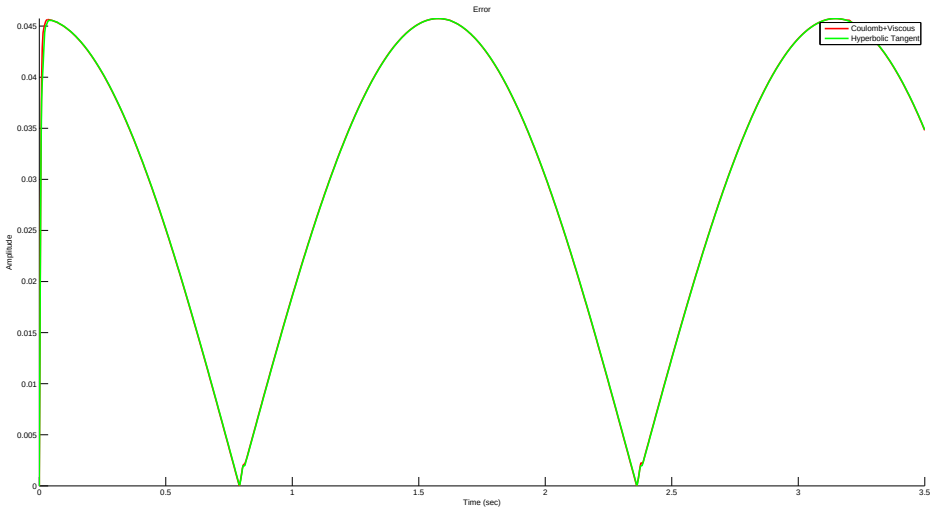

Figure 3.54: Error Signal of Position Control for a sinusoid with Unit Step disturbance based on Pole Placement Methodology in terms of settling time and overshoot

3.15.1.2 Sinusoidal Disturbance

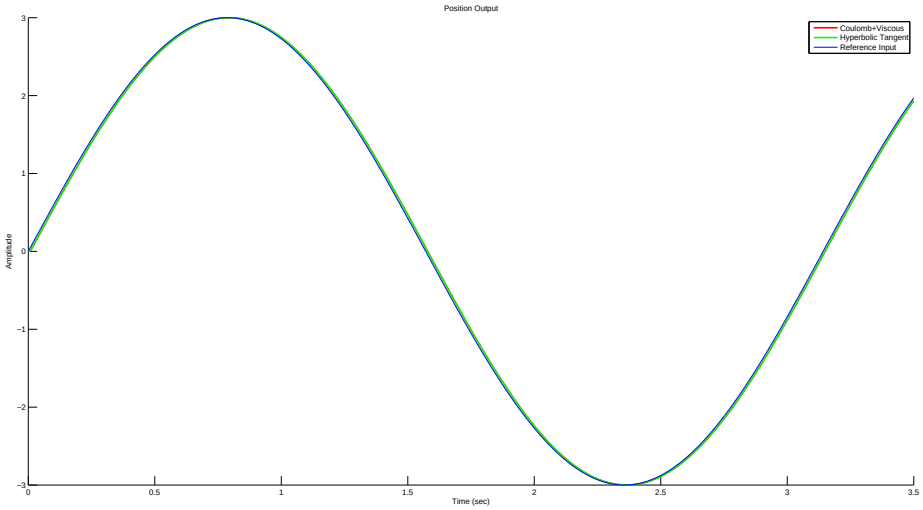

Figure 3.55: Sinusoidal Response of Position Control with Sinusoidal disturbance based on Pole Placement Methodology in terms of settling time and overshoot

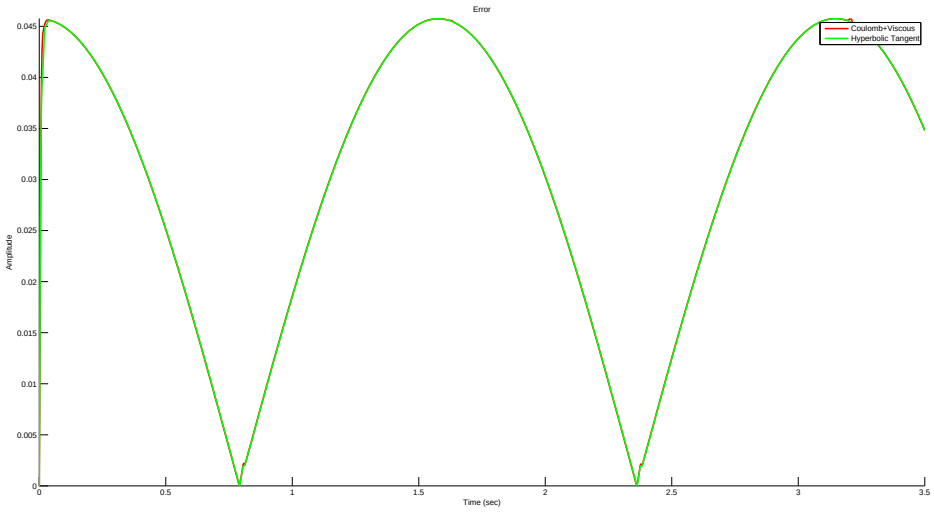

Figure 3.56: Error Signal of Position Control for a sinusoid with Sinusoidal disturbance based on Pole Placement Methodology in terms of settling time and overshoot

3.15.2 Pole Placement based on ITAE

3.15.2.1 Step Disturbance

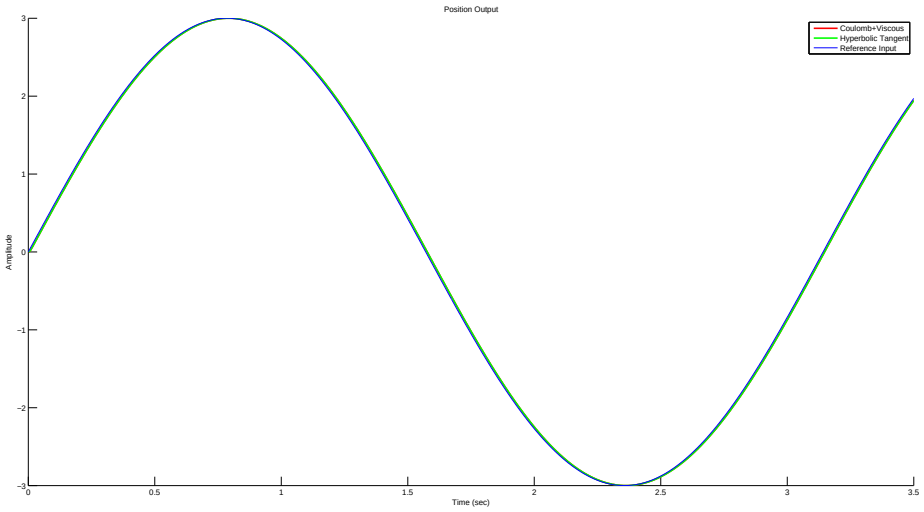

Figure 3.57: Sinusoidal Response of Position Control with Unit Step disturbance based on Pole Placement Methodology in terms of ITAE index

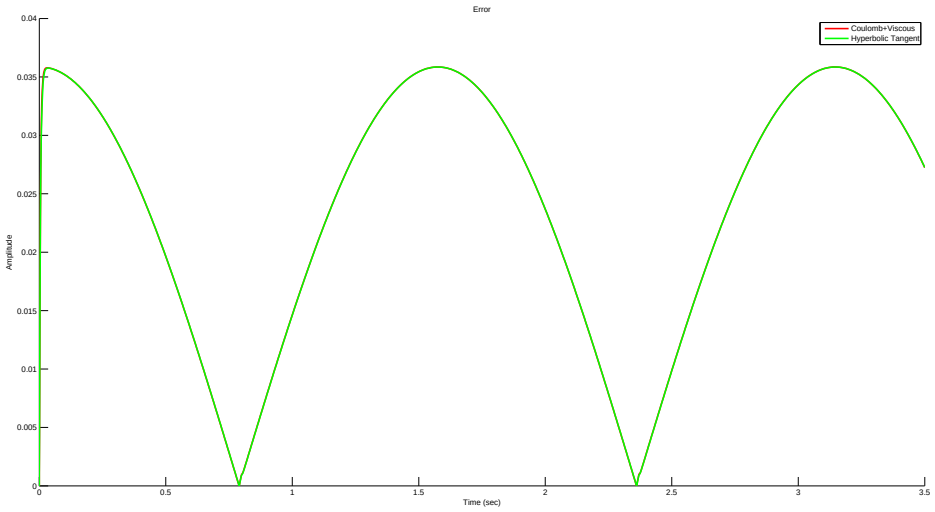

Figure 3.58: Error Signal of Position Control for a sinusoid with Unit Step disturbance based on Pole Placement Methodology in terms of ITAE index

3.15.2.2 Sinusoidal Disturbance

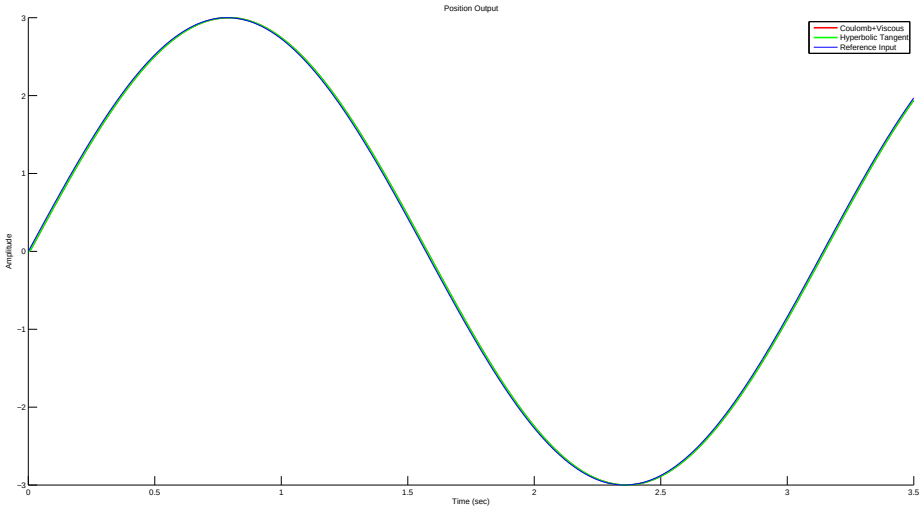

Figure 3.59: Sinusoidal Response of Position Control with Sinusoidal disturbance based on Pole Placement Methodology in terms of ITAE index

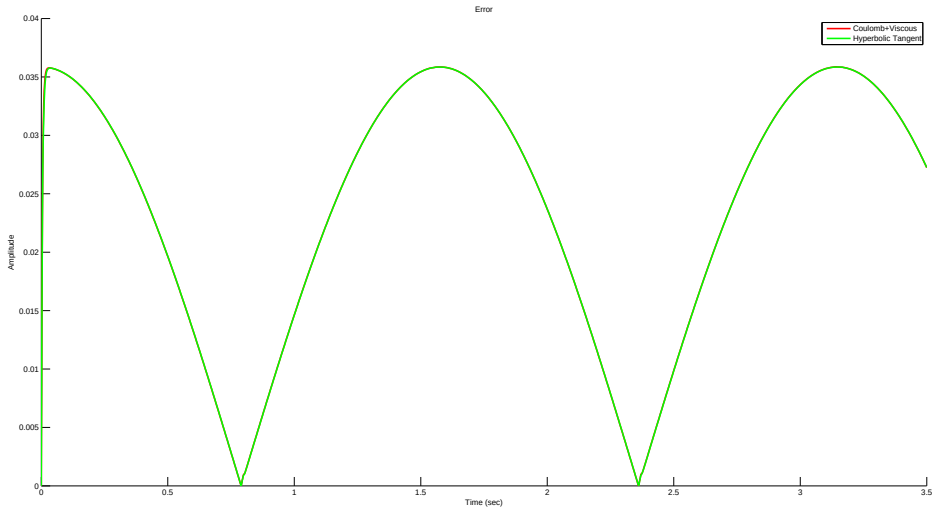

Figure 3.60: Error Signal of Position Control for a sinusoid with Sinusoidal disturbance based on Pole Placement Methodology in terms of ITAE index

3.16 Deadbeat Controller Based Position Control: Sinusoidal input with disturbance

The overall control system designed in Section 3.12, is also used for disturbance rejection. The disturbance input is added to the overall system designed in Section 3.12, as shown in Figure 1.1. For the disturbance input, we choose a step input $d(t) = u(t)$ and a sinusoidal signal $d(t) = Asin(2\pi ft)$, where we choose $A = 0.5$ and $f = 0.5$ rad/sec for simplicity.

3.16.1 Step Disturbance

Sinusoidal Responses and corresponding errors for pole placement + Deadbeat controller based control designs, for a Unit Step Disturbance, are shown in Figure 3.61 and Figure 3.62 respectively.

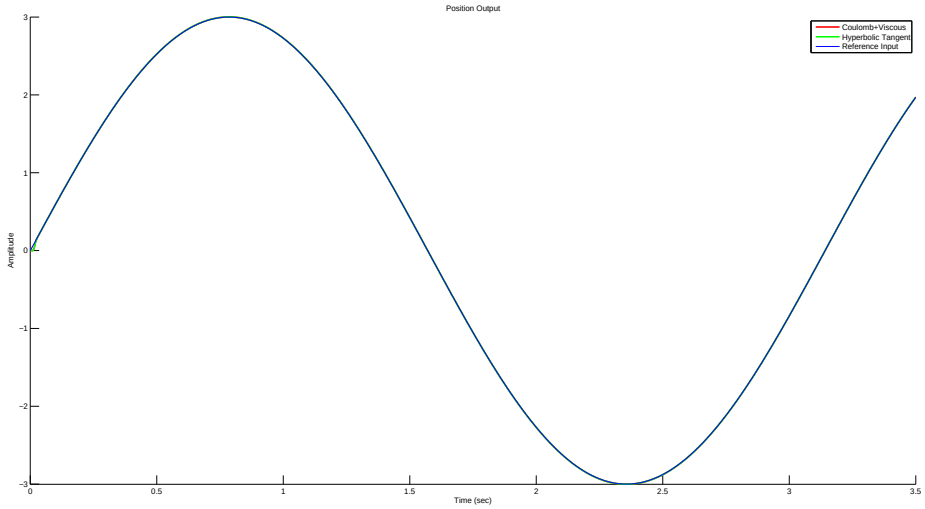

Figure 3.61: Sinusoidal Response of Position Control with Unit Step disturbance based on Deadbeat Controller in terms of settling time and overshoot

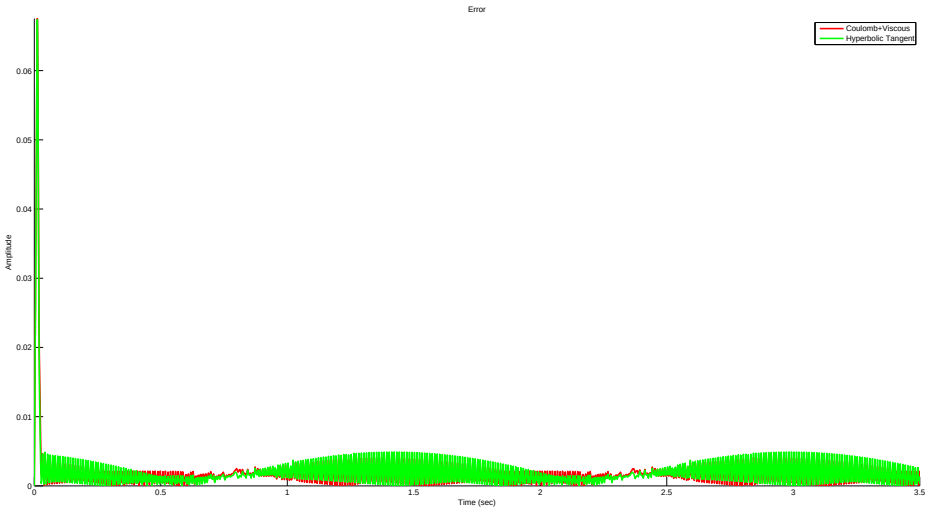

Figure 3.62: Error Signal of Position Control for a sinusoid with Unit Step disturbance based on Deadbeat Controller in terms of settling time and overshoot

3.16.2 Sinusoidal Disturbance

Sinusoidal Responses and corresponding errors for pole placement + Deadbeat controller based control designs, for a Sinusoidal Disturbance, are shown in Figure 3.63 and Figure 3.64 respectively.

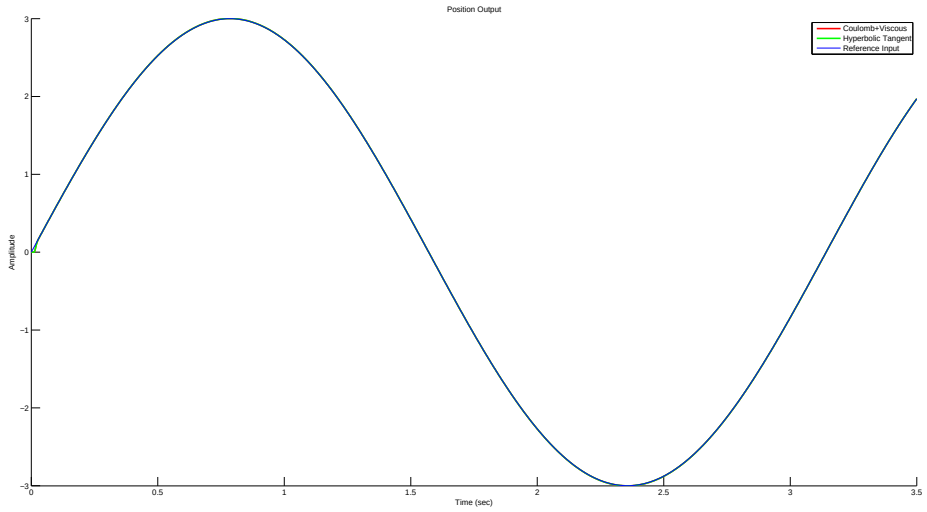

Figure 3.63: Sinusoidal Response of Position Control with Sinusoidal disturbance based on Deadbeat Controller in terms of settling time and overshoot

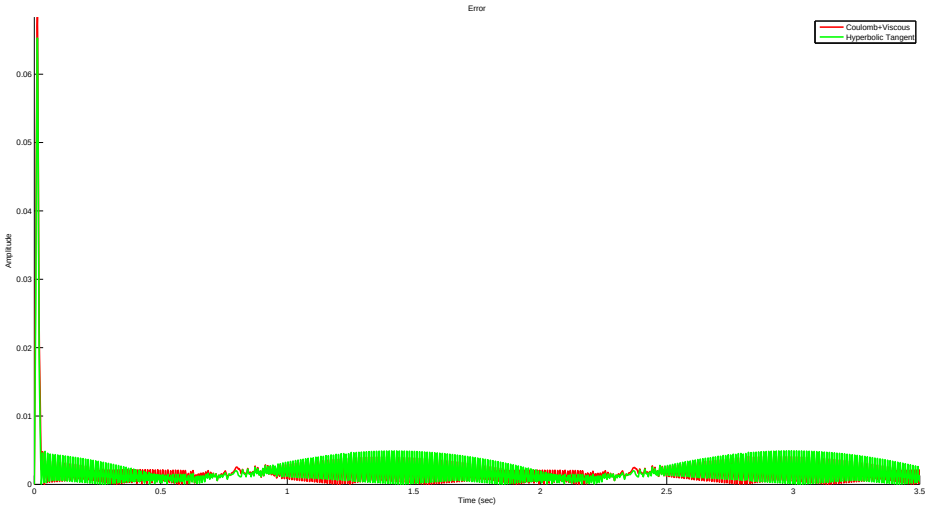

Figure 3.64: Error Signal of Position Control for a sinusoid with Sinusoidal disturbance based on Deadbeat Controller in terms of settling time and overshoot

Chapter 4

CONCLUSIONS

In this thesis, design of control systems based on Pole Placement and Deadbeat methodologies, in order to handle a mechanical system under the effect of friction, is studied. Pole Placement Methodology is based on different performance measures and indices such as settling time, overshoot and ITAE. Deadbeat Methodology is based on parameterization of Diophantine equations which depend on the reference signal to be tracked.

The first step of the pole placement methodology is to linearize and internally stabilize the system by feedback linearization. Next, pole placement method is applied by using state and output feedbacks, right after controllability and observability tests are carried out to check whether pole placement can be applied or not. As a third step, an integrator, combined with a unit feedback from the output, is added as a feedforward controller in order to form and reduce the error signal. As a last step, Root Locus Diagram of the overall system is analyzed to find a suitable gain in order to yield some predefined performance criteria such as settling time, overshoot etc.

A new deadbeat controller, to be utilized in addition to the overall control system

based on pole placement methodology, is proposed. The controller's parameters are obtained by solutions of the two independent Diophantine equations, constructed by the use of reference signal to be tracked and the transfer function of the linearized and stabilized control system.

Control system performance, depending on the applications of pole placement and deadbeat methodologies, is analyzed using a hierarchical closed loop feedback structure. Although this structure provides control for both position and velocity loops separately, the control system for the position loop depends on the closed loop transfer function of the control system for the velocity loop. Therefore; control system design is extended for the position loop right after the design of the control system for the velocity loop. The performance is criticized in terms of reference input tracking and disturbance rejection. For both velocity and position control, step and sinusoidal input tracking with and without disturbance cases are analyzed.

The plant contains Coulomb friction and linear viscous damping. As Coulomb friction contains a discontinuity at zero relative velocity, we cannot obtain an exact linearization. Therefore; during the design process, Coulomb friction is either omitted or approximated by tangent hyperbolic function. However, Coulomb friction is always used in our simulations. Ignoring Coulomb friction during control design is observed to be disadvantageous. Although Coulomb friction has a more accurate approximation for higher values in tangent hyperbolic function, tracking performances for unit step and sinusoidal inputs are improved with lower values. Indeed, tangent hyperbolic function with lower values seems to capture nonlinear and discontinuous properties of friction, such as at rest situation, better.

Pole placement methodology is observed to provide internally stable closed loop systems and served snugness in design according to various performance measures and indices. However, some of the results show that both velocity and position outputs track the reference inputs with some minimal delays and steady-state errors.

By the utilization of the deadbeat controller, both velocity and position outputs of the system are observed to be tracking the reference input from any initial state, with almost zero steady-state error and minimum settling time, compared to the pole placement methodology.

Some simulation results indicate initial overshoots, leading to a degradation in the start-up tracking response. A low-pass filter might be used to overcome this problem. In addition, for sinusoidal references/disturbances, both methodologies are observed to be open to improvement. The integral controller might be insufficient to completely compensate for Coulomb friction at velocity reversals. Instead of using an integral controller, different control strategies could be adapted in order to track a sinusoidal input. Disturbance rejection performance of the deadbeat controller is also better, compared to the pole placement methodology. However, this also remains to be an open research problem and both controllers might be improved for better disturbance rejection, such as trying to minimize the magnitude of the transfer function between disturbance and output, especially at the frequencies where disturbance is dominant.

A future work might be improvement and application of pole placement and deadbeat methodologies for more advanced friction models, especially dynamic friction models, such as Dahl, LuGre, Leuven and Generalized Maxwell-slip frictions.

Bibliography

[1] V. van Geffen, "A study of friction models and friction compensation," *DCT*, vol. 118, p. 24, 2009.

[2] F. Altpeter, *Friction modeling, identification and compensation*. PhD thesis, STI, Lausanne, 1999.

[3] J. O'Reilly, "The discrete linear time invariant time-optimal control problem-an overview," *Automatica*, vol. 17, no. 2, pp. 363 – 370, 1981.

[4] A. Isidori and M. Benedetto, "Feedback linearization of nonlinear systems," *Control Handbook, CRC, Boca Raton, FL*, pp. 909–917, 1996.

[5] R. A. Paz, "Ripple-free tracking with robustness," *International Journal of Control*, vol. 79, no. 6, pp. 543–568, 2006.

[6] C. Odabaş, "Observer based friction cancellation in mechanical systems," Master's thesis, Bilkent University, 2014.

[7] U. Taşdelen, "Smith predictor based controller design for a flexible robot arm," Master's thesis, Bilkent University, 2013.

[8] M. Tomizuka, "On the compensation of friction forces in precision motion control," in *Motion Control Proceedings, 1993., Asia-Pacific Workshop on Advances in*, pp. 69–74, Jul 1993.

[9] H. Olsson, *Control Systems with Friction*. PhD thesis, Department of Automatic Control, Lund Institute of Technology, 1996.

[10] B. Armstrong-Hélouvry, P. Dupont, and C. C. D. Wit, "A survey of models, analysis tools and compensation methods for the control of machines with friction," *Automatica*, vol. 30, no. 7, pp. 1083 – 1138, 1994.

[11] S. Lee and S. M. Meerkov, "Generalized dither," *International Journal of Control*, vol. 53, no. 3, pp. 741–747, 1991.

[12] I. Horowitz, S. Oldak, and A. Shapiro, "Extensions of dithered feedback systems," *International Journal of Control*, vol. 54, no. 1, pp. 83–109, 1991.

[13] N. Leonard and P. Krishnaprasad, "Adaptive friction compensation for bi-directional low-velocity position tracking," in *Decision and Control, 1992., Proceedings of the 31st IEEE Conference on*, pp. 267–273 vol.1, 1992.

[14] Y. Yoshida and M. Tanaka, "Position control of a flexible arm using a dither signal," *JSME international journal. Ser. C, Dynamics, control, robotics, design and manufacturing*, vol. 36, no. 1, pp. 93–99, 1993.

[15] A. A. Pervozvanski and C. C. de Wit, "Asymptotic analysis of the dither effect in systems with friction," *Automatica*, vol. 38, no. 1, pp. 105 – 113, 2002.

[16] T. Hägglund, "A friction compensator for pneumatic control valves," *Journal of Process Control*, vol. 12, no. 8, pp. 897 – 904, 2002.

[17] E. Tung, Y. Urushisaki, and M. Tomizuka, "Low velocity friction compensation for machine tool feed drives," in *American Control Conference, 1993*, pp. 1932–1936, June 1993.

[18] P. Dupont, "Avoiding stick-slip through pd control," *Automatic Control, IEEE Transactions on*, vol. 39, pp. 1094–1097, May 1994.

[19] P. Tataryn, N. Sepehri, and D. Strong, "Experimental comparison of some compensation techniques for the control of manipulators with stick-slip friction," *Control Engineering Practice*, vol. 4, no. 9, pp. 1209 – 1219, 1996.

[20] B. Armstrong and B. Amin, "PID control in the presence of static friction: A comparison of algebraic and describing function analysis," *Automatica*, vol. 32, no. 5, pp. 679 – 692, 1996.

[21] P. Rocco, "Stability of pid control for industrial robot arms," *Robotics and Automation, IEEE Transactions on*, vol. 12, pp. 606–614, Aug 1996.

[22] L. Cao and H. Schwartz, "Stick-slip friction compensation for pid position control," in *American Control Conference, 2000. Proceedings of the 2000*, vol. 2, pp. 1078–1082 vol.2, 2000.

[23] J.-H. Ryu, J. Song, and D.-S. Kwon, "A nonlinear friction compensation method using adaptive control and its practical application to an in-parallel actuated 6-dof manipulator," *Control Engineering Practice*, vol. 9, no. 2, pp. 159 – 167, 2001.

[24] B. Armstrong, D. Neevel, and T. Kusik, "New results in npid control: Tracking, integral control, friction compensation and experimental results," *Control Systems Technology, IEEE Transactions on*, vol. 9, pp. 399–406, Mar 2001.

[25] T.-Y. Lin, Y.-C. Pan, and C. Hsieh, "Precision-limit positioning of direct drive systems with the existence of friction," *Control Engineering Practice*, vol. 11, no. 3, pp. 233 – 244, 2003. Advances in Automotive Control.

[26] C. haur Wu and R. Paul, "Manipulator compliance based on joint torque control," in *Decision and Control including the Symposium on Adaptive Processes, 1980 19th IEEE Conference on*, pp. 88–94, Dec 1980.

[27] M. Hashimoto, "Robot motion control based on joint torque sensing," in *Robotics and Automation, 1989. Proceedings., 1989 IEEE International Conference on*, pp. 256–261 vol.1, May 1989.

[28] J. Karlen, J. Thompson, H. Vold, J. Farrell, and P. Eismann, "A dual-arm dexterous manipulator system with anthropomorphic kinematics," in *Robotics and Automation, 1990. Proceedings., 1990 IEEE International Conference on*, pp. 368–373 vol.1, May 1990.

[29] M. Hashimoto, T. Shimono, K. Koreyeda, H. Tanaka, Y. Koyosawa, and H. Hirabayashi, "Experimental study on torque control using harmonic drive built-in torque sensors," in *Robotics and Automation, 1992. Proceedings., 1992 IEEE International Conference on*, pp. 2026–2031 vol.3, May 1992.

[30] M. Hashimoto, Y. Kiyosawa, and R. Paul, "A torque sensing technique for robots with harmonic drives," *Robotics and Automation, IEEE Transactions on*, vol. 9, pp. 108–116, Feb 1993.

[31] K. Kosuge, H. Takeuchi, and K. Furuta, "Motion control of a robot arm using joint torque sensors," *Robotics and Automation, IEEE Transactions on*, vol. 6, pp. 258–263, Apr 1990.

[32] P. Lischinsky, C. Canudas-de Wit, and G. Morel, "Friction compensation for an industrial hydraulic robot," *Control Systems, IEEE*, vol. 19, pp. 25–32, Feb 1999.

[33] G. Morel and S. Dubowsky, "The precise control of manipulators with joint friction: a base force/torque sensor method," in *Robotics and Automation, 1996. Proceedings., 1996 IEEE International Conference on*, vol. 1, pp. 360–365 vol.1, Apr 1996.

[34] J. Garretson, W. Decker, and S. Dubowsky, "The design of a friction compensation control architecture for a heavy lift precision manipulator in contact with

the environment," in *Robotics and Automation, 2006. ICRA 2006. Proceedings 2006 IEEE International Conference on*, pp. 31–36, May 2006.

[35] L. Le Tien, A. Albu-Schäffer, A. De Luca, and G. Hirzinger, "Friction observer and compensation for control of robots with joint torque measurement," in *Intelligent Robots and Systems, 2008. IROS 2008. IEEE/RSJ International Conference on*, pp. 3789–3795, Sept 2008.

[36] B. S. Armstrong, "Dynamics for robot control: friction modeling and ensuring excitation during parameter identification," tech. rep., DTIC Document, 1988.

[37] N. van de Wouw and R. I. Leine, "Robust impulsive control of motion systems with uncertain friction," *International Journal of Robust and Nonlinear Control*, vol. 22, no. 4, pp. 369–397, 2012.

[38] T. Yang, *Impulsive control theory*, vol. 272. Springer Science & Business Media, 2001.

[39] L. Guzzella and A. H. Glattfelder, "Positioning of stick-slip systems - comparison of a conventional and a variable-structure controller design," *American Control Conference*, vol. 29, pp. 1277 – 1281, 1992.

[40] S.-J. Huang, J.-Y. Yen, and S.-S. Lu, "Dual mode control of a system with friction," *Control Systems Technology, IEEE Transactions on*, vol. 7, pp. 306–314, May 1999.

[41] A. Bonchis, P. Corke, D. Rye, and Q. Ha, "Variable structure methods in hydraulic servo systems control," *Automatica*, vol. 37, no. 4, pp. 589 – 595, 2001.

[42] P. I. Ro, W. Shim, and S. Jeong, "Robust friction compensation for submicrometer positioning and tracking for a ball-screw-driven slide system," *Precision Engineering*, vol. 24, no. 2, pp. 160 – 173, 2000.

[43] W.-H. Chen, D. Ballance, P. Gawthrop, and J. O'Reilly, "A nonlinear disturbance observer for robotic manipulators," *Industrial Electronics, IEEE Transactions on*, vol. 47, pp. 932–938, Aug 2000.

[44] L. R. Ray, A. Ramasubramanian, and J. Townsend, "Adaptive friction compensation using extended kalman–bucy filter friction estimation," *Control Engineering Practice*, vol. 9, no. 2, pp. 169 – 179, 2001.

[45] A. Ramasubramanian and L. Ray, "Stability and performance analysis for non-model-based friction estimators," in *Decision and Control, 2001. Proceedings of the 40th IEEE Conference on*, vol. 3, pp. 2929–2935 vol.3, 2001.

[46] V. Lampaert, J. Swevers, and F. Al-Bender, "Comparison of model and non-model based friction compensation techniques in the neighbourhood of pre-sliding friction," in *American Control Conference, 2004. Proceedings of the 2004*, vol. 2, pp. 1121–1126 vol.2, June 2004.

[47] Y. Wang, Z. Xiong, H. Ding, and X. Zhu, "Nonlinear friction compensation and disturbance observer for a high-speed motion platform," in *Robotics and Automation, 2004. Proceedings. ICRA '04. 2004 IEEE International Conference on*, vol. 5, pp. 4515–4520 Vol.5, April 2004.

[48] T. Dumitriu, M. Culea, T. Munteanu, and E. Ceangă, "Non-Model-Based Observer for Friction Compensation in Servo Drive Position Tracking," *Journal of Electrical Engineering*, vol. 7, no. 2, pp. 1–8, 2007.

[49] H. Olsson, K. Åström, C. C. de Wit, M. Gäfvert, and P. Lischinsky, "Friction models and friction compensation," *European Journal of Control*, vol. 4, no. 3, pp. 176 – 195, 1998.

[50] H. S. Lee and M. Tomizuka, "Robust motion controller design for high-accuracy positioning systems," *Industrial Electronics, IEEE Transactions on*, vol. 43, pp. 48–55, Feb 1996.

[51] G. Otten, T. de Vries, J. van Amerongen, A. Rankers, and E. Gaal, "Linear motor motion control using a learning feedforward controller," *Mechatronics, IEEE/ASME Transactions on*, vol. 2, pp. 179–187, Sep 1997.

[52] J. Moreno, R. Kelly, and R. Campa, "Manipulator velocity control using friction compensation," *Control Theory and Applications, IEE Proceedings -* , vol. 150, pp. 119–126, March 2003.

[53] J. Moreno and R. Kelly, "Manipulator velocity field control with dynamic friction compensation," in *Decision and Control, 2003. Proceedings. 42nd IEEE Conference on*, vol. 4, pp. 3834–3839 vol.4, Dec 2003.

[54] D. Kostic, B. de Jager, M. Steinbuch, and R. Hensen, "Modeling and identification for high-performance robot control: an rrr-robotic arm case study," *Control Systems Technology, IEEE Transactions on*, vol. 12, pp. 904–919, Nov 2004.

[55] E. G. Papadopoulos and G. C. Chasparis, "Analysis and model-based control of servomechanisms with friction," *Journal of dynamic systems, measurement, and control*, vol. 126, no. 4, pp. 911–915, 2004.

[56] D. Putra, L. Moreau, and H. Nijmeijer, "Observer-based compensation of discontinuous friction," in *Decision and Control, 2004. CDC. 43rd IEEE Conference on*, vol. 5, pp. 4940–4945 Vol.5, Dec 2004.

[57] G. Song, Y. Wang, L. Cai, and R. Longman, "A sliding-mode based smooth adaptive robust controller for friction compensation," in *American Control Conference, Proceedings of the 1995*, vol. 5, pp. 3531–3535 vol.5, Jun 1995.

[58] J. Gonzalez and G. Widmann, "A new model for nonlinear friction compensation in the force control of robot manipulators," in *Control Applications, 1997., Proceedings of the 1997 IEEE International Conference on*, pp. 201–203, Oct 1997.

[59] Z. Jamaludin, H. Van Brussel, and J. Swevers, "Quadrant glitch compensation using friction model-based feedforward and an inverse-model-based disturbance observer," in *Advanced Motion Control, 2008. AMC '08. 10th IEEE International Workshop on*, pp. 212–217, March 2008.

[60] Z. Jamaludin, H. V. Brussel, G. Pipeleers, and J. Swevers, "Accurate motion control of xy high-speed linear drives using friction model feedforward and cutting forces estimation," *CIRP Annals - Manufacturing Technology*, vol. 57, no. 1, pp. 403 – 406, 2008.

[61] C. De Wit, H. Olsson, K. Astrom, and P. Lischinsky, "A new model for control of systems with friction," *Automatic Control, IEEE Transactions on*, vol. 40, pp. 419–425, Mar 1995.

[62] Y. Zhang, G. Liu, and A. Goldenberg, "Friction compensation with estimated velocity," in *Robotics and Automation, 2002. Proceedings. ICRA '02. IEEE International Conference on*, vol. 3, pp. 2650–2655, 2002.

[63] M.-C. Tsai, I.-F. Chiu, and M.-Y. Cheng, "Design and implementation of command and friction feedforward control for cnc motion controllers," *Control Theory and Applications, IEE Proceedings* -, vol. 151, pp. 13–20, Jan 2004.

[64] N. van Dijk, H. Nijmeijer, N. van de Wouw, and I. M. Dorrepaal, "Adaptive friction compensation of an inertia supported by mos2 solid-lubricated bearings," *Eindhoven University of Technology, Mechanical Engineering, Dynamics and Control Group, no. DCT*, vol. 6, p. 2005, 2005.

[65] J. van Geenhuizen, *Friction compensation for the printer system.* PhD thesis, Master's thesis, Dept. Mech. Eng., Eindhoven Univ. Technol., Eindhoven, The Netherlands, 2008.

[66] C. Canudas, K. Astrom, and K. Braun, "Adaptive friction compensation in dc-motor drives," *Robotics and Automation, IEEE Journal of*, vol. 3, pp. 681–685, December 1987.

[67] B. Friedland and Y.-J. Park, "On adaptive friction compensation," *Automatic Control, IEEE Transactions on*, vol. 37, pp. 1609–1612, Oct 1992.

[68] H. Henrichfreise and C. Witte, "Observer-based nonlinear compensation of friction in a positioning system," *German-Polish Sem., Cologne*, pp. 1–10, 1997.

[69] M. Feemster, P. Vedagarbha, D. Dawson, and D. Haste, "Adaptive control techniques for friction compensation," in *American Control Conference, 1998. Proceedings of the 1998*, vol. 3, pp. 1488–1492 vol.3, Jun 1998.

[70] P. Vedagarbha, D. Dawson, and M. Feemster, "Tracking control of mechanical systems in the presence of nonlinear dynamic friction effects," *Control Systems Technology, IEEE Transactions on*, vol. 7, pp. 446–456, July 1999.

[71] Y. Tan and I. Kanellakopoulos, "Adaptive nonlinear friction compensation with parametric uncertainties," in *American Control Conference, 1999. Proceedings of the 1999*, vol. 4, pp. 2511–2515 vol.4, 1999.

[72] S. Andersson, A. Söderberg, and S. Björklund, "Friction models for sliding dry, boundary and mixed lubricated contacts," *Tribology International*, vol. 40, no. 4, pp. 580 – 587, 2007. NORDTRIB 2004.

[73] K. Tan, S. Huang, and T. Lee, "Robust adaptive numerical compensation for friction and force ripple in permanent-magnet linear motors," *Magnetics, IEEE Transactions on*, vol. 38, pp. 221–228, Jan 2002.

[74] Y. Zhu and P. Pagilla, "Static and dynamic friction compensation in trajectory tracking control of robots," in *Robotics and Automation, 2002. Proceedings. ICRA '02. IEEE International Conference on*, vol. 3, pp. 2644–2649, 2002.

[75] T. H. Lee, K. K. Tan, and S. Huang, "Adaptive friction compensation with a dynamical friction model," *Mechatronics, IEEE/ASME Transactions on*, vol. 16, pp. 133–140, Feb 2011.

[76] B. Bona and M. Indri, "Friction compensation in robotics: an overview," in *Decision and Control, 2005 and 2005 European Control Conference. CDC-ECC '05. 44th IEEE Conference on*, pp. 4360–4367, Dec 2005.

[77] C. Johnson and R. Lorenz, "Experimental identification of friction and its compensation in precise, position controlled mechanisms," *Industry Applications, IEEE Transactions on*, vol. 28, pp. 1392–1398, Nov 1992.

[78] M. Marrari, A. Emami-Naeni, and G. Franklin, "Output deadbeat control discrete-time multivariate systems," *Automatic Control, IEEE Transactions on*, vol. 34, pp. 644–648, Jun 1989.

[79] A. Emami-Naeini and G. Franklin, "Deadbeat control and tracking of discrete-time systems," *Automatic Control, IEEE Transactions on*, vol. 27, pp. 176–181, Feb 1982.

[80] A. Emami-Naeini, "Deadbeat control of linear multivariable generalized state-space systems," *Automatic Control, IEEE Transactions on*, vol. 37, pp. 648–652, May 1992.

[81] B. Leden, "Dead-beat control and the riccati equation," *Automatic Control, IEEE Transactions on*, vol. 21, pp. 791–792, Oct 1976.

[82] F. Lewis, "A general riccati equation solution to the deadbeat control problem," *Automatic Control, IEEE Transactions on*, vol. 27, pp. 186–188, Feb 1982.

[83] M. E. Salgado, D. A. Oyarzún, and E. I. Silva, "optimal ripple-free deadbeat controller design," *Automatica*, vol. 43, no. 11, pp. 1961 – 1967, 2007.

[84] Y. Zhao and H. Kimura, "Optimization of control input for deadbeat control systems," *International Journal of Control*, vol. 59, no. 4, pp. 1107–1117, 1994.

[85] H. Elaydi and R. A. Paz, "Optimal ripple-free deadbeat controllers for systems with time delays," in *Proceedings of the American Control Conference*, vol. 1, pp. 655–659, American Automatic Control Council, 1998.

[86] L. Jetto and S. Longhi, "Parameterized solution of the dead-beat ripple-free control problem for multirate sampled-data systems," in *Decision and Control, 1999. Proceedings of the 38th IEEE Conference on*, vol. 4, pp. 3914–3919 vol.4, 1999.

[87] S. Glad, "Output dead-beat control for nonlinear systems with one zero at infinity," *Systems & Control Letters*, vol. 9, no. 3, pp. 249–255, 1987.

[88] G. Bastin, F. Jarachi, and I. Mareels, "Output deadbeat control of nonlinear discrete-time systems with one-dimensional zero dynamics: global stability conditions," *Automatic Control, IEEE Transactions on*, vol. 44, pp. 1262–1266, Jun 1999.

[89] D. Nešic, *Dead-beat control for polynomial systems*. PhD thesis, The Australian National University, 1996.

[90] B. Burnett, *The Laws of Motion: Understanding Uniform and Accelerated Motion*. Library of physics, Rosen Publishing Group, 2004.

[91] A. Harnoy, B. Friedland, and S. Cohn, "Modeling and measuring friction effects," *Control Systems, IEEE*, vol. 28, pp. 82–91, Dec 2008.

[92] P. Green, K. Worden, and N. Sims, "On the identification and modelling of friction in a randomly excited energy harvester," *Journal of Sound and Vibration*, vol. 332, no. 19, pp. 4696 – 4708, 2013.

[93] R. C. Dorf and R. H. Bishop, *Modern Control Systems (11th Edition) (Pie)*. Prentice Hall, Aug. 2007.

[94] H. K. Khalil and J. Grizzle, *Nonlinear systems*, vol. 3. Prentice Hall New Jersey, 1996.

[95] H. Norlander, "Parameterization of state feedback gains for pole placement," in *European Control Conference (ECC), 2003*, pp. 115–120, Sept 2003.

[96] D. Graham and R. C. Lathrop, "The synthesis of optimum transient response: Criteria and standard forms," *American Institute of Electrical Engineers, Part II: Applications and Industry, Transactions of the*, vol. 72, pp. 273–288, Nov 1953.

[97] D. Baleanu, J. A. T. Machado, and A. C. Luo, *Fractional dynamics and control*. Springer Science & Business Media, 2011.

[98] A. Awouda and R. Bin Mamat, "Refine pid tuning rule using itae criteria," in *Computer and Automation Engineering (ICCAE), 2010 The 2nd International Conference on*, vol. 5, pp. 171–176, Feb 2010.

[99] V. Kučera, "Diophantine equations in control—a survey," *Automatica*, vol. 29, no. 6, pp. 1361 – 1375, 1993.

[100] A. Hansson, P. Gruber, and J. Tödtli, "Fuzzy anti-reset windup for PID controllers," *Control Engineering Practice*, vol. 2, no. 3, pp. 389 – 396, 1994.